CYTOCHROME P450 DERIVED EICOSANOIDS, ENDOTHELIAL FUNCTION AND CARDIOVASCULAR DISEASE

Craig R. Lee

A dissertation submitted to the faculty of the University of North Carolina at Chapel Hill in partial fulfillment of the requirements for the degree of Doctor of Philosophy in Pharmaceutical Sciences in the School of Pharmacy (Pharmacotherapy and Experimental Therapeutics).

Chapel Hill
2006

Approved by
Advisor: Darryl C. Zeldin
Advisor: Dhiren Thakker
Advisor: J. Herbert Patterson
Advisor: Kari E. North
Advisor: Celeste M. Lindley
Advisor: Kirkwood F. Adams, Jr.

ABSTRACT

CRAIG R. LEE: Cytochrome P450 Derived Eicosanoids, Endothelial Function and Cardiovascular Disease
(Under the direction of Darryl C. Zeldin, Dhiren Thakker, J. Herbert Patterson, Kari E. North Celeste M. Lindley and Kirkwood F. Adams, Jr.)

Endothelial dysfunction plays an integral role in the pathogenesis and progression of cardiovascular disease in humans. The development of endothelial dysfunction has been primarily ascribed to functional impairments in nitric oxide biosynthesis. However, arachidonic acid metabolism by the cyclooxygenase and cytochrome P450 epoxygenase pathways also appears to regulate endothelial function. Consequently, genetic variation in these pathways may be important modifiers of cardiovascular disease risk in humans. The collective objective of the studies outlined in this doctoral dissertation was to determine if genetic variation in these established (*NOS3*, *PTGS1* and *PTGS2*) and recently characterized (*EPHX2*, *CYP2J2* and *CYP2C8*) pathways are significantly associated with cardiovascular disease risk. First, metabolic studies conducted *in vitro* demonstrate that certain genetic variants in cyclooxygenase-1 possess significantly lower metabolic activity compared to wild-type cyclooxygenase-1. Second, the observed associations between genetic variation in *PTGS1*, *PTGS2* and *NOS3* and risk of incident coronary heart disease and ischemic stroke events further implicate these established pathways in the development of cardiovascular disease in humans. Third, the observed associations between genetic variation in *EPHX2*, *CYP2J2* and *CYP2C8* and risk of incident coronary heart disease events also demonstrate the potential importance of the cytochrome P450 epoxygenase pathway in the pathogenesis of

ischemic cardiovascular disease in humans. Fourth, the development and baseline characterization of transgenic mice that exhibit vascular endothelial cell-specific overexpression of either human CYP2J2 or CYP2C8 will enable further mechanistic characterization of the cytochrome P450 epoxygenase pathway in the regulation of endothelial function and the pathogenesis of cardiovascular disease.

ACKNOWLEDGEMENTS

Completion of this doctoral dissertation would not have been possible without the important contributions of many individuals in both my personal and professional life. First and foremost, I am forever indebted to my family for their constant love and support.

I would also like to acknowledge my dissertation committee members Dr. Darryl C. Zeldin, Dr. Dhiren Thakker, Dr. J. Herbert Patterson, Dr. Kari E. North, Dr. Celeste M. Lindley and Dr. Kirkwood F. Adams, Jr. for their guidance and support throughout my graduate training. In particular, I would like to thank Dr. Darryl C. Zeldin for all of opportunity he provided over the last four years.

Completion of my graduate training would not have been possible without the framework provided by the University of North Carolina at Chapel Hill, School of Pharmacy and Division of Pharmacotherapy and Experimental Therapeutics, and all those integrally involved in the establishment of the Ph.D. program in Experimental Therapeutics. In particular, I would like to thank Ms. Amber Allen and Ms. Sherrie Settle for all of their administrative support. I would also like to thank the National Institute of Environmental Health Sciences for its involvement in my training, including its financial support via the Ruth L. Kirschstein Individual National Research Service Award (F32 ES012856).

Completion of the work described in this doctoral dissertation would not have been possible without the important contributions of many individuals. I would first like to thank all those in the Zeldin lab for their guidance and support. In particular, I would like to thank

Ms. Alyce Bradbury, Ms. Joan Graves and Ms. Laura Miller-DeGraff. I would also like to thank our Atherosclerosis Risk in Communities (ARIC) study collaborators for making this investigation possible. In particular, I would like to thank Dr. Gerardo Heiss, Dr. Kari E. North, Dr. Molly S. Bray and Dr. David J. Couper for all of their input and vital contribution to this work. I would also like to thank the staff and participants of the ARIC study for their important contributions. I would like to acknowledge Ms. Christy L. Avery, Dr. M.J. Mosher, Dr. Josef Coresh, Dr. Aaron R. Folsom and Dr. Eric Boerwinkle for their contribution to the *NOS3* analysis, and Dr. Myriam Fornage, Dr. John M. Seubert, Dr. John W. Newman, Dr. Bruce D. Hammock and Mr. Rajan Gill for their contribution to the *EPHX2* analysis. I would also like to acknowledge Dr. Frank G. Bottone, Jr., Dr. Joseph M. Krahn, Dr. Leping Li, Dr. Harvey W. Mohrenweiser, Ms. Molly E. Cook, Dr. Robert M. Petrovich, Dr. Douglas A. Bell and Dr. Thomas E. Eling for their contribution to the *PTGS1* polymorphism studies. Lastly, I would like to acknowledge Ms. Julie Foley, Ms. Eli Ney, Mr. Fred B. Lih, Dr. Kenneth E. Tomer, Ms. Jessica Sherman, and Dr. Carl Pinkert for their important contributions to the transgenic mouse work.

TABLE OF CONTENTS

LIST OF TABLES

LIST OF FIGURES

LIST OF ABBREVIATIONS

ACE	angiotensin-converting enzyme
ANOVA	analysis of variance
ARIC	Atherosclerosis Risk in Communities
BHT	butylated hydroxytoluene
BMI	body mass index
cDNA	complementary DNA
CHAPS	3-[(3-Cholamidopropyl)dimethylammonio]-1-propanesulfonate
CHD	coronary heart disease
CI	confidence intervals
COX	cyclooxygenases
CRS	cohort random sample
CYP	cytochrome P450
CYP2C8	CYP2C8 gene
CYP2J2	CYP2J2 gene
DBP	diastolic blood pressure
DHET	dihydroxyeicosatrienoic acid
DHOME	dihydroxyoctadecenoic acid
DHN	dihydroxynonadecanoic acid
DNA	deoxyribonucleic acid
dNTPs	deoxynucleotide triphosphates
DTT	dithiothreitol
EDHF	endothelial-derived hyperpolarization factor

EDTA	ethylenediaminetetraacetic acid
EETs	epoxyeicosatrienoic acids
egSNP	environmental genome single nucleotide polymorphism
eNOS	endothelial nitric oxide synthase
EpHep	epoxyheptadecanoic acid
EPHX2	soluble epoxide hydrolase gene
EpOME	epoxyoctadecenoic acid
FDR	false discovery rate
GFP	green fluorescent protein
HDL	high density lipoprotein
HMG-CoA	3-hydroxy-3-methylglutaryl coenzyme A
HPLC	high performance liquid chromatography
HRR	hazard rate ratio
IC_{50}	inhibitor concentration 50%
IκB-α	inhibitor kappa B-alpha
LB	Luria-Bertani
LD	linkage disequilibrium
LDL	low density lipoprotein
MALDI-TOF	matrix-assisted laser desorption/ionization time-of-flight
MAPK	mitogen-activated protein kinase
MCA	middle cerebral artery
MMP	matrix metalloproteinase
MS	mass spectrometry

NADPH	nicotinamide adenine dinucleotide phosphate
NF-κB	nuclear factor kappa B
NOS3	endothelial nitric oxide synthase gene
NSAIDs	nonsteroidal anti-inflammatory drugs
PCR	polymerase chain reaction
PG	prostaglandin
polyA	polyadenylation
PPAR	peroxisome proliferator-activated receptor
PTGS1	cycloxygenase-1 gene
PTGS2	cycloxygenase-2 gene
RNA	ribonucleic acid
ROS	reactive oxygen species
RT	reverse transcriptase
SBP	systolic blood pressure
sEH	soluble epoxide hydrolase
SEM	standard error of the mean
SNPs	single nucleotide polymorphisms
TBS	tris-buffered saline
Tg	transgenic
Tie2	endothelial-specific receptor tyrosine kinase gene
UTR	untranslated region
WT	wild-type

CHAPTER I

INTRODUCTION

Endothelial Function and Cardiovascular Disease

Ischemic cardiovascular disease is the leading cause of morbidity and mortality in the U.S. (1). It is estimated that 1.2 million Americans will experience an acute coronary heart disease (CHD) event and 0.7 million will experience an acute stroke event this year (1). Endothelial dysfunction plays an integral role in the pathogenesis and progression of ischemic cardiovascular disease in humans (2). Inflammation is also a key regulator in the pathogenesis of atherosclerotic cardiovascular disease, particularly via its role in the development and progression of endothelial dysfunction (2, 3). Endothelial dysfunction is typically manifested by substantially reduced endothelial-dependent vasodilation in the coronary, cerebral and peripheral vasculature, and increased expression of various pro-inflammatory mediators such as vascular adhesion molecules and chemokines (2-5). Risk factors including cigarette smoking (6), hypercholesterolemia (7), and diabetes (8) significantly contribute to the development and progression of endothelial dysfunction, which is markedly impaired in patients with established atherosclerosis (9) and independently associated with an increased risk of myocardial infarction and ischemic stroke events (10, 11). Moreover, pharmacological therapies such as HMG-CoA reductase inhibitors (statins) and angiotensin-converting enzyme (ACE) inhibitors significantly

improve endothelial function and reduce the risk of cardiovascular disease events in patients (2).

Nitric Oxide. The development of endothelial dysfunction has been primarily ascribed to functional impairments in nitric oxide biosynthesis and activity. Nitric oxide is synthesized by endothelial nitric oxide synthase (eNOS, *NOS3*) in the vasculature, where it possesses potent vasodilatory (12), anti-inflammatory (13), and anti-remodeling (14) effects. Impairment in eNOS-mediated nitric oxide synthesis significantly contributes to endothelial dysfunction and promotes the development of atherosclerosis (15, 16). In particular, cigarette smoking elicits many of its deleterious endothelial effects via attenuation of nitric oxide synthesis and activity (17, 18). Although nitric oxide is considered the primary endothelial-derived relaxing factor, arachidonic acid metabolism also appears to be important in the regulation of endothelial function, as illustrated in Figure 1.

Endothelial Arachidonic Acid Metabolism

Arachidonic acid is a polyunsaturated fatty acid present in mammalian cell membranes via esterification to membrane glycerophospholipids. Upon release by activation of cellular phospholipases, arachidonic acid is available for enzymatic oxidation by cyclooxygenases (COX) (19) and cytochromes P450 (20) into various biologically active mediators important in the regulation of endothelial and myocardial function. Lipoxygenase-mediated arachidonic acid metabolism is also an important and well-characterized pathway; however, its contribution to endothelial function will not be discussed (21).

Cyclooxygenases. The role of the COX metabolic pathway in cardiovascular physiology and disease pathogenesis has been extensively characterized. Briefly, COX-1 and COX-2 catalyze the oxidative conversion of arachidonic acid to prostaglandin (PG) H_2, which is subsequently metabolized by specific prostaglandin synthases to biologically active products including prostacyclin (PGI_2), thromboxane A_2 and PGE_2 (19). Although both COX-1 and COX-2 catalyze the same metabolic reaction with similar efficiencies, they are encoded by distinct gene products and differ substantially in their regulation and expression (19). COX-1 is constitutively expressed and is responsible for the biosynthesis of prostaglandins involved in various housekeeping functions, such as the regulation of renal, gastrointestinal, and platelet function (19). COX-2 is induced by multiple biological mediators, and primarily catalyzes prostaglandin synthesis in cells involved in both local and systemic inflammatory responses (19). However, the relative contribution of both COX-1 and COX-2-mediated prostaglandin biosynthesis appears to be a critical regulator of vascular function *in vivo* (22). For instance, despite their potential anti-inflammatory and atherosclerotic plaque stabilizing effects, nonselective COX-1/COX-2 and selective COX-2 antagonists inhibit endothelial prostacyclin biosynthesis without influencing platelet thromboxane A_2 production and appear to increase risk of myocardial infarction, particularly in high risk patients (23, 24). Although preferential inhibition of COX-1 derived thromboxane A_2 in platelets via low-dose aspirin administration significantly reduces the risk of myocardial infarction, ischemic stroke and death in high-risk patients (25), suppression of *endothelial* COX metabolism appears to worsen endothelial function and predispose patients to higher risk of acute cardiovascular events.

Cytochromes P450. Multiple cytochromes P450 also metabolize arachidonic acid to various eicosanoid products, including four regioisomeric epoxyeicosatrienoic acids (EETs) via olefin epoxidation (5,6-EET, 8,9-EET, 11,12-EET and 14,15-EET) (20, 26). Multiple P450 isoforms can catalyze the regio- and stereoselective formation of EETs in various species and tissues; however, the CYP2J and CYP2C subfamilies constitute the primary P450 epoxygenases (20). In humans, CYP2J2 and CYP2C8 are the primary isoforms responsible for the formation of EETs in endothelial cells and cardiomyocytes, where they possess potent biological effects (20). Once formed, EETs are rapidly hydrolyzed to their corresponding dihydroxyeicosatrienoic acid (DHET) metabolites by soluble epoxide hydrolase (sEH, *EPHX2*) (27-29). In general, DHETs are much less active than EETs in the cardiovascular system (20). Therefore, it has been proposed that sEH regulates steady-state EET levels *in vivo*, as illustrated in Figure 2.

P450 Epoxygenase Pathway – Biological Relevance

Previous work has demonstrated that EETs have substantial vasodilatory (30, 31), anti-inflammatory (32), fibrinolytic (33), post-ischemic cardioprotective (34, 35), pro-angiogenic (36), and vascular smooth muscle cell anti-migratory (37) effects. The EETs are potent vasodilators in the coronary microcirculation in both animals and humans, and are leading candidates for endothelial-derived hyperpolarization factor (EDHF) since their vasodilator effects are mediated via opening of vascular smooth muscle cell Ca^{2+}-dependent K^+ (BK_{Ca}) channels (30, 31). These effects are most pronounced in the presence of inhibitors of nitric oxide and PGI_2 biosynthesis, suggesting that this pathway may serve as an important reserve system to these primary endothelial-derived relaxing factors. In fact, EET-mediated

vasodilation may play a substantially larger role in patients with established endothelial dysfunction and reduced nitric oxide availability, since nitric oxide is known to inhibit P450 enzymatic activity (38) and attenuate the release of EDHF (39).

In addition, both CYP2J2 overexpression and exogenous administration of EETs have potent anti-inflammatory effects in endothelial cells by significantly attenuating cytokine-induced endothelial cell adhesion molecule expression and leukocyte adhesion to the vascular wall via inhibition of inhibitor kappa B-α (IκB-α) phosphorylation and nuclear factor kappa B (NF-κB) subunit RelA translocation to the nucleus (32), a well-characterized initiating event of pro-inflammatory signaling in the vasculature (5). Subsequent work has further characterized the anti-inflammatory properties of EETs via mechanisms involving activation of peroxisome proliferator-activated receptor-α (PPAR-α) (40) and PPAR-γ (41), and attenuation of COX-2-mediated PGE_2 synthesis (42). The EETs also play a significant role in the regulation of cardiac function following ischemia (34, 35). Specifically, transgenic mice with cardiomyocyte-specific overexpression of CYP2J2 and enhanced cardiac EET biosynthesis exhibit significant cardioprotection and improvement in post-ischemic recovery of left ventricular function via activation of mitochondrial K_{ATP} channels and p42/p44 mitogen-activated protein kinase (MAPK) signaling (35). Lastly, P450-derived EETs also contribute to the regulation of eNOS and COX-2 expression in the endothelium (43, 44), demonstrating the inter-related contribution of each of these pathways in the vasculature.

Importantly, sEH is integrally involved in regulation of both cellular levels and the cardiovascular effects of EETs. For instance, *Ephx2*$^{-/-}$ mice have significantly lower blood pressure (45) and significantly greater post-ischemic recovery of heart contractile function

(46) compared to wild type mice. Moreover, sEH inhibitors significantly lower blood pressure in spontaneously and angiotensin II-induced hypertensive rats (28, 47), inhibit vascular smooth muscle cell proliferation (48), and possess potent anti-inflammatory effects (41, 49). Hence, inhibition of sEH may represent a novel therapeutic strategy for the prevention and/or treatment of endothelial dysfunction and cardiovascular disease via augmentation of the cardiovascular effects of P450-derived EETs.

Although both CYP2J and CYP2C isoforms catalyze EET biosynthesis in endothelial cells, the source of EETs may be a critical determinant of their biological effects due to simultaneous formation of pro-inflammatory reactive oxygen species (ROS). For instance, unlike most other P450s CYP2J2 expression minimized ROS formation in the presence of enhanced oxidative stress (50), a characteristic common to patients with endothelial dysfunction. However, it has been reported that even though CYP2C overexpression in endothelial cells increased EET synthesis *in vitro*, no net anti-inflammatory effect was observed after cytokine challenge due to a simultaneous increase in ROS formation (51). These preliminary studies suggest that the source of EETs may be a critical factor related to their biological properties; however, evaluation of the relative differences between CYP2J2 and CYP2C8-mediated EET biosynthesis and ROS formation *in vivo* under controlled conditions remains to be characterized.

Perspective. Collectively, the results from various cellular and rodent models have demonstrated the importance of P450-mediated EET biosynthesis in cardiovascular physiology. However, the role of CYP2J2 and CYP2C8-derived EETs in the regulation of endothelial function, intravascular inflammation and atherosclerotic lesion development *in*

vivo remains poorly understood. Development of genetically altered mice overexpressing human *CYP2J2* or *CYP2C8* in the vasculature will be necessary to further characterize the *in vivo* role of both CYP2J2 and CYP2C8-derived EETs in these processes, which have proven vital to the development and progression of cardiovascular disease in humans.

Genetic Variation in Endothelial Pathways

Genetic polymorphisms have become increasingly recognized as important contributors to disease risk and variability in response to certain medications in humans (52) (Appendix I). Numerous polymorphisms in the genes encoding eNOS (*NOS3*), COX-1 (*PTGS1*), COX-2 (*PTGS2*), CYP2J2 (*CYP2J2*), CYP2C8 (*CYP2C8*) and sEH (*EPHX2*) have been recently discovered. The NIEHS Environmental Genome Single Nucleotide Polymorphism (egSNP) program has resequenced the *PTGS1*, *PTGS2*, *CYP2J2*, *CYP2C8* and *EPHX2* genes (https://dir-apps.niehs.nih.gov/egsnp/home.htm). Many of the identified variants include functionally relevant polymorphisms in either the proximal promoter or exonic regions of the gene which encode amino acid changes in the protein (i.e., nonsynonymous). However, their relevance to cardiovascular disease susceptibility remains poorly understood.

***NOS3*, *PTGS1* and *PTGS2*.** Multiple genetic polymorphisms in *NOS3* have been discovered, including the *T-786C* and Glu298Asp variants which have been associated with reduced nitric oxide biosynthesis (53, 54). Numerous clinical studies evaluating potential associations between *NOS3* polymorphisms and cardiovascular disease risk have reported inconsistent results (55). However, few investigations have evaluated incident clinical

events. Moreover, few have considered the potential influence of cigarette smoking despite their potential synergistic contribution to worsening endothelial function *in vivo* (56, 57).

The identification and functional characterization of genetic polymorphisms in *PTGS2* have also been reported (58, 59). These studies have demonstrated that certain variants significantly alter COX-2 expression and/or activity and may be important risk factors for disease in humans (58-60). In particular, the *G-765C* polymorphism in the proximal promoter of *PTGS2* disrupts a Sp1 binding site and is associated with significantly lower *PTGS2* transcription (59). Moreover, due to its anti-inflammatory effects, the variant *-765C* allele was associated with significantly lower risk of prevalent myocardial infarction or ischemic stroke events in a high-risk Italian population (60). However, associations between *PTGS2* polymorphisms and risk of incident cardiovascular events have not been investigated.

In contrast, characterization of genetic variation in *PTGS1* has not been as widely investigated. Polymorphisms in both coding and noncoding regions of human *PTGS1* have been identified, including nonsynonymous variants encoding amino acid substitutions in the COX-1 protein (61, 62). However, the functional consequences of these variants, in terms of their influence on basal COX-1-mediated arachidonic acid metabolism, have not been studied. Moreover, putative associations between *PTGS1* polymorphisms and cardiovascular disease risk have not been evaluated to date.

***CYP2J2*, *CYP2C8* and *EPHX2*.** Multiple genetic polymorphisms in *CYP2J2* have also been recently discovered (63, 64). The Thr143Ala (*CYP2J2*2*), Arg158Cys (*CYP2J2*3*), Ile192Asn (*CYP2J2*4*) and Asn404Tyr (*CYP2J2*6*) nonsynonymous variants were associated with significant reductions in EET biosynthesis *in vitro* compared to wild-type

protein; however, these variants were prevalent at very low frequencies (<2%) in the general population (63). A *G-50T* (*CYP2J2*7*) polymorphism in the proximal promoter of *CYP2J2* was also identified; although the minor allele was present at higher frequencies than the described nonsynonymous variants (approximately 8% in Caucasians) (63, 64). Presence of this variant resulted in loss of a critical Sp1 transcription factor binding site, and led to reduced transcription of *CYP2J2 in vitro* and EET biosynthesis *in vivo* (64). Importantly, the *-50T* variant allele was associated with higher risk of prevalent coronary artery disease in a German population (64), suggesting that genetic variation in *CYP2J2* may impact the development of cardiovascular disease in humans.

Numerous genetic polymorphisms in *CYP2C8* have also been recently discovered, including the nonsynonymous Ile269Phe (*CYP2C8*2*), Arg139Lys/Lys399Arg (*CYP2C8*3*) and Ile264Met (*CYP2C8*4*) variants which possess reduced CYP2C8 metabolic activity *in vitro* compared to wild-type protein (65, 66). The Ile264Met and Arg139Lys/Lys399Arg variant alleles are more frequent in Caucasian populations, while the Ile269Phe variant is more frequent in African-Americans. The Ile264Met and Ile269Phe variants have exhibited reduced capacity to metabolize the anticancer drug paclitaxel (65, 66). The Arg139Lys/Lys399Arg variant was markedly defective in the metabolism of both arachidonic acid and paclitaxel (65). Moreover, the Arg139Lys/Lys399Arg variant allele was associated with higher risk of prevalent myocardial infarction in a Swedish cohort (67).

Multiple single nucleotide polymorphisms in *EPHX2* have also been discovered (68, 69). These include nonsynonymous polymorphisms that demonstrate either increased (Lys55Arg, Glu470Gly) or decreased (Arg103Cys, Arg287Gln, 402InsArg) sEH-mediated conversion of EETs to DHETs *in vitro* compared to wild-type protein (68, 69). An association between the

Arg287Gln polymorphism variant allele and increased coronary artery calcification, a subclinical measure of atherosclerotic burden, has been reported in African-Americans (70); however, since this variant carries reduced sEH activity, the observed association appears in contrast to the current hypotheses regarding the protective effects of EETs in the cardiovascular system. Importantly, associations between polymorphisms in *CYP2J2*, *CYP2C8* and *EPHX2* and the risk of incident clinical events have not been evaluated to date.

Perspective. Although preliminary associations have been reported between variation in these established (*NOS3*, *PTGS2*) and recently characterized (*CYP2J2*, *CYP2C8* and *EPHX2*) genes involved in the regulation of endothelial function and cardiovascular disease risk, future gene-association studies evaluating risk of incident clinical events such as myocardial infarction and ischemic stroke will be necessary to further characterize the role of these pathways in cardiovascular disease susceptibility. Moreover, evaluation of the potential influence of environmental factors known to impair endothelial function, such as cigarette smoking, on these associations will also be necessary to characterize potential gene-environment interactions relevant to cardiovascular disease risk. Lastly, *in vitro* functional characterization of selected variants in *PTGS1* will be critical in order to guide the design and interpretation of epidemiological studies evaluating associations between *PTGS1* variants and cardiovascular disease risk.

Specific Aims

I. To determine if nonsynonymous polymorphisms in *PTGS1* significantly alter cyclooxygenase-1 metabolic activity *in vitro*.

Hypothesis. Certain nonsynonymous variants will be associated with significantly lower basal cyclooxygenase-1 metabolic activity *in vitro* compared to wild-type.

II. To determine if genetic variation in *PTGS1*, *PTGS2* and/or *NOS3* is significantly associated with the development of incident coronary heart disease or ischemic stroke clinical events in humans.

Hypothesis A. Polymorphisms associated with lower cyclooxygenase-1 or cyclooxygenase-2 metabolic activity or expression will be associated with significantly higher risk of incident coronary heart disease and ischemic stroke events. These associations will be most pronounced in individuals not receiving aspirin therapy.

Hypothesis B. Polymorphisms associated with lower nitric oxide synthase metabolic activity or expression will be associated with significantly higher risk of incident coronary heart disease and ischemic stroke events. These associations will be most pronounced in cigarette smokers.

III. To determine if genetic variation in *CYP2J2*, *CYP2C8* and/or *EPHX2* is significantly associated with the development of incident coronary heart disease clinical events in humans.

Hypothesis A. Polymorphisms associated with higher and lower soluble epoxide hydrolase metabolic activity will be associated with significantly higher and lower risk of incident coronary heart disease events, respectively.

Hypothesis B. Polymorphisms associated with lower CYP2J2 or CYP2C8 metabolic activity or expression will be associated with significantly higher risk of incident coronary heart disease events.

IV. To develop transgenic mice that exhibit vascular endothelial cell-specific overexpression of human CYP2J2 or CYP2C8.

Hypothesis. Constitutive, vascular endothelial cell-specific overexpression of CYP2J2 and CYP2C8 can be achieved using the *Tie2* promoter and *Tie2* full enhancer, resulting in increased systemic epoxyeicosatrienoic acid concentrations.

Chapter Outline

Part I. Cyclooxygenase and Nitric Oxide Pathways and Cardiovascular Disease Risk.

Chapter II. Identification and functional characterization of polymorphisms in human cyclooxygenase-1 (*PTGS1*).

Chapter III. Cyclooxygenase polymorphisms and risk of cardiovascular events: the Atherosclerosis Risk in Communities (ARIC) study.

Chapter IV. *NOS3* polymorphisms, cigarette smoking, and cardiovascular disease risk: the Atherosclerosis Risk in Communities (ARIC) study.

Part II. P450 Epoxygenase Pathway and Cardiovascular Disease Risk.

Chapter V. Genetic variation in soluble epoxide hydrolase (*EPHX2*) and risk of coronary heart disease: the Atherosclerosis Risk in Communities (ARIC) study.

Chapter VI. *CYP2J2* and *CYP2C8* polymorphisms and coronary heart disease risk: the Atherosclerosis Risk in Communities (ARIC) study.

Chapter VII. Development and baseline characterization of Tie2-CYP2J2 and Tie2-CYP2C8 transgenic mice.

Figure 1: Endothelial pathways of interest.

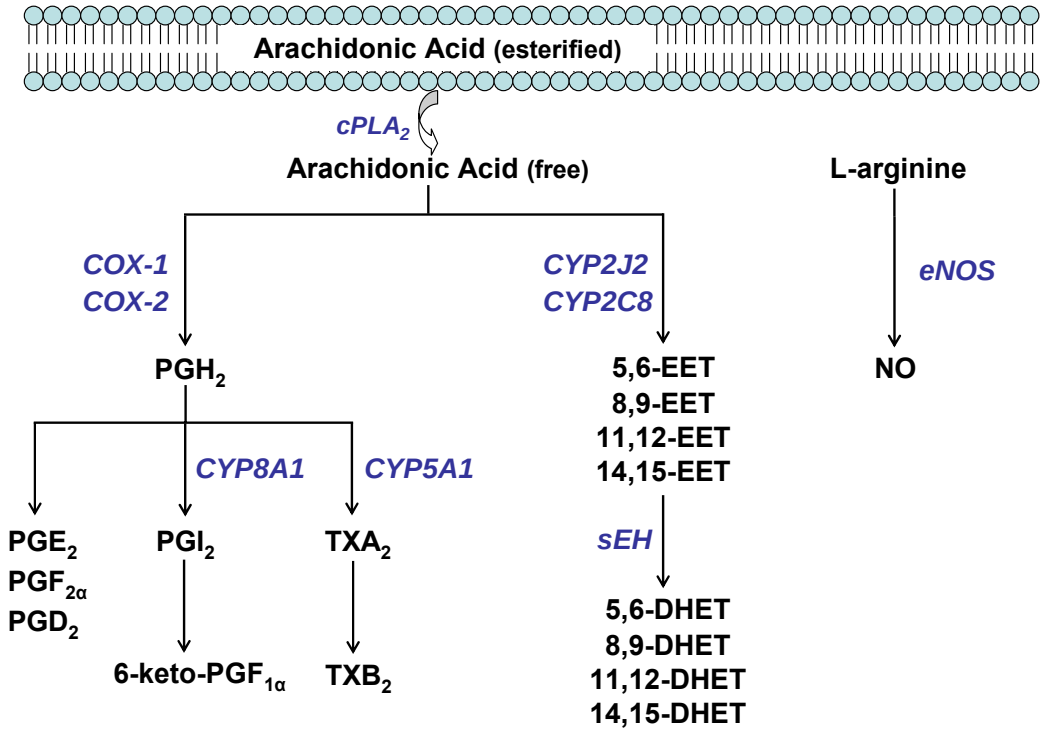

Figure 2: Regulation of steady-state EET levels by P450 epoxygenases and sEH.

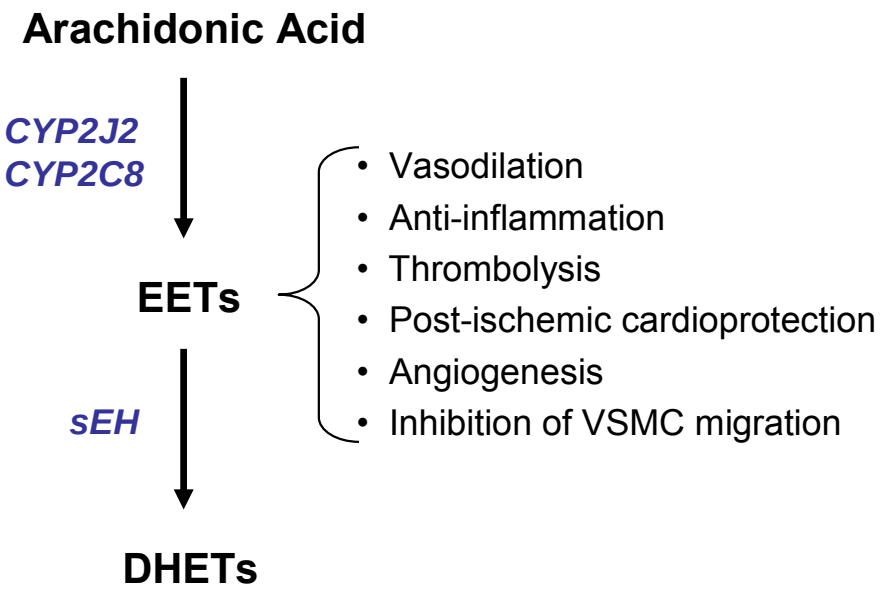

PART I

CYCLOOXYGENASE AND NITRIC OXIDE PATHWAYS AND CARDIOVASCULAR DISEASE RISK

CHAPTER II

IDENTIFICATION AND FUNCTIONAL CHARACTERIZATION OF POLYMORPHISMS IN HUMAN CYCLOOXYGENASE-1 (*PTGS1*)

Lee CR, Bottone FG, Krahn JM, Li L, Mohrenweiser HW, Cook ME, Petrovich RM, Bell DA, Eling TE, Zeldin DC. Identification and functional characterization of polymorphisms in human cyclooxygenase-1 (*PTGS1*). Pharmacogenet Genomics 2006; (accepted with minor revision; resubmitted 6/6/06).

Introduction

Cyclooxygenases (COX)-1 and -2 catalyze the oxidative conversion of arachidonic acid to prostaglandin (PG) H_2, which is subsequently metabolized to various biologically active metabolites such as prostacyclin and thromboxane A_2 (19). Although both COX-1 and COX-2 catalyze the same metabolic reaction with similar efficiencies, they are encoded by distinct gene products and differ substantially in their regulation and expression (19).

The gene encoding human COX-1 (*PTGS1*) has been mapped to chromosome 9q32-q33.3, is approximately 22 kilobases in length, and contains 11 exons (71, 72). COX-1 is constitutively expressed and is responsible for the biosynthesis of PGs involved in various housekeeping functions, such as the regulation of renal, gastrointestinal, and platelet function (19). COX-2 is induced by multiple biological mediators, and primarily catalyzes PG synthesis in cells involved in both local and systemic inflammatory responses (19). Nonsteroidal anti-inflammatory drugs (NSAIDs) inhibit COX-mediated PG synthesis and are widely used for the prevention and/or treatment of various diseases (73). As a therapeutic class, these agents demonstrate a wide range of relative selectivity for COX-1 and COX-2,

and significant inter-individual variability in clinical response exists (73). Due to the inducible nature of COX-2 regulation and its potential role in the pathogenesis of various inflammatory disorders, the overwhelming majority of research characterizing the role of COXs in human disease to date has focused on COX-2. However, recent evidence, including associations between selective COX-2 inhibitor utilization and myocardial infarction risk, suggests the *relative* contribution of COX-1 and COX-2-mediated PG synthesis is important (23, 24). Consequently, genetic variation in both *PTGS1* and *PTGS2* may be important modifiers of disease risk in humans.

The identification and functional characterization of genetic polymorphisms in *PTGS2* have been reported (58, 59). These studies demonstrate that certain variants significantly alter COX-2 expression and/or activity and may be important risk factors for disease in humans (58-60). In contrast, characterization of genetic variation in *PTGS1* has not been as widely investigated, even though the presence of functionally relevant variants may significantly influence PG biosynthesis, disease risk, and NSAID pharmacodynamics in humans. Polymorphisms in both coding and noncoding regions of human *PTGS1* have been previously identified (61, 62, 74, 75), including by resequencing as part of the SeattleSNPs Variation Discovery Resource (http://pga.mbt.washington.edu/). In particular, nonsynonymous variants encoding amino acid substitutions in the COX-1 protein have been identified (61, 62, 74, 75). However, the functional consequences of these variants, in terms of their influence on basal COX-1-mediated arachidonic acid metabolism, have not been characterized to date. Human studies have evaluated the potential influence of certain variants on NSAID-mediated inhibition of COX metabolism *in vivo* and *ex vivo* (62, 76-78); however, the functional consequences of most variants on NSAID pharmacodynamics are not

well understood. The primary objectives of this investigation were to: 1) identify or confirm the existence of polymorphisms in *PTGS1* by resequencing, 2) characterize the linkage disequilibrium (LD) structure in *PTGS1*, and 3) evaluate the functional consequences of selected variants using established *in vitro* assays.

Methods

Chemicals. All chemicals were purchased from Sigma (St. Louis, MO), unless otherwise noted.

DNA Samples. Genomic DNA was extracted from 72 human lymphoblastoid cell lines (Coriell Institute, Camden, NJ) obtained from healthy individuals with the following ancestries: 24 Africans [16 African-Americans, 8 African Pygmy], 24 Asians [5 Indo-Pakistani, 5 native Taiwanese, 5 mainland Chinese, 3 Cambodian, 3 Japanese, 3 Melanesian], 24 European/Caucasians [9 European-Americans, 5 Druze, 5 Adygei, 5 Russian], and an additional 20 anonymous healthy U.S. residents (DNA Polymorphism Discovery Resource, NIH) (79), as part of the NIEHS Environmental Genome Single Nucleotide Polymorphism (egSNP) program (https://dir-apps.niehs.nih.gov/egsnp/home.htm) (58, 63, 69, 80).

Genotyping. A resequencing strategy was used to identify variants in both coding and noncoding regions of *PTGS1*. Sequencing spanned all 11 exons, including approximately 75 base pairs 3' and 5' of each intron-exon boundary, and 2.4 kilobases into the 5' untranslated region (5'UTR). Amplified polymerase chain reaction (PCR) products containing these regions were generated using oligonucleotide primers specific to *PTGS1*. All sequencing

was performed in both directions, as previously described, at the Lawrence Livermore National Laboratory (58, 63, 69, 80). Since all DNA samples came from commercially available cell lines, this protocol was considered exempt by the Lawrence Livermore National Laboratory Institutional Review Board.

LD Statistics. Minor allele frequencies and pairwise LD statistics were calculated for each polymorphism, and the corresponding LD plots were generated (Haploview 3.2) (81). All analyses were completed independently in the African, Asian, and European/Caucasian ethnic groups.

Evaluation of COX-1 Gene and Protein Sequences. Approximately 1.8 kilobases of the human *PTGS1* 5'UTR sequence was extracted from the University of California Santa Cruz Genome Browser (http://genome.ucsc.edu/), and the corresponding human, mouse, rat, dog and chimp sequences for this region were aligned to screen for nucleotide conservation across species at each of the polymorphic sites. The sequences surrounding each polymorphism were then evaluated for potential location within putative transcription factor binding sites using the TRANSFAC database (82).

The human, rat, mouse, and sheep COX-1 amino acid sequences were obtained from Genbank and aligned using the ClustalW program (83) to determine if the identified nonsynonymous polymorphisms occurred in conserved regions of the protein. A model of the human COX-1 protein was constructed based on the ovine COX-1 crystal structure (PDB accession 1Q4G) (84), which has 96% sequence identity to human COX-1. The model was also compared with the murine COX-2 crystal structure (PDB accession 1CVU) (85, 86).

Additional crystallographic refinement was performed for both structures using the deposited diffraction data after analysis by MolProbity (87). In both cases, the crystallographic R-factor was reduced by more than 1% in working and test reflection sets. The procedure for modeling human COX-1 from the refined ovine structure consisted primarily of selecting preferred rotamers (87). The high level of sequence conservation and lack of insertions or deletions eliminated the need for changes to the C-alpha backbone coordinates. Substitution of side chains using common side-chain rotamers produced an acceptable fit in all cases, so no energy minimization was performed. In order to predict the potential impact of amino acid substitutions on the structure and function of the COX-1 protein, the R53H, R78W, K185T, G230S, L237M, and V481I variant amino acids were individually built into the wild-type human COX-1 model. Since the R8W and P17L polymorphisms occur in the COX-1 signal peptide and the ovine COX-1 crystal structure starts at amino acid residue 25 (84), the impact of these variants were not evaluated in the model.

Plasmid Construction and Site-Directed Mutagenesis. The full-length COX-1 cDNA was subcloned into pcDNA3.1 (Invitrogen, Carlsbad, CA), as previously described (88). Single nucleotide polymorphisms (SNPs) were introduced into the wild-type COX-1 cDNA by site-directed mutagenesis using the QuikChange Site-Directed Mutagenesis Kit (Stratagene, La Jolla, CA) per the manufacturer instructions. The specific primer sequences used to generate each of the 8 mutations are provided in Table 1. Presence of the desired mutation in each ampicillin-resistant clone was confirmed by sequencing the entire COX-1 cDNA using the BigDye Terminator Reaction Ready Mix (Applied Biosystems, Foster City, CA) and ABI Prism 377 DNA sequencer (Applied Biosystems). Wild-type and variant cDNAs with the

desired substitutions and no secondary mutations were then subcloned into the *Bam*HI/*Not*I sites of the pVL1393 Baculovirus Transfer Vector (BD Biosciences, San Diego, CA) via the intermediate pCR Blunt II-TOPO vector (Invitrogen). The orientation and sequence of the wild-type and variant cDNAs in pVL1393 were confirmed by direct sequencing.

Expression of Human COX-1 in Sf9 Cells. Sf9 cells were plated in T-25 tissue culture flasks at 2 x 10^6 cells/flask, cotransfected with 0.5 μg of BaculoGold Bright linearized baculovirus DNA (BD Biosciences) and 2 μg of pVL1393 containing the COX-1 inserts, and incubated at 27°C for 96 hours. Recombinant baculovirus was amplified by infecting 50 mL of Sf9 cells (70% confluent) in HyQ SFX-Insect cell culture media (Fisher Chemical, Fairlawn, NJ) and 5% fetal bovine serum with 1 mL of the transfection supernatant, and incubated in spinner flasks for 72 hours at 27°C at 120 rpm. Cells were harvested and lysed by sonication in a 80 mM Tris, 2 mM EDTA buffer (pH=7.2). Viral amplification was qualitatively confirmed by visualizing GFP fluorescence in the lysed cells under ultraviolet light. Uninfected negative control cells demonstrated no fluorescence. For large scale COX-1 expression, 1 liter of Sf9 cells (70% confluent) were infected with each amplification supernatant and incubated for 72 hours in spinner flasks at 27°C at 120 rpm, as described (58, 89, 90). Cells were centrifuged for 20 minutes at 4°C at 3000 rpm, washed with ice cold phosphate buffered saline, and centrifuged again. Cell pellets were stored at -80°C after removal of the supernatant.

Cell pellets were thawed on ice and lysed by sonication in a 80 mM Tris, 2 mM EDTA buffer (pH=7.2) containing 0.1 M silver diethyldithiocarbamate and protease inhibitors, as described (58, 89, 90). Cell lysates were ultracentrifuged at 40,000 rpm at 4°C for 1 hour,

and the microsomal pellets were homogenized in a 200 mM Tris, 0.1 mM EDTA buffer (pH=8.0) containing 0.4% CHAPS. Homogenates were stirred for 1.5 hours at 4°C while bringing the final volume to 1% CHAPS (w/v), and ultracentrifuged at 40,000 rpm at 4°C for 45 minutes. Supernatants, which contained the solubilized COX-1 enzyme, were stored in aliquots at -80°C.

Immunoblotting. Protein concentrations of the solubilized microsomal fractions were quantified using the Bio-Rad protein assay (Bio-Rad, Hercules, CA). Protein normalized samples were added to 4X sample buffer containing β-mercaptoethanol and boiled for 5 minutes. Proteins were separated by 10% Novex Tris-glycine polyacrylamide gels (Invitrogen) and transferred to nitrocellulose membranes (Invitrogen) in transfer buffer containing 20% methanol. The membranes were blocked in 5% nonfat milk in Tris-buffered saline (TBS) for 2 hours, incubated in a 1:250 dilution of COX-1 specific monoclonal antibody (Cayman Chemical, Ann Arbor, MI) at 4°C overnight, and then washed in 0.05% TBS-Tween 20 four times. After incubation with a 1:2000 dilution of horseradish peroxidase conjugated bovine anti-mouse secondary antibody (Santa Cruz Biotechnology, Santa Cruz, CA) and additional washing, COX-1 immunoreactive bands were detected by chemiluminescence using the SuperSignal West Pico chemiluminescent substrate (Pierce, Rockford, IL).

In order to estimate differences in COX-1 expression across each preparation, densitometry was completed after multiple immunoblots and mean fold differences in COX-1 immunoreactivity were calculated for each variant relative to wild-type. The total amount of solubilized microsomal protein used in all subsequent activity studies was normalized to

COX-1 immunoreactivity based on these calculations. Similar protein normalization methods have been utilized for the functional characterization of nonsynonymous polymorphisms in other genes using a baculovirus/insect cell expression system (58, 69).

COX-1 Enzymatic Assay. COX-1 enzymatic activity was determined by measuring oxygen consumption at 37°C in an oxygraph chamber using an YSI Model 53 oxygen monitor and electrode (YSI International, Yellow Springs, OH), as described (58, 89-91). The reaction buffer consisted of 100 mM Tris (pH=8.0) containing 500 μM phenol. Solubilized microsomal protein from the wild-type (3.4 mg of total protein) and 8 variant (total protein amounts normalized to COX-1 immunoreactivity) preparations were reconstituted in reaction buffer with 10 μM hematin for 1 minute on ice. Solubilized microsomal protein from uninfected Sf9 cells (3.4 mg of total protein) was used as a negative control. Samples were then equilibrated in reaction buffer for 1 minute at 37°C. Oxygen consumption was measured for 120 seconds following the addition of 100 μM arachidonic acid (Cayman Chemical), and the rate of oxygen consumption was calculated and expressed as μM O_2/minute/mg microsomal protein. Three independent experiments were completed, each in triplicate.

Inhibitor studies were completed with 0 (vehicle), 0.1, 1, 5, 10, and 25 μM indomethacin (Cayman Chemical) in the wild-type, R8W, P17L, G230S, and L237M preparations. Solubilized microsomal proteins were reconstituted on ice for 10 minutes with hematin plus indomethacin, each completed in triplicate, and oxygen consumption was measured using the experimental conditions described above.

Statistical Analysis. The rate of oxygen consumption was expressed relative to wild-type and averaged. Data are presented as mean±standard error of the mean (SEM), and were compared across COX-1 preparation by analysis of variance (ANOVA). A post-hoc Dunnett's test assessed the presence of statistical differences between each mutant relative to wild-type. A *P*-value <0.05 was considered statistically significant.

In order to determine if certain variants significantly influenced indomethacin-mediated inhibition of COX-1, IC_{50} values were estimated. First, the data for each preparation were plotted as percent activity relative to control (vehicle) versus natural log indomethacin concentration. The IC_{50} value for each was estimated according to the Hill equation by nonlinear regression (WinNonlin, Pharsight Corporation), where Emax=1.0, C=natural log indomethacin concentration, and the IC_{50} and γ (an exponential term influencing the sigmoidal shape of the curve) values were estimated according to the model's fit of the data:

$$\text{Effect} = \text{Emax} * \left[1 - \left(C^{\gamma} \Big/ C^{\gamma} + IC_{50}{}^{\gamma} \right) \right]$$

Triplicate values at each indomethacin concentration were simultaneously modeled for estimation of a single IC_{50} value (±95% confidence intervals) for each preparation. Inclusion of a $1/Y^2$ weighting factor substantially improved the model's fit of the data according to the Akaike Information Criterion value.

Results

Identification of *PTGS1* Variants. Sequencing the *PTGS1* gene in 72 individuals of known ethnicity identified 44 variants (42 SNPs, 1 nucleotide insertion, and 1 nucleotide deletion). Evaluation of an additional 20 anonymous individuals of unknown ethnicity identified one

additional SNP. Of these 45 variants, 14 were located in the 5'UTR, 12 were in exons, and 19 were in introns. Seven of the 12 exonic substitutions were nonsynonymous (R8W, R8P, P17L, R78W, K185T, L237M, and V481I) and 5 were synonymous. The R8P and R78W variants have not been previously reported. The R8P variant was identified in a single individual of African descent. The R78W variant was identified in a single individual of unknown ethnicity. The R53H and G230S variants reported in other populations (61, 62) were not identified in this resequencing analysis; however, their existence was confirmed at frequencies <1% in an independent African-American population (n=367) (see Chapter III). The minor allele frequencies of most polymorphisms differed significantly across ethnicity, with the Asian sample demonstrating the least genetic variation. The location and minor allele frequencies of all 45 variants are summarized in Table 2. Given the magnitude of genetic diversity and admixture across human populations, and the small number of chromosomes screened within each ethnic group, the reported minor allele frequencies should be considered an approximation.

LD Structure of the *PTGS1* Gene. The LD structure across *PTGS1* is presented for each ethnicity (Figure 3). A substantial degree of LD was observed throughout the 5'UTR. This LD pattern specifically involved seven polymorphisms (*T-1749C*, *G-1598A*, *A-1202G*, *A-1201G*, *G-1006A*, *A-918G* and *A-707G*) (Table 2) and was observed in both the European/Caucasian (D'=1.0, r^2=0.73-1.0) and African (D'=1.0, r^2=1.0) samples, suggesting these seven polymorphisms are on the same haplotype. In European/Caucasians, these 5'UTR polymorphisms were also in significant LD with the P17L variant in exon 2. Interestingly, only two of the identified 5'UTR polymorphisms (*C-1160G* and *G-951A*) are

located in regions relatively conserved across human, mouse, rat, dog and chimp, suggesting that most are in regions that are not selectively constrained. The completed transcription factor binding site search suggests the *T-1749C* polymorphism could weaken a putative AML/RUNX1 binding site by changing the core motif from *TGTTGT* to *TGCTGT*, the linked *A-1202G* and *A-1201G* polymorphisms could destroy a putative NF-Y binding site by changing the core NF-Y motif from *CCAAT* to *CCGGT*, and the *G-951A* polymorphism could disrupt a putative NF-AT binding site. In addition, the *G-1006A* polymorphism could create a putative heat shock protein (HSF) binding site.

Structural Analysis of the COX-1 Protein. Alignment of human, mouse, rat and sheep COX-1 amino acid sequences demonstrated that the R78, G230 and L237 amino acids are conserved across each of these species (Figure 4). Interestingly, L237 is also conserved across all COX-2 protein sequences. The R53H, R78W, K185T, G230S, L237M, and V481I variants were individually incorporated into the wild-type human COX-1 model (Figure 5). Substitution of a serine for glycine at residue 230 (G230S) appears to significantly impact the structure of COX-1 (Figure 6). First, glycine 230 is located on a 3_{10} helical turn, suggesting that this tight turn requires a glycine residue. The equivalent residue in COX-2 is asparagine 231. Comparison of the current model to murine COX-2 (PDB accession 1CVU) (85, 86) reveals that some of the backbone interactions in COX-2 are less favorable than observed in COX-1, but these are offset through favorable interactions by the asparagine 231 side chain to the backbone carbonyl of glutamine 208 and the side chain of aspartic acid 229 (Figure 6C). In the current human COX-1 model, there is a single sterically-compatible rotamer conformation for serine 230 substitution, which can interact favorably with only one

hydrogen-bond acceptor (Figure 6B). The minimum conformational change to avoid a negative interaction is the rotation of aspartic acid 228 to a position within hydrogen-bonding distance to arginine 332. However, this position requires a displacement of tryptophan 138' which perturbs the dimer interface association, potentially influencing enzyme activity (Figure 6D, where 'prime' indicates a residue from the dimer associated molecule). Moreover, arginine 332 is solvent-accessible at the bottom of a narrow crevasse where arachidonic acid could form hydrogen bonds and prevent stabilization of the proposed alternate conformation of aspartic acid 228.

In the presence of the R53H, R78W, K185T, L237M, or V481I substitutions, common rotamer conformations yielded reasonable accommodation of the substituted amino acid; however, in certain cases potential minor alterations in structure that could influence enzyme activity were noted. For instance, arginine 53 is in a solvent exposed region where substitution with histidine (R53H) has no obvious effects; however, this substitution could have a minor influence on glycosylation of asparagine 67 or the adjacent dimerization contact, both of which are approximately about 10-11Å away. The arginine 78 residue is at the membrane binding surface and, although conserved, a tryptophan substitution at this position (R78W) is also favorable for membrane binding and unlikely to directly influence enzyme activity. The most feasible functional role for arginine at this site would be to assist retrieval of arachidonic acid into the active site. The lysine 185 residue is on a solvent exposed loop, distant from any functional site likely to influence catalysis; however, this residue is in a positively charged region with several arginines, which could serve some non-obvious function potentially altered by a threonine substitution (K185T). The leucine 237 residue is likely involved in a dimerization interaction, with significant contacts to sugars

linked to asparagine 143 of the related monomer. A methionine substitution (L237M) fits reasonably well into this site with favorable hydrophobic interactions, but it is larger and more flexible. This mutation is predicted to have a small effect on the dimerization interface. Moreover, oxidation of methionine could conceivably impact the dimerization contact; however, it is unclear whether either of these effects could significantly influence enzyme activity. The valine 481 residue is distant from both the catalytic site and dimerization surface. Since an isoleucine substitution (V481I) is conservative, this mutation appears unlikely to influence enzyme activity.

Expression of the Wild-type and Variant COX-1 Proteins. The COX-1 wild-type and mutant R8W, P17L, R53H, R78W, K185T, G230S, L237M, and V481I proteins were expressed in Sf9 cells using a single promoter baculovirus system. The R8P variant was not expressed since the R8W variant occurred at the same amino acid position and was more frequent. Expression was verified by immunoblotting, with a molecular mass of approximately 70-kDa for the wild-type and mutant proteins (Figure 7A). COX-1 expression was not observed in uninfected Sf9 cells. Consistent with previous studies of COX-1 expression in Sf9 cells (89, 90), the relative amount of COX-1 in the solubilized microsomal fraction to the total amount of protein was fairly low. However, large scale expression of each preparation generated enough COX-1 protein for functional characterization.

Densitometry analysis of multiple immunoblots demonstrated variability in the level of COX-1 immunoreactivity across preparations, with an approximate range of 0.3-1.4-fold differences relative to wild-type. Immunoblots were repeated with varying amounts of solubilized microsomal protein according to these densitometry results in order to normalize

each preparation for COX-1 immunoreactivity, as presented in Figure 7A. Such an approach normalized these preparation differences in COX-1 expression and yielded approximately 0.9-1.1-fold differences in COX-1 immunoreactivity across each preparation relative to wild-type. Subsequently, equivalent amounts of immunoreactive COX-1 for each preparation were included in the activity studies.

COX-1 Enzymatic Activity. The mean rate of oxygen consumption calculated for the wild-type COX-1 preparation was 19.7±2.0 μM O_2/minute/mg microsomal protein. The uninfected negative control demonstrated undetectable oxygen consumption, suggesting detectable oxygen consumption in the COX-1 preparations was due to recombinant COX-1-mediated arachidonic acid metabolism. Pooled analysis of three independent experiments demonstrated the R53H (35.0±4.9%), R78W (36.1±3.9%), K185T (59.2±6.4%), G230S (56.6±3.5%) and L237M (51.0±2.5%) variants had significantly lower metabolic activity relative to wild-type COX-1 (100.0±7.2%) (Figure 7B, $P<0.05$ of each variant versus wild-type). No significant differences in enzymatic activity were detected in the R8W (103.8±10.0%), P17L (113.3±7.0%), and V481I (121.3±10.2%) variants compared to wild-type (Figure 7B). Similar results were obtained in each of the three independent experiments. Moreover, weight-adjusting the calculated oxygen consumption rates according to the mean 0.9-1.1-fold differences in COX-1 immunoreactivity observed across each normalized preparation did not significantly alter these results (data not shown).

Inhibition of COX-1 Enzymatic Activity. The sensitivity of the wild-type and R8W, P17L, G230S, and L237M variants to inhibition by indomethacin, a nonselective COX inhibitor

with greater potency for COX-1 than COX-2 in recombinant systems, was evaluated. The R8W and P17L variants were selected since they are the most frequent nonsynonymous polymorphisms. The G230S and L237M variants were selected based on the basal metabolic activity and modeling results reported above. The effects of increasing indomethacin concentrations on metabolic activity for each preparation relative to vehicle-incubated controls are presented (Figures 8A-D). From these data, IC_{50} values for each preparation were estimated (Table 3). The P17L and G230S variants demonstrated significantly lower IC_{50} values compared to wild-type, suggesting presence of these mutations significantly increase COX-1 sensitivity to inhibition by indomethacin. This increase in sensitivity is evident in Figures 8B and 8C, respectively. No significant differences in IC_{50} values were observed with the R8W and L237M variants compared to wild-type. The R8W variant appeared more resistant to inhibition at lower indomethacin concentrations relative to wild-type (Figure 8A); however, this effect was lost at higher indomethacin concentrations and the estimated IC_{50} value was not statistically different from wild-type. The L237M variants appeared more sensitive to inhibition at higher indomethacin concentrations relative to wild-type (Figure 8D); however, the estimated IC_{50} value was not statistically different from wild-type.

In order to take into account basal COX-1 activity, the rate of oxygen consumption in each preparation was compared after treatment with 25 μM indomethacin relative to wild-type after treatment with vehicle control (Figure 8E). The P17L (13.8±1.7%), G230S (4.1±1.3%), and L237M (6.9±2.6%) variants each demonstrated significantly lower metabolic activity compared to wild-type (36.7±0.5%) (P<0.05 of each variant versus wild-type). Significant differences were not observed with the R8W variant (29.4±4.1%) compared to wild-type.

These findings suggest that combination of indomethacin treatment and the P17L, G230S and L237M variants significantly reduce COX-1 metabolic activity compared to indomethacin treatment of wild-type COX-1.

Discussion

COX-1 and COX-2 derived PGs play a vital role in the regulation of various biological processes in humans, such that nonselective and selective NSAIDs are routinely administered for the prevention and/or treatment of a variety of clinical conditions (19, 23, 24, 73). Genetic variation in *PTGS1* and *PTGS2* may significantly modify disease risk in humans and/or contribute to inter-individual variability in the pharmacodynamic response to NSAIDs. Although the functional relevance of genetic variants in *PTGS2* has been evaluated (58, 59), functional characterization of human *PTGS1* variants has not been as widely investigated. In order to guide the design and interpretation of future genetic epidemiology and pharmacogenomic studies, the primary aim of this investigation was to identify or confirm the existence of genetic polymorphisms in *PTGS1*, characterize the LD structure, and evaluate the functional consequences of selected variants *in vitro*.

Multiple variants were identified in both coding and noncoding regions of human *PTGS1* by resequencing 92 healthy individuals. Twenty-four of the 45 variants had been previously reported in the published literature (61, 62, 74, 75) and/or publicly available databases (http://www.ncbi.nlm.nih.gov/snp), and were present at comparable frequencies within each ethnic group. Interestingly, seven of the 45 variants were nonsynonymous changes (R8W, R8P, P17L, R78W, K185T, L237M, and V481I), most of which were present at low (≤6%) frequencies in distinct ethnic groups. The previously reported R53H and G230S variants

(61) were not identified in the egSNP population, but their existence was confirmed at low frequencies in an independent African-American population (Chapter III). Multiple polymorphisms in the *PTGS1* 5'UTR were also identified, including seven (*T-1749C*, *G-1598A*, *A-1202G*, *A-1201G*, *G-1006A*, *A-918G* and *A-707G*) on the same haplotype in the European/Caucasian and African samples. Moreover, these 5'UTR polymorphisms were also in near complete LD with the P17L variant in European/Caucasian, but not African individuals. The presence of LD between the *A-707G* and P17L polymorphisms in Caucasians has been previously reported (62, 74, 76, 92); however, the current analysis is the first to suggest that this LD pattern involves six additional polymorphisms further upstream in the 5'UTR. A recent human investigation demonstrated that presence of this variant haplotype was not associated with *PTGS1* RNA expression in oral mucosa (92). Preliminary sequence analysis in the current investigation suggests that certain 5'UTR variant alleles may disrupt putative transcription factor binding sites. Further functional characterization of these promoter polymorphisms via transcriptional activation and DNA binding studies appears necessary.

Recombinant wild-type COX-1 and the R8W, P17L, R53H, R78W, K185T, G230S, L237M, and V481I mutant proteins were expressed and basal COX-1 metabolic activity was evaluated *in vitro*. As summarized in Table 4, the R53H, R78W, K185T, G230S, and L237M variants demonstrated significantly lower metabolic activity (35-60%) relative to wild-type COX-1; although, none completely abolished activity, most likely since these variants did not occur at or in immediate proximity to residues critical for substrate binding and/or enzyme activity such as arginine 120 or tyrosine 385 (93-96). Protein modeling suggests the G230S variant may significantly alter COX-1 protein structure. These structural

observations, in conjunction with the observed functional effects, suggest that the G230S variant disrupts the active conformation of COX-1 by shifting the dimer interface via D228 and W138'. This conformational change could also influence catalysis more directly through an interaction between D228 and R332. R332 is a member of helix 6 (84), which also includes residues contributing to formation of the active site. A shift in this helix could serve as the mechanism underlying the observed effect on catalytic function.

Similar reductions in enzyme activity were also observed with the R53H, R78W, K185T, and L237M variants; although, their predicted impact on COX-1 structure were not as obvious. The L237 residue is conserved across all known COX-1 and COX-2 species, and the L237M variant presumably could influence catalytic activity through its predicted impact on dimerization; however, the association between alterations in COX dimerization and metabolic activity has not been well characterized. The mechanism underlying the alterations in activity observed with the R53H, R78W, and K185T variants does not appear to be explained by the protein modeling results. However, recent COX-1 structure-function studies suggest that several amino acid substitutions with modest influence on arachidonic acid binding to the COX-1 active site can alter the catalytic efficiency and metabolite profile of COX-1-mediated arachidonic acid metabolism (96, 97). Perhaps these variants could reduce overall metabolic efficiency by altering the interaction between arachidonic acid and the active site. Future studies evaluating the mechanism underlying these functional effects appear necessary. No significant changes in enzymatic activity were detected with the R8W, P17L, and V481I variants relative to wild-type. The R8W and P17L variants occur at amino acids lying within the COX-1 signal peptide sequence, which is post-translationally cleaved (84, 95), and would be unlikely to significantly impact enzymatic activity. Protein modeling

suggests the V481I variant is also unlikely to significantly alter COX-1 structure or activity. Additional low frequency nonsynonymous variants in *PTGS1* have also been recently discovered (L15-L16del, R108Q, I136V, K341R, R458Q) (61, 75, 78, 98); however, their potential influence on COX-1 metabolic activity has not been investigated. Moreover, the *in vivo* functional consequences of the R53H, R78W, K185T, G230S, L237M and 5'UTR variants remain to be evaluated via quantification of systemic (plasma, urine) and local (tissue-, cell-specific) PG concentrations, particularly since the relative contribution of COX-2 to PG biosynthesis may also be altered in individuals with certain *PTGS1* polymorphisms. *In vitro* and *in vivo* functional studies will substantially aid in the interpretation of genetic epidemiological studies evaluating associations between *PTGS1* polymorphisms and risk of diseases known to involve altered COX-derived PG synthesis, such as cardio- and cerebrovascular disease, colorectal cancer, and asthma (23, 73).

Inhibition studies with indomethacin demonstrated the P17L and G230S variants were significantly more sensitive to indomethacin-mediated inhibition of COX-1 activity relative to wild-type, as determined by estimation of IC_{50} values for each preparation. Since the P17L variant resides within the COX-1 signal peptide sequence, the mechanism underlying the observed alteration in indomethacin sensitivity is unclear. The estimated IC_{50} values for the R8W and L237M variants were not significantly different from wild-type; however, COX-1 metabolic activity was significantly lower with the L237M variant relative to wild-type after inhibition with indomethacin since the L237M variant also had significantly lower basal activity. The estimated indomethacin IC_{50} value for the wild-type preparation in the current study (8.37 μM) was higher than those previously reported with purified COX-1

preparations (approximately 1 μM) (89, 90). This is likely due to utilization of crude microsomal protein preparations.

Interestingly, a recent human study demonstrated that platelets isolated from Caucasian individuals heterozygous for the P17L variant allele were significantly more sensitive to aspirin-mediated inhibition of $PGF_{2\alpha}$ production compared to wild-type individuals (62). The *in vitro* data with the P17L variant and indomethacin from the current study are consistent with these findings (Table 4), even though aspirin and indomethacin inhibit COX-1 activity via different mechanisms, suggesting individuals carrying this variant may be significantly more sensitive to NSAID-mediated inhibition of COX-1 activity and potentially more susceptible to adverse events such as gastrointestinal bleeding, renal dysfunction, and/or cardiovascular events (73). Similar associations may also exist with the G230S and L237M variants; although, the population impact of the P17L polymorphism may be more substantial since it is significantly more frequent in both European/Caucasian and African populations. In contrast, human studies have also suggested that the P17L variant may be associated with resistance to aspirin-mediated inhibition of platelet aggregation (76) and aspirin-mediated reduction in risk of colorectal polyps (78). Importantly, these investigations were also conducted in Caucasian populations, such that presence of the aforementioned *PTGS1* 5'UTR variant alleles, and not the P17L variant allele, may be driving these observed interactions with aspirin therapy. Presence of the P17L variant has also been associated with rofecoxib and celecoxib-mediated inhibition of thromboxane formation *in vivo* (77). The population evaluated in this investigation consisted of Caucasian, African-American and Asian individuals. Since the ethnicities of those carrying the P17L variant allele were not reported, the potential contribution of *PTGS1* 5'UTR polymorphisms could not be

ascertained. Collectively, the mechanisms underlying these conflicting *in vitro* and *in vivo* observations remain to be characterized; however, the relative contribution of the P17L and 5'UTR polymorphisms may be an important determinant of NSAID pharmacodynamics in humans. Additional human pharmacogenomic studies evaluating potential associations between *PTGS1* polymorphisms and NSAID pharmacodynamics in both Caucasians and African-Americans, including risk of adverse events, appear warranted.

Certain limitations exist in the current analysis. First, utilization of a non-mammalian expression system could significantly impact the expression and function of a recombinant protein, particularly glycosylated proteins such as COX-1. However, recombinant COX-1 has been expressed in insect cell systems previously, and has exhibited similar post-translational processing, glycosylation and activity profiles compared to native COX-1 (89, 90). Second, the limitations related to evaluation of metabolic activity at a single substrate concentration are recognized. The observed differences in the rate of oxygen consumption in certain mutant preparations compared to wild-type may be a reflection of reduced metabolic capacity (decreased V_{max}) and/or reduced substrate binding (increased K_m). Evaluation of metabolic activity across a range of substrate concentrations will ultimately be necessary to more completely characterize the enzyme kinetics of each mutant relative to wild-type. However, quantification of oxygen consumption after addition of 100 μM of arachidonic acid has been previously utilized to evaluate COX-1 metabolic activity in recombinant systems (89, 90). Moreover, similar conditions have been employed for IC_{50} determinations of multiple COX inhibitors, including indomethacin (89, 90). Since indomethacin is not utilized clinically as widely as aspirin, or for the same indication, the clinical applicability of the completed inhibition studies may not extend to all NSAIDs. However, indomethacin has

demonstrated greater potency for inhibition of COX-1 than COX-2 and has been widely studied in this recombinant *in vitro* system under these experimental conditions (89, 90). Consequently, indomethacin was a more appropriate inhibitor for the initial characterization of selected COX-1 variants.

In summary, the R53H, R78W, K185T, G230S, and L237M variants in *PTGS1* demonstrated significantly lower basal metabolic activity *in vitro* relative to wild-type COX-1, suggesting individuals carrying these variant alleles may have significantly altered PG biosynthesis *in vivo*. In addition, the P17L and G230S variants were significantly more sensitive to indomethacin-mediated inhibition of COX-1 activity relative to wild-type, suggesting individuals carrying these variant alleles may be more susceptible to NSAID-associated adverse events. Future studies confirming the *in vivo* relevance of these variants, including their influence on disease susceptibility and NSAID pharmacodynamics, are warranted.

Table 1. Primers used for the site-directed mutagenesis of human COX-1.

Mutation	Sequences of Forward (F) and Reverse (R) Primers*
Arg8Trp (R8W)	(F) 5'–CCATGAGCCGGAGTCTCTTGCTC**T**GGTTCTTGCTGTTCCTGCTCC–3'
	(R) 5'–GGAGCAGGAACAGCAAGAACC**A**GAGCAAGAGACTCCGGCTCATGG–3'
Pro17Leu (P17L)	(F) 5'–GCTGTTCCTGCTCCTGCTCC**T**GCCGCTCCCCGTCCTGCTCG–3'
	(R) 5'–CGAGCAGGACGGGGAGCGGC**A**GGAGCAGGAGCAGGAACAGC–3'
Arg53His (R53H)	(F) 5'–CCGCTTCGGCCTTGACC**A**CTACCAGTGTGACTGC–3'
	(R) 5'–GCAGTCACACTGGTAG**T**GGTCAAGGCCGAAGCGG–3'
Arg78Trp (R78W)	(F) 5'–GCCTGTGGACCTGGCTC**T**GGAATTCACTGCGGCCC–3'
	(R) 5'–GGGCCGCAGTGAATTCC**A**GAGCCAGGTCCACAGGC–3'
Lys185Thr (K185T)	(F) 5'–GCTTCCTGCTCAGGAGGA**C**GTTCATACCTGACCCCC–3'
	(R) 5'–GGGGGTCAGGTATGAAC**G**TCCTCCTGAGCAGGAAGC–3'
Gly230Ser (G230S)	(F) 5'–GGGCCATGGGGTAGACCTC**A**GCCACATTTATGGAGAC–3'
	(R) 5'–GTCTCCATAAATGTGGC**T**GAGGTCTACCCCATGGCCC–3'
Leu237Met (L237M)	(F) 5'–CGGCCACATTTATGGAGACAAT**A**TGGAGCGTCAGTATCAACTGCGGC–3'
	(R) 5'–GCCGCAGTTGATACTGACGCTCCA**T**ATTGTCTCCATAAATGTGGCCG–3'
Val481Ile (V481I)	(F) 5'–CCTCCTTCCAGGAGCTC**A**TAGGAGAGAAGGAGATGGC–3'
	(R) 5'–GCCATCTCCTTCTCTCCTA**T**GAGCTCCTGGAAGGAGG–3'

*Primers were PAGE-purified (Invitrogen). Bold/underlined bases indicate the mutated nucleotides. The R8P mutant was not expressed.

Table 2. *PTGS1* variants identified from the NIEHS egSNP sequencing project.*

Polymorphism	Nucleotide[†]	Location	Amino Acid	Estimated Minor Allele Frequency[‡]			
				Caucasian (n=24)	African (n=24)	Asian (n=24)	All (n=72 or 92[§])
(1) C>G	-1862	5'UTR	-	0	0.02	0	0.01[§]
(2) T>C[‖]	-1749	5'UTR	-	0.06	0.04	0	0.07[§]
(3) T>G	-1702	5'UTR	-	0	0	0.02	0.01[§]
(4) G>A[‖]	-1598	5'UTR	-	0.06	0.04	0	0.07[§]
(5) T>C	-1541	5'UTR	-	0.19	0.33	0.46	0.39[§]
(6) A>G[‖]	-1202	5'UTR	-	0.06	0.04	0.02	0.07[§]
(7) A>G[‖]	-1201	5'UTR	-	0.06	0.04	0.02	0.07[§]
(8) C>G	-1160	5'UTR	-	0.02	0.04	0	0.02[§]
(9) G>A[‖]	-1006	5'UTR	-	0.08	0.04	0	0.08[§]
(10) G>A	-951	5'UTR	-	0	0.02	0	0.01
(11) A>G[‖]	-918	5'UTR	-	0.08	0.04	0	0.04
(12) Insertion AA	-748	5'UTR	-	0	0.08	0	0.03
(13) A>G[‖]	-707	5'UTR	-	0.08	0.04	0	0.04
(14) T>C	-640	5'UTR	-	0	0.02	0	0.01
(15) C>T	250	Exon 2	R8W	0.04	0	0.06	0.05[§]
(16) G>C	251	Exon 2	R8P	0	0.02	0	0.01[§]
(17) C>T[#]	278	Exon 2	P17L	0.06	0.06	0	0.06[§]
(18) G>C	6817	Intron 2	-	0.02	0	0	0.01
(19) C>T	6843	Intron 2	-	0	0.02	0	0.01

Table 2 (con't).

Polymorphism	Nucleotide[†]	Location	Amino Acid	Estimated Minor Allele Frequency[‡]			
				Caucasian (n=24)	African (n=24)	Asian (n=24)	All (n=72 or 92[§])
(20) G>A (rs3842788)	6975	Exon 3	Q41Q	0.02	0.23	0.02	0.09
(NI)*G>A (rs3842789)	7010	Exon 3	R53H	0	0	0	0
(21) C>T (rs10306139)	7056	Exon 3	C68C	0	0.02	0	0.01
(22) G>A (rs876567)	7095	Intron 3	-	0.04	0.02	0	0.02
(23) G>C (rs2282169)	7465	Intron 3	-	0.13	0.35	0.06	0.22[§]
(24) C>T	7501	Exon 4	R78W	0	0	0	0.01[§]
(25) C>G (rs10306148)	10153	Intron 5	-	0.08	0.42	0.04	0.24
(26) T>C	10203	Intron 5	-	0.02	0	0	0.01
(27) A>G	10354	Intron 5	-	0	0.02	0	0.01
(28) A>C (rs3842792)	10476	Exon 6	K185T	0	0.04	0	0.01
(29) C>A (rs5788)	10561	Exon 6	G213G	0.04	0.46	0.04	0.21
(30) G>A (rs3842794)	10651	Intron 6	-	0	0.02	0	0.01
(NI)*G>A	10721	Exon 7	G230S	0	0	0	0
(31) C>A (rs5789)	10742	Exon 7	L237M	0.04	0	0	0.01
(32) G>A	10805	Intron 7	-	0	0.02	0	0.01
(33) Deletion A (rs3215925)	10809	Intron 7	-	0.13	0.40	0.04	0.26
(34) C>G	12754	Intron 8	-	0.02	0	0	0.01[§]
(35) G>A	12867	Intron 8	-	0	0.06	0	0.02[§]
(36) G>A (rs10306153)	12880	Intron 8	-	0	0.31	0	0.09[§]

Table 2 (con't).

Polymorphism	Nucleotide[†]	Location	Amino Acid	Estimated Minor Allele Frequency[‡]			
				Caucasian (n=24)	African (n=24)	Asian (n=24)	All (n=72 or 92[§])
(37) T>C	12921	Intron 8	-	0	0.04	0	0.01[§]
(38) A>G	13020	Intron 8	-	0	0.02	0	0.02[§]
(39) T>C (rs4836885)	13138	Intron 8	-	0.04	0.41	0.02	0.23[§]
(40) G>A (rs10306230)	13148	Intron 8	-	0.02	0.02	0.02	0.02[§]
(41) G>A (rs5794)	19389	Exon 10	V481I	0.04	0	0	0.01[§]
(42) A>T	21195	Intron 10	-	0	0.04	0	0.01[§]
(43) T>C (rs3842801)	21205	Intron 10	-	0	0.17	0	0.07[§]
(44) G>A (rs3842802)	21286	Exon 11	A499A	0	0.06	0	0.02[§]
(45) T>C (rs3842803)	21301	Exon 11	P504P	0	0.23	0	0.08[§]

5'UTR = 5' untranslated region

*The R53H and G230S nonsynonymous variants were not identified (NI) in the egSNP population.

[†]Nucleotide position relative to the transcriptional start site (Genbank accession number AF440204).

[‡]Number of individuals.

[§]Indicates sequencing data that was obtained in an additional 20 anonymous individuals of unknown ethnicity (n=92 total).

[‖]These polymorphisms are in complete or near complete linkage disequilibrium with one another in both the African (D'=1.0, r^2=1.0) and Caucasian (D'=1.0, r^2=0.73-1.0) populations. See Figure 3.

[#]The P17L polymorphism is in complete or near complete linkage disequilibrium with the 5'UTR[e] polymorphisms in the Caucasian population only (D'=1.0, r^2=0.73-1.0). See Figure 3.

Table 3. Estimated IC_{50} values for indomethacin with wild-type COX-1 and the R8W, P17L, G230S, and L237M variants.

COX-1 Variant	Estimated IC_{50} (μM) (95% confidence interval)
Wild-type	8.37 (5.00–14.0)
R8W	15.3 (11.1–21.0)
P17L	2.80 (1.72–4.56)*
G230S	1.36 (0.54–3.42)*
L237M	3.55 (1.73–7.29)

**P*-value <0.05 versus wild-type.

Table 4. Functional relevance of nonsynonymous polymorphisms in *PTGS1*.*

***PTGS1* Variant**	**Amino Acid Conserved Across Species†**	**Modeling Predicted Functional Impact†**	***In Vitro* Metabolic Activity†**	***In Vitro* Sensitivity to Indomethacin†**	***Ex Vivo* Sensitivity to Aspirin‡**
R8W	No	No	↔	↔	↔
P17L	No	No	↔	↑	↑ or ↓
R53H	No	? / Yes (minor)	↓	?	?
R78W	Yes	? / No	↓	?	?
K185T	No	? / No	↓	?	?
G230S	Yes	Yes (major)	↓	↑	?
L237M	Yes	Yes (minor)	↓	↔ / ↑	?
V481I	No	No	↔	?	?

*Functional effects indicated as increased (↑), decreased (↓), unchanged (↔), or unknown (?) compared to wild-type.

†Based on the analyses and *in vitro* functional studies completed in the current investigation.

‡Based on the previously published studies by Halushka et al. (62) and Maree et al. (76) in humans. Conflicting results have been reported with the P17L variant, which was in complete linkage disequilibrium with the *A-707G* polymorphism in both populations.

Figure Legends

Figure 3. Pairwise estimates of LD between each *PTGS1* polymorphism are plotted for the (A) African, (B) European/Caucasian, and (C) Asian ethnic groups using Haploview 3.2. Each polymorphism is numbered according to its position in the *PTGS1* gene as presented in Table 2. Black squares indicate complete LD (r^2=1.0), white squares indicate zero LD (r^2=0.0), and increasing intensity of gray indicates increasing degrees of LD.

Figure 4. Alignment of the human (Genbank accession number P23219), mouse (AAH05573), rat (NP_058739), and sheep (P05979) COX-1 amino acid sequences using the ClustalW program. Amino acid locations of the eight evaluated nonsynonymous variants are highlighted.

Figure 5. Overview of the COX-1 dimer and the R53H, R78W, K185T, G230S, L237M, and V481I variants, with (A) a top view of the dimer complex, and (B) a side view of one monomer facing the dimerization surface. Mutations are illustrated with space-filling atoms. The heme group is shown in maroon, and arachidonic acid is shown in yellow. Sugars are shown in cyan, with two sugars per glycosylation site.

Figure 6. Structural characterization of the G230S variant. (A) The vicinity of G230 in the model of wild-type COX-1. The position of D228 is stabilized by a hydrogen-bond to the backbone nitrogen of G230. (B) The G230S substitution allows for only one rotamer position without significant structural changes. (C) The corresponding site in human COX-2 has an N231 in a similar position to the modeled S230 substitution; however, N231 also

provides several interactions that help stabilize the observed conformation. (D) In COX-1, S230 destabilizes the observed conformation, which could be avoided by a rotation of D228 towards R332, which also requires a shift in the dimer interaction with W138'.

Figure 7. (A) Representative immunoblot of solubilized microsomes containing recombinant wild-type and eight variant COX-1 proteins. The amount of solubilized microsomal protein loaded per lane for each preparation was normalized to COX-1 immunoreactivity based on previous immunoblots. The wild-type lane contains 34 μg of microsomal protein. Lane 1 contains COX-1 ovine protein standard (Cayman Chemical, 1 μg) as a positive control. Lane 11 contains solubilized microsomes made from uninfected Sf9 cells (34 μg) as a negative control. (B) Mean±SEM rate of oxygen consumption for each of the 8 variant COX-1 preparations relative to wild-type. Solubilized microsomal protein from uninfected Sf9 cells were used as a negative control. The data presented are pooled from three independent experiments, each completed in triplicate. The rate of oxygen consumption was significantly associated with the COX-1 microsomal preparation (ANOVA: $P<0.001$, $r^2=0.78$). *$P<0.05$ versus wild-type by a post-hoc Dunnett's test.

Figure 8. Inhibition of COX-1-mediated arachidonic acid metabolism by increasing concentrations of indomethacin in the (A) R8W, (B) P17L, (C) G230S, and (D) L237M variants compared to wild-type. Values represent the mean±SEM rate of oxygen consumption calculated at each indomethacin concentration (0.1, 1, 5, 10, and 25 μM) relative to the rate of oxygen consumption detected with vehicle control for each preparation. Each data point includes three independent measurements. (E) Mean±SEM rate of oxygen

consumption for the wild-type and R8W, P17L, G230S, and L237M variants after incubation with 25 μM indomethacin relative to the rate of oxygen consumption detected after incubation with vehicle control in the wild-type preparation. Each data point includes three independent measurements. The rate of oxygen consumption after incubation with 25 μM indomethacin was significantly associated with the COX-1 preparation (ANOVA: $P<0.001$, $r^2=0.93$). *$P<0.05$ versus wild-type by a post-hoc Dunnett's test.

Figure 3. *PTGS1* linkage disequilibrium plots.

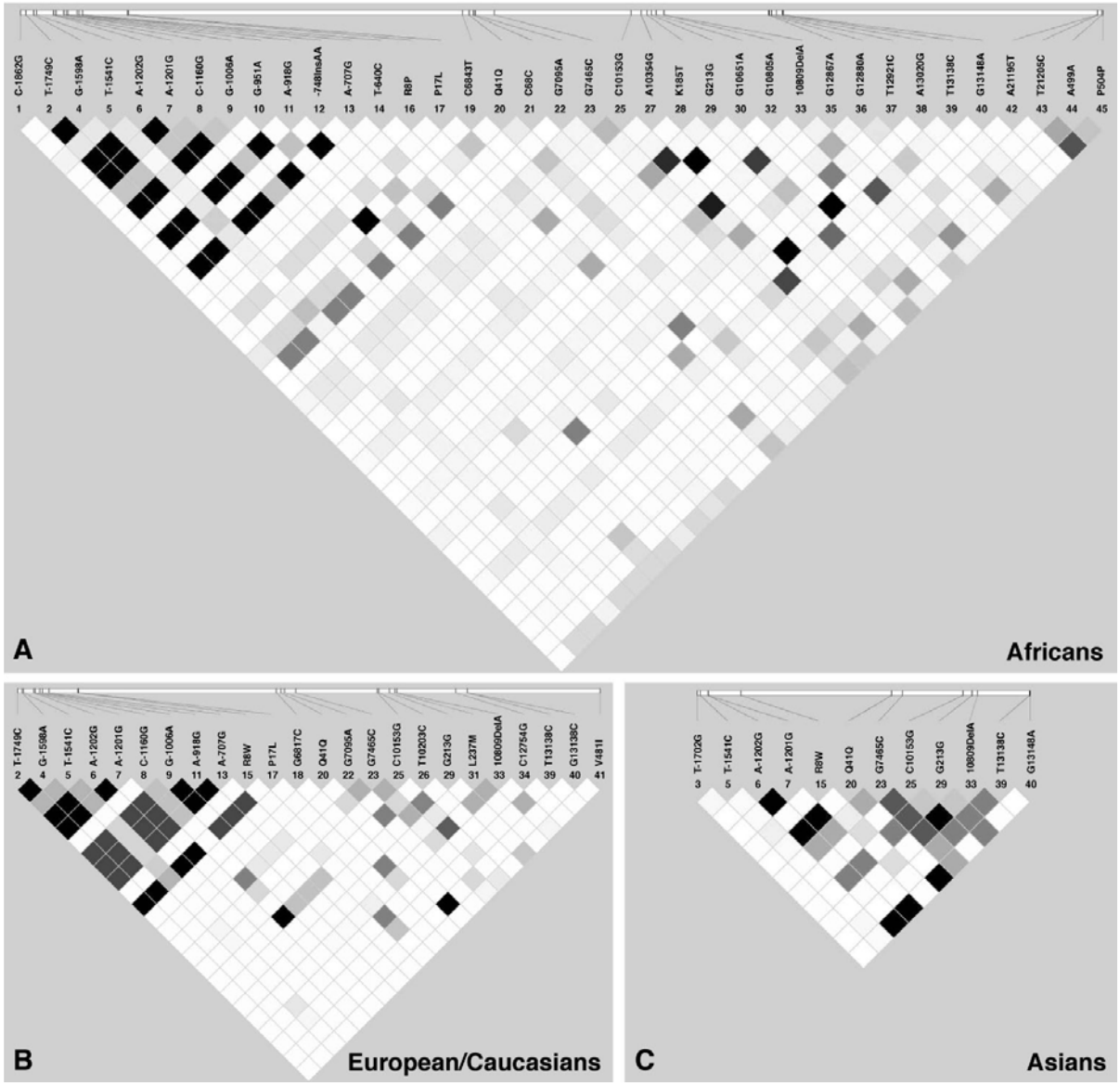

Figure 4. COX-1 amino acid sequence alignment.

```
                        R8W      P17L                                        R53H
PTGS1_human_WT      MSR-SLLLRFLLFLLLLPPL--PVLLADPGAPTPVNPCCYYPCQHQGICVRFGLDRYQCD 57
PTGS1_mouse         MSRRSLSLWFPLLLLLLLPPTPSVLLADPGVPSPVNPCCYYPCQNQGVCVRFGLDNYQCD 60
PTGS1_rat           MSRRSLSLQFPLLLLLLLLPPPPVLLTDAGVPSPVIPCCYYPCQNQGVCVRFGLDHYQCD 60
PTGS1_sheep         MSRQSISLRFPLLLLLLSPS--PVFSADPGAPAPVNPCCYYPCQHQGICVRFGLDRYQCD 58

                                 R78W
PTGS1_human_WT      CTRTGYSGPNCTIPGLWTWLRNSLRPSPSFTHFLLTHGRWFWEFVNATFIREMLMRLVLT 117
PTGS1_mouse         CTRTGYSGPNCTIPEIWTWLRNSLRPSPSFTHFLLTHGYWLWEFVNATFIREVLMRLVLT 120
PTGS1_rat           CTRTGYSGPNCTIPEIWTWLRSSLRPSPSFTHFLLTHGYWIWEFVNATFIREVLMGWVLT 120
PTGS1_sheep         CTRTGYSGPNCTIPEIWTWLRTTLRPSPSFIHFMLTHGRWLWDFVNATFIRDTLMRLVLT 118

PTGS1_human_WT      VRSNLIPSPPTYNSAHDYISWESFSNVSYYTRILPSVPKDCPTPMGTKGKKQLPDAQLLA 177
PTGS1_mouse         VRSNLIPSPPTYNSAHDYISWESFSNVSYYTRILPSVPKDCPTPMGTKGKKQLPDVQLLA 180
PTGS1_rat           VRSNLIPSPPTYNTAHDYISWESFSNVSYYTRILPSVPKDCPTPMGTKGKKQLPDIHLLA 180
PTGS1_sheep         VRSNLIPSPPTYNIAHDYISWESFSNVSYYTRILPSVPRDCPTPMGTKGKKQLPDAEFLS 178

                         K185T                                          G230S  L237M
PTGS1_human_WT      RRFLLRRKFIPDPQGTNLMFAFFAQHFTHQFFKTSGKMGPGFTKALGHGVDLGHIYGDNL 237
PTGS1_mouse         QQLLLRREFIPAPQGTNILFAFFAQHFTHQFFKTSGKMGPGFTKALGHGVDLGHIYGDNL 240
PTGS1_rat           QRLLLRREFIPAPQGTNVLFAFFAQHFTHQFFKTSGKMGPGFTKALGHGVDLGHIYGDSL 240
PTGS1_sheep         RRFLLRRKFIPDPQGTNLMFAFFAQHFTHQFFKTSGKMGPGFTKALGHGVDLGHIYGDNL 238

PTGS1_human_WT      ERQYQLRLFKDGKLKYQVLDGEMYPPSVEEAPVLMHYPRGIPPQSQMAVGQEVFGLLPGL 297
PTGS1_mouse         ERQYHLRLFKDGKLKYQVLDGEVYPPSVEQASVLMRYPPGVPPERQMAVGQEVFGLLPGL 300
PTGS1_rat           ERQYHLRLFKDGKLKYQVLDGELYPPSVEQASVKMRYPPGVPPEKQMAVAQEVFGLLPGL 300
PTGS1_sheep         ERQYQLRLFKDGKLKYQMLNGEVYPPSVEEAPVLMHYPRGIPPQSQMAVGQEVFGLLPGL 298

PTGS1_human_WT      MLYATLWLREHNRVCDLLKAEHPTWGDEQLFQTTRLILIGETIKIVIEEYVQQLSGYFLQ 357
PTGS1_mouse         MLFSTIWLREHNRVCDLLKEEHPTWDDEQLFQTTRLILIGETIKIVIEEYVQHLSGYFLQ 360
PTGS1_rat           MLFSTIWLREHNRVCDLLKEEHPTWDDEQLFQTTRLILRGETIEIIIEEYVQHLSGYFLQ 360
PTGS1_sheep         MLYATIWLREHNRVCDLLKAEHPTWGDEQLFQTARLILIGETIKIVIEEYVQQLSGYFLQ 358

PTGS1_human_WT      LKFDPELLFGVQFQYRNRIAMEFNHLYHWHPLMPDSFKVGSQEYSYEQFLFNTSMLVDYG 417
PTGS1_mouse         LKFDPELLFRAQFQYRNRIAMEFNHLYHWHPLMPNSFQVGSQEYSYEQFLFNTSMLVDYG 420
PTGS1_rat           LKFDPELLFRAQFQYRNRIAMEFNHLYHWHPFMPDSFQVGSQEYSYEQFLFNTSMLVDYG 420
PTGS1_sheep         LKFDPELLFGAQFQYRNRIAMEFNQLYHWHPLMPDSFRVGPQDYSYEQFLFNTSMLVDYG 418

PTGS1_human_WT      VEALVDAFSRQIAGRIGGGRNMDHHILHVAVDVIRESREMRLQPFNEYRKRFGMKPYTSF 477
PTGS1_mouse         VEALVDAFSRQRAGRIGGGRNFDYHVLHVAVDVIKESREMRLQPFNEYRKRFGLKPYTSF 480
PTGS1_rat           VEALVDAFSRQRAGRIGGGRNFDYHVLHVAEDVIKESREMRLQSFNEYRKRFGLKPYTSF 480
PTGS1_sheep         VEALVDAFSRQPAGRIGGGRNIDHHILHVAVDVIKESRVLRLQPFNEYRKRFGMKPYTSF 478

                    V481I
PTGS1_human_WT      QELVGEKEMAAELEELYGDIDALEFYPGLLLEKCHPNSIFGESMIEIGAPFSLKGLLGNP 537
PTGS1_mouse         QELTGEKEMAAELEELYGDIDALEFYPGLLLEKCQPNSIFGESMIEMGAPFSLKGLLGNP 540
PTGS1_rat           QEFTGEKEMAAELEELYGDIDALEFYPGLMLEKCQPNSLFGESMIEMGAPFSLKGLLGNP 540
PTGS1_sheep         QELTGEKEMAAELEELYGDIDALEFYPGLLLEKCHPNSIFGESMIEMGAPFSLKGLLGNP 538

PTGS1_human_WT      ICSPEYWKPSTFGGEVGFNIVKTATLKKLVCLNTKTCPYVSFRVPDASQDDGPAVERPSTEL 599
PTGS1_mouse         ICSPEYWKPSTFGGDVGFNLVNTASLKKLVCLNTKTCPYVSFRVPDYPGDDGSVLVRRSTEL 602
PTGS1_rat           ICSPEYWKPSTFGGDVGFNIVNTASLKKLVCLNTKTCPYVSFRVPDYPGDDGSVFVRPSTEL 602
PTGS1_sheep         ICSPEYWKASTFGGEVGFNLVKTATLKKLVCLNTKTCPYVSFHVPDPRQEDRPGVERPPTEL 600
```

Figure 5. COX-1 protein model.

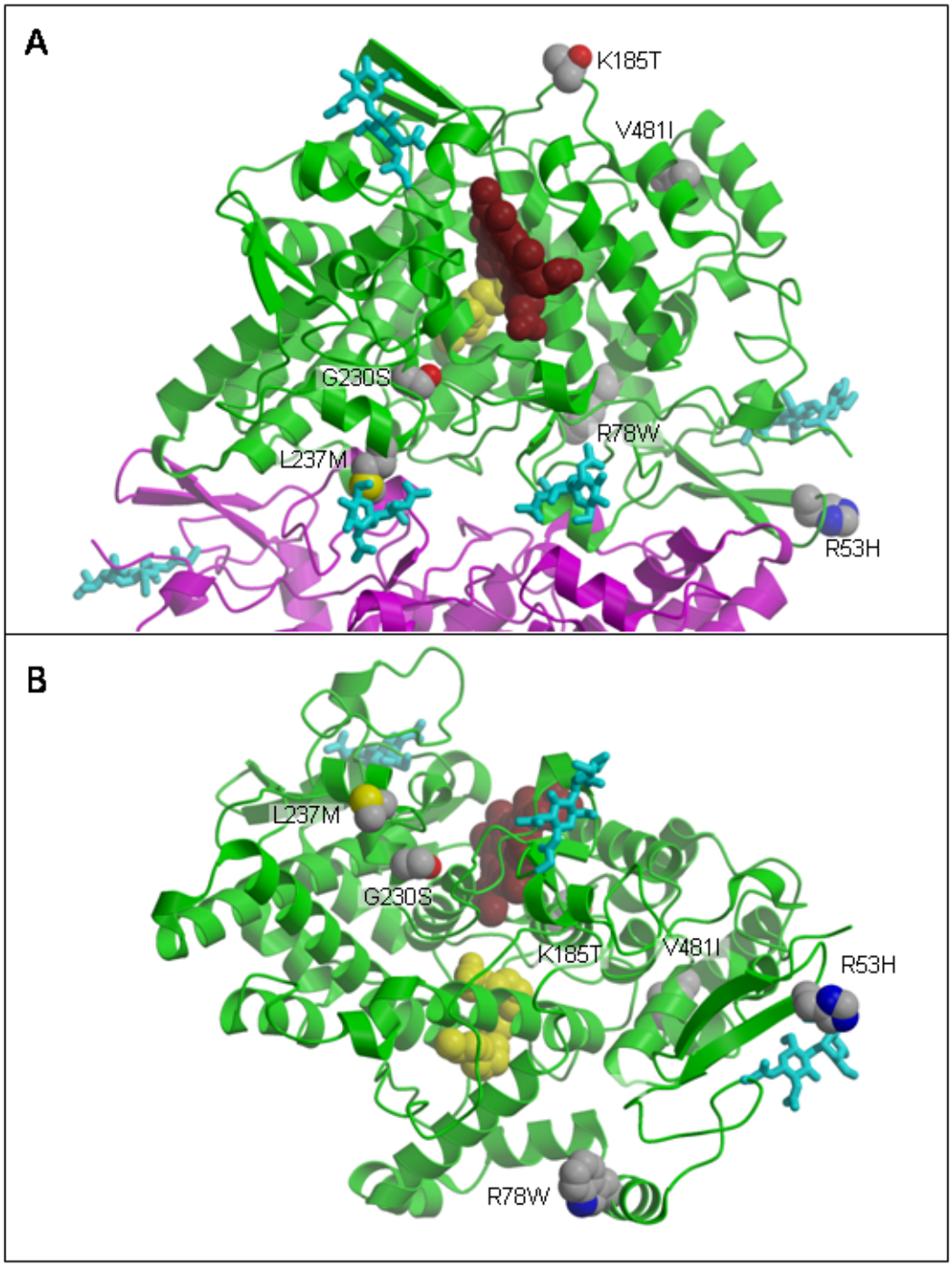

Figure 6. Structural characterization of the G230S variant.

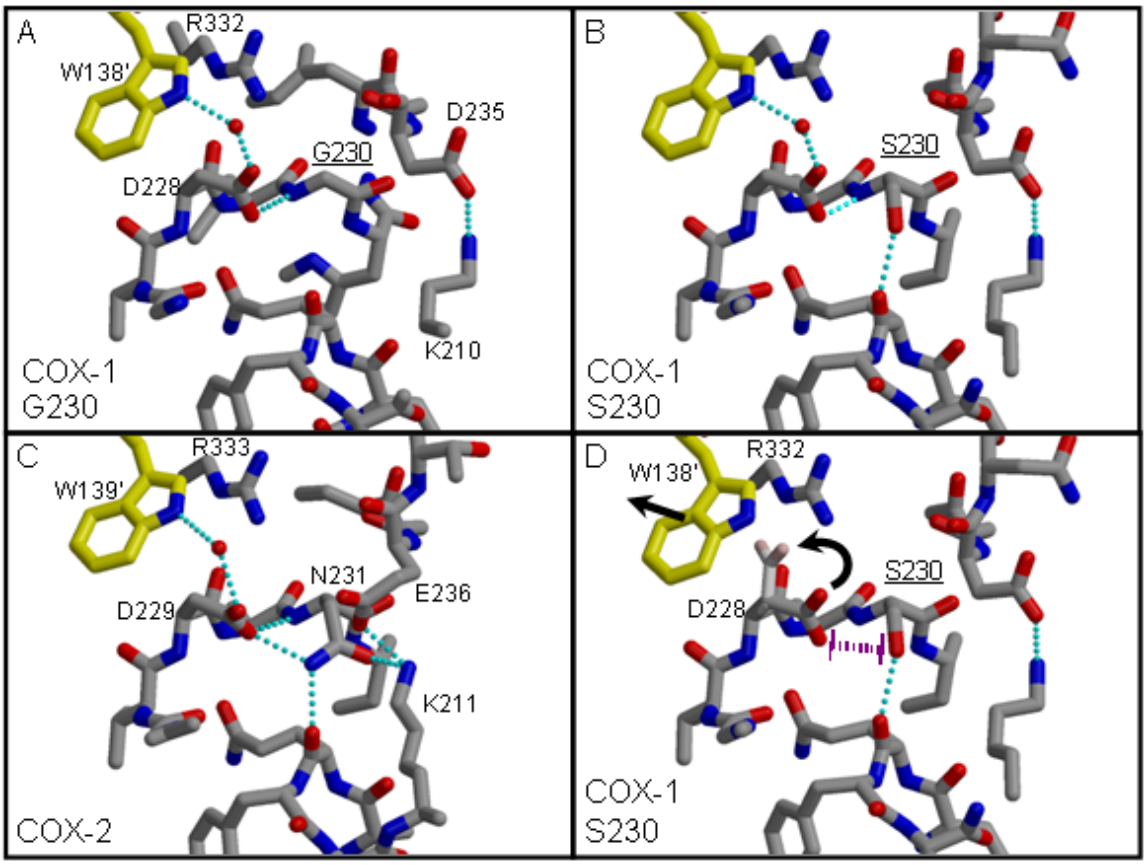

Figure 7. Expression and functional characterization of COX-1 polymorphisms.

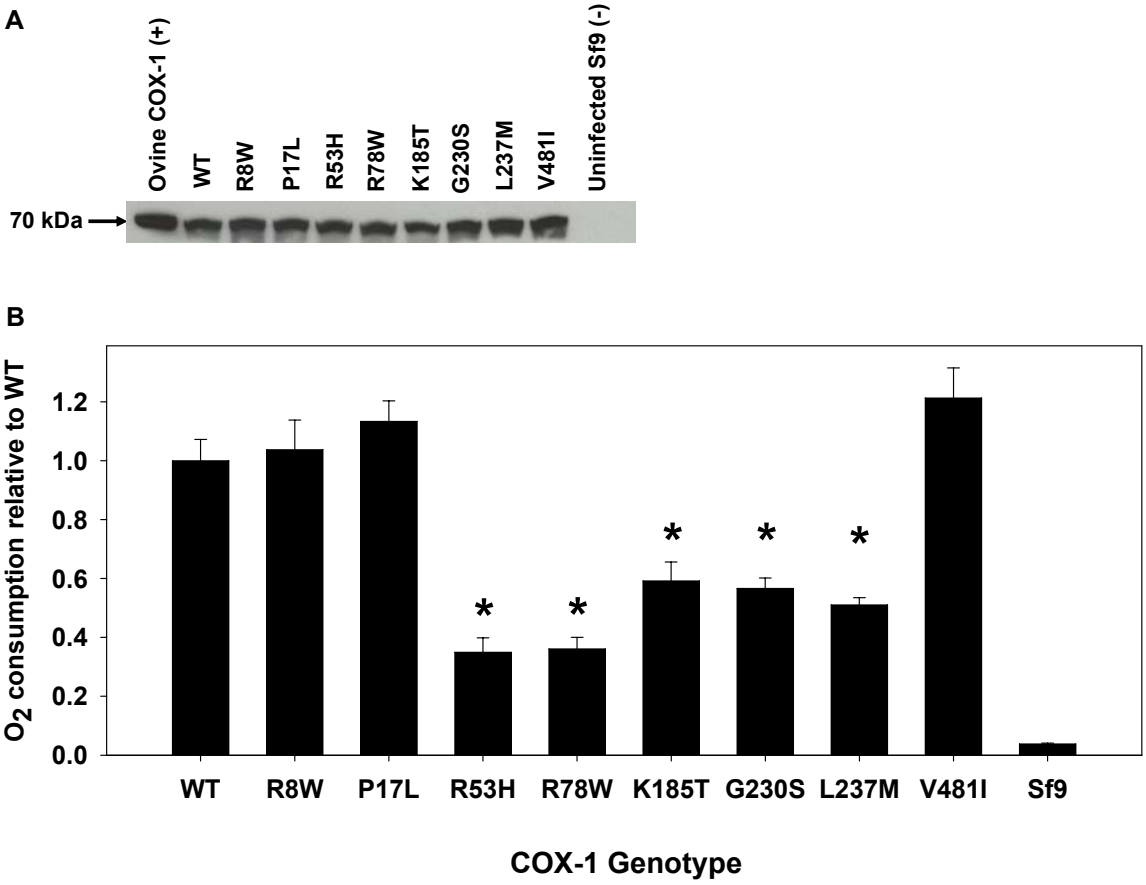

Figure 8. COX-1 polymorphisms and indomethacin inhibition.

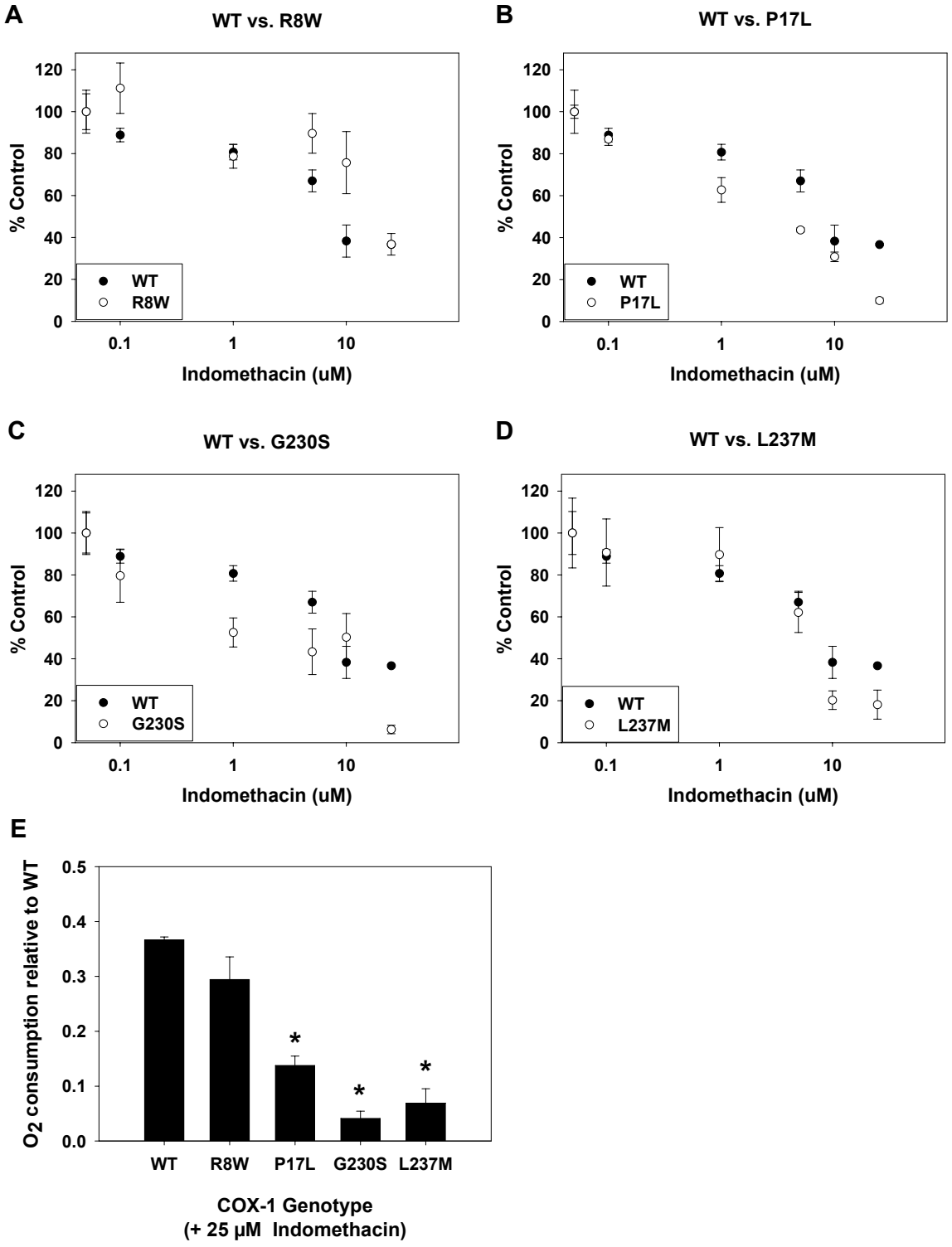

CHAPTER III

CYCLOOXYGENASE POLYMORPHISMS AND RISK OF CARDIOVASCULAR EVENTS: THE ATHEROSCLEROSIS RISK IN COMMUNITIES (ARIC) STUDY

Introduction

Ischemic cardiovascular disease is a major public health problem. It is estimated that 1.2 million Americans will experience an acute coronary heart disease (CHD) event and 0.7 million will experience an acute stroke event this year (1). Cyclooxygenase (COX)-1 and COX-2 derived prostaglandins are critical regulators of vascular, myocardial and platelet function, and alterations in their expression and/or activity can significantly modify risk of cardiovascular disease events in humans (22-25, 99, 100). Although both COX-1 and COX-2 catalyze the same metabolic reaction with similar efficiencies, they are encoded by distinct gene products and differ substantially in their regulation and expression (19). Recent evidence demonstrating associations between selective COX-2 inhibitor utilization and elevated risk of myocardial infarction (23, 24), coupled with the well-known protective effects of low-dose aspirin (25), suggests the relative contribution of COX-1 and COX-2-mediated prostaglandin synthesis is an integral mediator of cardiovascular homeostasis. Consequently, genetic variation in both COX-1 (*PTGS1*) and COX-2 (*PTGS2*) may be important modifiers of cardiovascular disease risk.

Numerous genetic polymorphisms in coding and noncoding regions of *PTGS1* and *PTGS2* have been identified (58, 59, 61, 62). For instance, the *G-765C* polymorphism in the

proximal promoter of *PTGS2* disrupts a Sp1 binding site and is associated with significantly lower *PTGS2* transcription (59). Moreover, due to its anti-inflammatory effects, the variant -*765C* allele was associated with significantly lower risk of prevalent myocardial infarction or ischemic stroke events in a high-risk Italian population (60). However, associations between *PTGS2* polymorphisms and incident events have not been investigated. Certain nonsynonymous polymorphisms in *PTGS1*, such as the *G230S* variant, have significantly lower COX-1 metabolic activity *in vitro* (101) (Chapter II); however, potential associations between *PTGS1* polymorphisms and cardiovascular disease risk have not been evaluated to date. The primary aim of this investigation was to determine if genetic variation in *PTGS1* and *PTGS2* was associated with risk of incident CHD or ischemic stroke events in individuals enrolled in the biethnic Atherosclerosis Risk in Communities (ARIC) study. An important secondary aim was to determine if this risk was modified by aspirin utilization.

Methods

Study Population. Participants were selected from the ARIC study, a longitudinal, population-based cohort study of 15,792 men and women aged 45 to 64 years from four U.S. communities (Forsyth County, NC; Jackson, MS; Minneapolis, MN; and Washington County, MD) enrolled between 1987 and 1989 (102). Since enrollment, participants have been followed prospectively via annual phone interviews, clinic examinations approximately every three years through 1998, and ongoing abstraction of hospital and death certificate records. The study protocol was approved by the Institutional Review Board of each center, and consent was obtained from each participant.

Ascertainment of Incident CHD and Stroke Cases. All incident cases that occurred between baseline and December 31, 1998 were evaluated (median follow-up 9.1 years), excluding participants with a history of a physician-diagnosed CHD or stroke event at baseline (n=1434), whose self-reported race was neither Caucasian nor African-American (n=48), and African-Americans enrolled in the Minneapolis, MN and Washington County, MD study centers (n=55). Incident CHD (n=1085) was defined as 1) definite or probable myocardial infarction (n=520), 2) electrocardiographic evidence of silent myocardial infarction (n=112), 3) definite CHD death (n=110), or 4) coronary revascularization procedure (n=343). Incident stroke was defined as a definite or probable ischemic stroke (n=300). Of note, n=68 individuals experienced an incident CHD and ischemic stroke event on separate occasions.

The ascertainment of cases and criteria for classification have been previously described (103, 104). All potential events were systematically reviewed and adjudicated by the ARIC Morbidity and Mortality Classification Committee (102-104). Hospitalized myocardial infarction was classified as definite or probable based on chest pain symptoms, cardiac enzyme levels, and electrocardiographic changes. Definite CHD death was classified based on chest pain symptoms, underlying cause of death, hospitalization records, and medical history. Coronary revascularization procedures included coronary artery bypass grafting and percutaneous coronary intervention. Using the National Survey of Stroke criteria (105), a stroke event was classified as definite or probable if there was 1) rapid onset of neurological symptoms that lasted >24 hours or led to death within 24 hours, 2) no evidence of pathology that could have mimicked stroke, and 3) one major (e.g., aphasia or hemiparesis) or two minor (e.g., diplopia or dysarthria) neurological deficits. Qualifying cases were further

classified as ischemic (thrombotic brain infarction, cardioembolic stroke) or hemorrhagic (subarachnoid hemorrhage, intracerebral hemorrhage) on the basis of neuroimaging studies and autopsy, when available (104).

Baseline Measurements. Detailed demographic, clinical, and biochemical data were obtained from each subject at baseline. Race was self-reported. Prevalent CHD and stroke were defined as history of a physician-diagnosed event. Hypertension was defined as systolic blood pressure ≥140 mmHg, diastolic blood pressure ≥90 mmHg, or current antihypertensive medication use. Diabetes was defined as fasting blood glucose ≥126 mg/dL, nonfasting blood glucose ≥200 mg/dL, physician diagnosis, or pharmacologic treatment. Detailed information on cigarette smoking was obtained through an interview-administered questionnaire. Aspirin utilization (yes/no), including aspirin-containing products, was assessed through a detailed medication history, as described (106). Dose and duration of use were not determined.

Cohort Random Sample. A random sample of all ARIC participants without history of CHD or stroke at baseline was assembled to serve as the reference group for the case-cohort comparisons (n=1065; 85 and 29 of which are also incident CHD and stroke cases, respectively). Sampling of the cohort was stratified on age (≥55 or <55 years), gender, and race (Caucasian or African-American). Sampling proportions varied across each stratum.

Genotyping. Genomic DNA from all incident CHD and ischemic stroke cases and the cohort random sample was genotyped for the *G-1006A*, *R8W*, *P17L*, *R53H*, *G230S* and

L237M polymorphisms in *PTGS1* and the *V511A* polymorphism in *PTGS2* using multiplex matrix-assisted laser desorption/ionization time-of-flight (MALDI-TOF) mass spectrometry methods (Sequenom Inc., San Diego, CA), as described (107) (Appendix II). Since MALDI-TOF methods were unsuccessful, the *G-765C* polymorphism in *PTGS2* was genotyped using the BeadArray system (Illumina, Inc., San Diego, CA), as described (108) (Appendix III). Blind replicates were included for quality control. Missing genotypes were present in <5% of individuals.

These polymorphisms were identified from a resequencing effort as part of the NIEHS Environmental Genome Single Nucleotide Polymorphism program (https://dir-apps.niehs.nih.gov/egsnp/home.htm) and/or the published literature (Table 5) (58, 59, 61, 62, 101) (Chapter II). The *G-1006A* polymorphism is one of seven polymorphisms in the 5' untranslated region (UTR) of *PTGS1* present in significant linkage disequilibrium (LD), and on the same haplotype, in both European/Caucasian and African individuals (101) (Chapter II). The *G-1006A* polymorphism was selected to capture variation at each of these loci since the functional relevance of each variant remains to be characterized. The other selected polymorphisms represent either functionally relevant variants (*PTGS1*: *R53H*, *G230S*, *L237M*; *PTGS2*: *G-765C*) or the most frequent nonsynonymous variants (*PTGS1*: *R8W*, *P17L*; *PTGS2*: *V511A*) identified to date in each gene (58, 59, 101) (Chapter II).

Data Analysis. Inverse sampling fractions from each stratum were used as weights in variance estimation of adjusted covariate means and proportions by linear and logistic regression, respectively. Cohort random sample allele frequencies were evaluated for deviation from Hardy-Weinberg equilibrium, and pairwise LD statistics were calculated

(Haploview 3.2) (81). Hazard rate ratios (HRR) and 95% confidence intervals (CI) for the development of incident CHD or ischemic stroke in relation to genotype were calculated by weighted proportional hazards regression, using Barlow's method to account for the stratified random sampling and case-cohort design (109). Model 1 included baseline age, gender, and study center as covariates. Model 2 also included significant clinical covariates, which were current smoking status, diabetes, hypertension, high density lipoprotein cholesterol, total cholesterol, and body mass index at baseline for the CHD endpoint, and current smoking status, diabetes, and hypertension for the stroke endpoint. Assuming an autosomal dominant mode of inheritance, individuals with one or two variant alleles were combined for comparison to wild-type individuals. All analyses were completed separately in Caucasians and African-Americans. Assuming a case-control design, type I error α=0.05 and 20% variant genotype frequency, there was approximately 99% and 94% power for the CHD endpoint and 94% and 83% power for the stroke endpoint to detect an odds ratio of 2.0 in Caucasians and African-Americans, respectively.

Interaction testing was completed on a multiplicative scale between baseline aspirin utilization (yes/no) and both *G-1006A* (*PTGS1*) and *G-765C* (*PTGS2*) genotype for both endpoints in Caucasians, using a Wald chi-square test for significance of the estimated β-coefficient for the interaction term (110). Gene-aspirin interaction testing was not completed in African-Americans due to low aspirin utilization and sample size limitations. Because interaction hypothesis testing on a multiplicative scale is underpowered, the critical value for statistical significance was set to α=0.15, two-sided (111). Stratified weighted proportional hazards regression was also completed to further explore potential interactions.

To minimize the impact of the multiple statistical tests conducted in this analysis, the false discovery rate (FDR) *q*-value was estimated for each comparison, separately for each endpoint, which is defined as the proportion of statistical tests deemed significant that are actually false-positives (QVALUE) (112). In order to calculate conservative *q*-value estimates, statistical tests from the unadjusted, model 1 and model 2 association analyses for each *PTGS1* and *PTGS2* polymorphism were considered, even though each model assessed the same independent variable. Additional *q*-value estimates were also calculated for the gene-aspirin interaction analysis. Only *q*-values for significant findings are presented.

Results

Study Population. Significant baseline differences in various risk factors were observed between CHD and stroke cases and non-cases included in the cohort random sample (Table 6). Incident CHD and stroke cases were significantly older and more likely to be male, smokers, diabetic, hypertensive and have abnormal fasting lipid panels compared to non-cases. Stroke cases were also more likely to be African-American and less likely to report aspirin use at baseline. Aspirin utilization at baseline was significantly lower in African-Americans compared to Caucasians in the cohort random sample (11.3% versus 29.9%, $P<0.001$), CHD cases (13.8% versus 30.2%, $P<0.001$) and ischemic stroke cases (13.3% versus 23.6%, $P=0.021$), respectively.

***PTGS1/PTGS2* Genotype.** The location and observed race-specific allele frequencies of the 6 *PTGS1* and 2 *PTGS2* polymorphisms evaluated are listed in Table 5. The *G-1006A* and *P17L* polymorphisms in *PTGS1* were in almost complete LD in Caucasians (D'=0.99,

r^2=0.96), but not African-Americans (D'=0.46, r^2=0.16). No evidence of LD was observed between the other variants in either ethnic group (r^2<0.01). The allelic distribution of the *PTGS1 P17L* polymorphism deviated significantly from Hardy-Weinberg equilibrium in Caucasians (*P*=0.002); however, all other polymorphisms were in Hardy-Weinberg equilibrium in both Caucasians and African-Americans (*P*>0.05).

***PTGS1* Polymorphisms.** In Caucasians, the variant *-1006A* allele was significantly more common among ischemic stroke cases compared to cohort random sample non-cases (18.2% versus 10.6%, respectively, *P*=0.027) (Table 7). Presence of at least one variant *-1006A* allele was associated with significantly higher risk of incident ischemic stroke events relative to *-1006G* homozygotes after adjusting for age, gender and study center (model 1, HRR 1.78, 95% CI 1.08-2.92, *P*=0.024, *q*=0.080) (Table 8). A similar association was observed after also adjusting for cigarette smoking, diabetes and hypertension status (model 2, HRR 1.70, 95% CI 0.99-2.93, *P*=0.056, *q*=0.120); however, this did not attain statistical significance. This relationship was not modified by gender (*P*=0.252). No evidence of a significant association between the variant *-1006A* allele and risk of ischemic stroke in African-Americans, or risk of CHD in either Caucasians or African-Americans, was observed (Tables 7-10). Similar associations with each endpoint were also observed with common reconstructed haplotypes tagged by the variant *-1006A* allele (data not shown).

In African-Americans, the rare *G230S* variant allele appeared to be more common in ischemic stroke cases compared to non-cases (2.6% versus 1.2%, respectively) (Table 7). Moreover, presence of the *G230S* variant allele was associated with significantly higher risk of incident ischemic stroke events after covariate adjustment (model 2, HRR 14.8, 95% CI

1.94-112.4, *P*=0.009, *q*=0.085) (Table 8). A similar, but less pronounced association was also observed between this rare variant and risk of incident CHD events (model 2, HRR 7.42, 95% CI 1.21-45.7, *P*=0.031, *q*=0.465) (Table 10). One individual carrying the *G230S* variant allele experienced both an incident ischemic stroke and CHD event on separate occasions. When considering the composite endpoint, presence of the *G230S* variant allele was also associated with significantly higher risk of an incident ischemic stroke or CHD event after covariate adjustment (model 2, HRR 8.37, 95% CI 1.53-45.8, *P*=0.014). No associations between the *R8W*, *P17L*, *R53H* or *L237M* variant alleles and risk of either endpoint were observed (Tables 7-10).

***PTGS2* Polymorphisms.** In African-Americans, the variant *-765C* allele was significantly more common among ischemic stroke cases compared to cohort random sample non-cases (61.4% versus 49.4%, respectively, *P*=0.032) (Table 11). Presence of at least one variant *-765C* allele was associated with significantly higher risk of incident ischemic stroke events relative to *-765G* homozygotes after covariate adjustment (model 2, HRR 1.76, 95% CI 1.05-2.94, *P*=0.031, *q*=0.146) (Table 12). This relationship was not modified by gender (*P*=0.645). The *-765C* allele was not significantly associated with risk of ischemic stroke in Caucasians, or risk of CHD in either Caucasians or African-Americans (Tables 11 and 12). No association between the *V511A* variant allele and risk of either endpoint was observed in African-Americans (Tables 11 and 12).

Aspirin Utilization. In Caucasians, aspirin utilization at baseline appeared to modify the relationship between the *G-765C* polymorphism in *PTGS2* and risk of incident CHD events

(*P* for interaction=0.065, *q*=0.102) (Table 13). When stratified by aspirin use at baseline, the variant *-765C* allele demonstrated a non-significant association with higher risk of CHD in aspirin non-users (model 2, HRR 1.37, 95% CI 0.98-1.92, *P*=0.064) and lower risk of CHD in those receiving aspirin therapy (model 2, HRR 0.60, 95% CI 0.36-1.02, *P*=0.058); however, these stratified associations did not attain statistical significance. Aspirin utilization did not modify the relationship between the G-*765C* polymorphism and risk of ischemic stroke (*P* for interaction=0.630), or the relationship between the *G-1006A* polymorphism in *PTGS1* and risk of either ischemic stroke (*P* for interaction=0.228) or CHD (*P* for interaction=0.933).

Discussion

The current analysis demonstrated that genetic variation in *PTGS1* and *PTGS2* was associated with risk of incident ischemic cardiovascular disease events in Caucasians and African-Americans enrolled in the ARIC study. Specifically, the variant *-1006A* allele in *PTGS1* and *-765C* allele in *PTGS2* were associated with higher risk of ischemic stroke events in Caucasians and African-Americans, respectively. Moreover, the rare *G230S* variant allele in *PTGS1* was associated with significantly higher risk of both ischemic stroke and CHD events in African-Americans. Although the *G-765C* polymorphism in *PTGS2* was not significantly associated with CHD incidence, aspirin utilization appeared to modify this relationship in Caucasians. The variant *-765C* allele appeared to be associated with higher risk of CHD in aspirin non-users and lower risk in those receiving aspirin therapy.

Cyclooxygenase derived prostaglandins are important regulators of vascular, myocardial and platelet function *in vivo*, and the relative contribution of COX-1 and COX-2-mediated

prostaglandin biosynthesis appears to be a critical determinant of cardio- and cerebrovascular disease risk (22-25). For instance, the balance between prostacyclin and thromboxane A_2 significantly modifies atherosclerotic lesion development (100). Moreover, preferentially inhibiting COX-1 derived thromboxane A_2 in platelets via low-dose aspirin administration significantly reduces the risk of myocardial infarction, ischemic stroke and death in high-risk patients (25). In contrast, despite their potential anti-inflammatory and atherosclerotic plaque stabilizing effects, selective COX-2 antagonists inhibit endothelial prostacyclin biosynthesis without influencing platelet thromboxane A_2 production and increase risk of myocardial infarction events, particularly in higher risk patients (23, 24). COX-1 and COX-2 derived prostaglandins are also important mediators of cerebrovascular function. Selective inhibition of COX-1 significantly reduces cerebral blood flow and vasodilatory responses, and COX-$1^{-/-}$ mice have significantly larger cerebral infarct volumes compared to wild-type mice after middle cerebral artery (MCA) occlusion (113, 114). Moreover, cerebral COX-1 gene transfer prior to MCA occlusion significantly reduces cerebral infarct volume in rats via increased prostacyclin production (115). Selective inhibition of COX-2 also abolishes cerebral vasodilatory responses to bradykinin (116). However, COX-$2^{-/-}$ mice have significantly smaller infarct volumes compared to wild-type mice after MCA occlusion (117), and transgenic mice with neuronal overexpression of COX-2 have larger infarct volumes, implicating the post-ischemic inflammatory effects of increased COX-2 expression and PGE_2 production in brain injury (118). Collectively, preclinical and clinical investigations have demonstrated the importance of COX-1 and COX-2-mediated prostaglandin biosynthesis in the pathogenesis of ischemic stroke and CHD. Consequently,

genetic variation in *PTGS1* and *PTGS2* may be important modifiers of ischemic stroke and CHD susceptibility in humans.

The rare *G230S* variant allele in *PTGS1*, which is monomorphic in Caucasians, was associated with significantly higher risk of ischemic stroke events in African-Americans. The *G230S* variant has been previously shown to have significantly lower COX-1 metabolic activity *in vitro* compared to wild-type enzyme (101) (Chapter II). Moreover, molecular modeling suggests this variant may indirectly disrupt the active conformation of COX-1, leading to the observed reductions in metabolic activity (101) (Chapter II). Association between the *G230S* variant and risk of ischemic stroke incidence is consistent with the described preclinical data demonstrating the protective role of COX-1 in cerebrovascular function (113-115). A significant association was also observed between the *G230S* variant allele and higher risk of CHD events; although, this association was less pronounced and carried a substantial FDR estimate (q=0.465). Due to the rare frequency of the *G230S* variant allele, the observed associations with both endpoints carried wide confidence intervals and should be interpreted with caution. In Caucasians, the variant *-1006A* allele in *PTGS1* was associated with greater risk of incident ischemic stroke. This polymorphism is one of seven variants within the *PTGS1* 5'UTR present in substantial LD (101) (Chapter II); however, the functional relevance of the variant haplotype and each individual variant has not been characterized to date. Consequently, the *G-1006A* polymorphism may not be the functionally relevant locus driving the observed association with ischemic stroke risk. Future studies evaluating the functional effects of these variants are necessary.

A significant association was also observed between the variant *-765C* allele in *PTGS2* and higher risk of ischemic stroke incidence in African-Americans. No significant

association was observed in Caucasians. This variant has previously been shown to disrupt a Sp1 binding site in the *PTGS2* proximal promoter, reduce COX-2 transcription and expression, and carry significant anti-inflammatory effects (59, 60). Moreover, presence of this variant has been associated with lower risk of prevalent myocardial infarction or ischemic stroke in a high-risk Italian population (60), contrasting epidemiological and clinical trial evidence demonstrating associations between selective COX-2 inhibitor use and increased risk of cardiovascular events (23, 24). The current analysis suggests that the *-765C* allele is associated with higher risk of ischemic stroke events in African-Americans. Importantly, post-event complications and outcomes were not evaluated, even though preclinical evidence suggests that lower COX-2 expression reduces the extent of ischemic brain injury after a cerebral infarct (117). Future studies evaluating the influence of the *G-765C* polymorphism on prognosis after ischemic stroke events appear necessary.

A significant association between the *-765C* allele and risk of incident CHD events was not observed. However, aspirin utilization appeared to modify this relationship in Caucasians, such that the *-765C* allele appeared to be associated with higher risk of CHD in aspirin non-users and lower risk in those receiving aspirin therapy. This observation is consistent with the hypothesis that concomitant aspirin utilization may mitigate the cardiovascular hazard associated with selective COX-2 inhibition via restoration of prostacyclin-thromboxane A_2 balance, which is altered in favor of thromboxane A_2 with COX-2 inhibition (24). However, this hypothesis has not been rigorously validated in prospective clinical trials. Nonetheless, presence of this potential interaction with aspirin utilization could help explain, at least in part, the aforementioned association between the *-765C* allele and lower cardiovascular risk observed by Cipollone et al. (60). Since this

analysis of prevalent outcomes targeted a population at high-risk of cardiovascular events, 67% were receiving aspirin therapy (60). Although the variant -*765C* allele was not associated with overall risk of incident CHD events in Caucasians in the current analysis, -*765C* allele carriers receiving aspirin at baseline tended to be at lower risk of CHD while those not receiving aspirin tended to be at higher risk. Perhaps aspirin use in -*765C* allele carriers restores prostacyclin-thromboxane A_2 balance, allows the plaque stabilizing effects related to suppression of COX-2 mediated PGE_2 synthesis and matrix metalloproteinase activity to predominate (60), and results in lower risk of CHD events. Thus, aspirin use may not just attenuate risk associated with the variant -*765C* allele, the combination may provide synergistic benefit in the prevention of CHD events. Moreover, perhaps presence of the -*765C* allele without concomitant aspirin therapy leads to altered prostacyclin-thromboxane A_2 balance and greater risk of CHD events, similar to what has been observed with the selective COX-2 inhibitors. However, due to the power limitations in the current interaction analysis, these findings must be interpreted with caution and confirmed in larger populations.

Although the current study evaluated rigorously ascertained incident events, mechanisms underlying the observed associations were not elucidated. The limitations related to the evaluation of aspirin utilization at baseline in an observational study are also recognized. Patients were not randomized at baseline, and aspirin therapy was likely initiated in those at highest risk of cardiovascular events. Although potential confounders related to cardiovascular disease risk were adjusted for in the current regression analysis, additional confounding factors such as misclassification bias, changes in aspirin utilization throughout follow-up, duration of therapy and dose could have influenced these observations. Thus, the reported gene-aspirin interaction findings should be considered exploratory and hypothesis-

generating. Future studies evaluating the mechanisms underlying this potential interaction are necessary. Moreover, it may be difficult to gauge the statistical significance of the polymorphism-disease association findings considering the number of comparisons completed in the current analysis. Consequently, the FDR was assessed across all completed tests in the association analysis. Since all *q*-values related to the association between the *G-1006A* (Caucasians), *G230S* (African-Americans) and *G-765C* (African-Americans) polymorphisms and ischemic stroke risk were conservatively estimated to be <0.15, there is a high level of confidence in these findings; however, validation in an independent population is necessary.

In summary, the current analysis suggests that genetic variation in *PTGS1* and *PTGS2* may be important risk factors for the development of ischemic stroke events. Moreover, aspirin utilization may modify the association between the *G-765C* polymorphism in *PTGS2* and risk of CHD events in Caucasians. Future studies in multiple populations will be required to validate these findings, in addition to molecular, biochemical and physiological studies to elucidate the mechanisms underlying the observed associations.

Table 5. Selected *PTGS1* and *PTGS2* polymorphisms for genotyping.

Polymorphism	Nucleotide*	Location	Amino Acid	CRS Minor Allele Frequency		Function†
				Caucasian (N=698)	African-American (N=367)	
PTGS1						
G>A	-1006	5' UTR	-	0.059	0.116	Unknown
C>T (rs1236913)	250	Exon 2	R8W	0.070	0.012	Normal
C>T (rs3842787)	278	Exon 2	P17L	0.061	0.145	Normal
G>A (rs3842789)	7010	Exon 3	R53H	0	0.002	Dec. activity
G>A	10721	Exon 7	G230S	0	0.005	Dec. activity
C>A (rs5789)	10742	Exon 7	L237M	0.033	0.005	Dec. activity
PTGS2						
G>C (rs20417)	-765	Promoter	-	0.164	0.301	Dec. transcription
T>C (rs5273)	5792	Exon 10	V511A	0	0.045	Normal

CRS=cohort random sample, UTR=untranslated region

*Nucleotide position relative to gene transcriptional start site (Genbank accession numbers: *PTGS1* AF440204; *PTGS2* AY229989).

†Based on previous functional studies (58, 59, 101) (Chapter II).

Table 6. ARIC baseline characteristics by incident case status.

Characteristic*	CRS	CHD Cases†	Stroke Cases‡
N	1065	1085	300
Gender (% male)	41.4%	67.4%	53.0%
Race (% Caucasian)	72.8%	76.6%	55.0%
Age (years)	53.8 ± 0.10	55.8 ± 0.17	56.7 ± 0.32
Current smoker (% yes)	24.8%	36.1%	36.8%
Pack-years >20 (% yes)	29.0%	48.6%	41.4%
Diabetes (%)	11.1%	25.1%	34.6%
Hypertension (%)	29.8%	49.4%	66.0%
SBP (mmHg)	120.4 ± 0.58	128.3 ± 0.63	134.8 ± 1.30
DBP (mmHg)	73.3 ± 0.37	76.2 ± 0.38	79.4 ± 0.81
BMI (kg/m^2)	27.7 ± 0.20	28.3 ± 0.15	29.0 ± 0.31
HDL cholesterol (mg/dL)	53.3 ± 0.61	43.4 ± 0.39	48.4 ± 0.90
LDL cholesterol (mg/dL)	133.7 ± 1.31	151.5 ± 1.26	144.7 ± 2.55
Total cholesterol (mg/dL)	211.7 ± 1.32	226.2 ± 1.34	222.4 ± 2.90
Triglycerides (mg/dL)	125.2 ± 2.39	165.2 ± 3.52	153.0 ± 6.33
Aspirin (% yes)	24.8%	26.4%	19.0%

*Characteristics weighted according to the sampling fraction. Data presented as mean±standard error of the mean. CRS=cohort random sample, SBP=systolic blood pressure, DBP=diastolic blood pressure, BMI=body mass index, HDL=high density lipoprotein, LDL=low density lipoprotein.

†$P<0.05$ for comparison of CHD cases to 980 non-cases in the CRS for all characteristics, except aspirin use.

‡$P<0.05$ for comparison of stroke cases to 1036 non-cases in the CRS for all characteristics.

Table 7. *PTGS1* polymorphism frequency by incident ischemic stroke case status.

	Caucasian			African-American		
Genotype*	**Non-cases**	**Stroke cases**	***P*-value**	**Non-cases**	**Stroke cases**	***P*-value**
G-1006A						
G/G	583 (89.4%)	121 (81.8%)		246 (76.9%)	84 (73.0%)	
G/A + A/A	71 (10.6%)	27 (18.2%)	*P*=0.027	70 (23.1%)	31 (27.0%)	*P*=0.436
R8W						
C/C	571 (86.7%)	131 (87.9%)		308 (97.1%)	112 (97.4%)	
C/T + T/T	85 (13.3%)	18 (12.1%)	*P*=0.694	8 (2.9%)	3 (2.6%)	*P*=N/A
P17L						
C/C	564 (89.3%)	123 (84.3%)		229 (72.1%)	81 (71.7%)	
C/T + T/T	69 (10.7%)	23 (15.7%)	*P*=0.125	90 (27.9%)	32 (28.3%)	*P*=0.758
G230S						
G/G	654 (100%)	149 (100%)		311 (98.8%)	112 (97.4%)	
G/A + A/A	0 (0%)	0 (0%)	*P*=N/A	3 (1.2%)	3 (2.6%)	*P*=N/A
L237M						
C/C	604 (93.6%)	143 (94.7%)		312 (99.2%)	114 (99.1%)	
C/A + A/A	43 (6.4%)	8 (5.3%)	*P*=0.613	3 (0.8%)	1 (0.9%)	*P*=N/A

*Genotype data presented as absolute (percent) genotype frequency. Frequencies are weighted according to the sampling fraction. The *R53H* variant allele in *PTGS1* (rs3842789) was identified in only one African-American non-case.

Table 8. Hazard rate ratio between *PTGS1* polymorphisms and risk of incident ischemic stroke events.

	Caucasian			African-American		
Polymorphism	**HRR**	**95% CI**	***P*-value**	**HRR**	**95% CI**	***P*-value**
G-1006A	*G/A + A/A* versus *G/G*			*G/A + A/A* versus *G/G*		
Model 1*	1.78	1.08 – 2.92	*P*=0.024	1.46	0.88 – 2.40	*P*=0.137
Model 2†	1.70	0.99 – 2.93	*P*=0.056	1.16	0.64 – 2.10	*P*=0.616
R8W	*C/T + T/T* versus *C/C*			*C/T + T/T* versus *C/C*		
Model 1*	0.80	0.46 – 1.38	*P*=0.418	0.97	0.25 – 3.74	*P*=0.965
Model 2†	0.72	0.40 – 1.30	*P*=0.278	2.21	0.44 – 11.2	*P*=0.339
P17L	*C/T + T/T* versus *C/C*			*C/T + T/T* versus *C/C*		
Model 1*	1.48	0.88 – 2.50	*P*=0.143	1.10	0.68 – 1.78	*P*=0.701
Model 2†	1.36	0.77 – 2.40	*P*=0.296	1.04	0.60 – 1.80	*P*=0.882
G230S	*G/A + A/A* versus *G/G*			*G/A + A/A* versus *G/G*		
Model 1*	N/A			4.46	0.72 – 27.7	*P*=0.109
Model 2†	N/A			14.8	1.94 – 112.4	*P*=0.009
L237M	*C/A + A/A* versus *C/C*			*C/A + A/A* versus *C/C*		
Model 1*	0.77	0.34 – 1.74	*P*=0.534	1.26	0.12 – 13.7	*P*=0.850
Model 2†	0.96	0.43 – 2.18	*P*=0.925	0.58	0.05 – 6.66	*P*=0.661

HRR=hazard rate ratio, CI=confidence interval, N/A=modeling not completed since 0% frequency in case and/or non-case group.

*Adjusted for age, gender, and study center.

†Adjusted for age, gender, study center, current smoker, diabetes, and hypertension.

Table 9. *PTGS1* polymorphism frequency by incident CHD case status.

	Caucasian			African-American		
Genotype*	**Non-cases**	**CHD cases**	***P*-value**	**Non-cases**	**CHD cases**	***P*-value**
G-1006A						
G/G	542 (89.2%)	666 (86.6%)		234 (75.9%)	168 (76.4%)	
G/A + A/A	68 (10.8%)	103 (13.4%)	*P*=0.164	72 (24.1%)	52 (23.6%)	*P*=0.906
R8W						
C/C	533 (86.7%)	669 (86.6%)		298 (97.0%)	218 (98.2%)	
C/T + T/T	79 (13.3%)	104 (13.5%)	*P*=0.952	8 (3.0%)	4 (1.8%)	*P*=N/A
P17L						
C/C	524 (89.1%)	671 (87.9%)		219 (71.5%)	159 (72.0%)	
C/T + T/T	66 (10.9%)	92 (12.1%)	*P*=0.534	90 (28.5%)	62 (28.0%)	*P*=0.913
G230S						
G/G	610 (100%)	773 (100%)		301 (98.8%)	215 (98.2%)	
G/A + A/A	0 (0%)	0 (0%)	*P*=N/A	3 (1.2%)	4 (1.8%)	*P*=N/A
L237M						
C/C	563 (93.7%)	733 (94.0%)		301 (99.2%)	220 (99.6%)	
C/A + A/A	39 (6.3%)	47 (6.0%)	*P*=0.851	3 (0.8%)	1 (0.4%)	*P*=0.659

*Genotype data presented as absolute (percent) genotype frequency. Frequencies are weighted according to the sampling fraction. The *R53H* variant allele in *PTGS1* (rs3842789) was identified in only one African-American non-case.

Table 10. Hazard rate ratio between *PTGS1* polymorphisms and risk of incident CHD events.

	Caucasian			African-American		
Polymorphism	**HRR**	**95% CI**	***P*-value**	**HRR**	**95% CI**	***P*-value**
G-1006A	*G/A + A/A* versus *G/G*			*G/A + A/A* versus *G/G*		
Model 1*	1.13	0.80 – 1.60	*P*=0.487	1.15	0.76 – 1.75	*P*=0.509
Model 2†	1.28	0.87 – 1.89	*P*=0.206	1.25	0.77 – 2.04	*P*=0.367
R8W	*C/T + T/T* versus *C/C*			*C/T + T/T* versus *C/C*		
Model 1*	1.04	0.75 – 1.44	*P*=0.824	0.69	0.20 – 2.34	*P*=0.548
Model 2†	1.00	0.69 – 1.44	*P*=0.991	0.91	0.20 – 4.03	*P*=0.899
P17L	*C/T + T/T* versus *C/C*			*C/T + T/T* versus *C/C*		
Model 1*	1.01	0.71 – 1.46	*P*=0.940	1.05	0.71 – 1.54	*P*=0.823
Model 2†	1.11	0.74 – 1.65	*P*=0.620	1.25	0.80 – 1.94	*P*=0.330
G230S	*G/A + A/A* versus *G/G*			*G/A + A/A* versus *G/G*		
Model 1*	N/A			3.47	0.60 – 19.9	*P*=0.163
Model 2†	N/A			7.42	1.21 – 45.7	*P*=0.031
L237M	*C/A + A/A* versus *C/C*			*C/A + A/A* versus *C/C*		
Model 1*	0.94	0.58 – 1.51	*P*=0.794	0.60	0.06 – 6.36	*P*=0.674
Model 2†	0.92	0.55 – 1.53	*P*=0.749	0.33	0.03 – 4.45	*P*=0.407

HRR=hazard rate ratio, CI=confidence interval, N/A=modeling not completed since 0% frequency in case and/or non-case group.

*Adjusted for age, gender, and study center.

†Adjusted for age, gender, study center, current smoker, diabetes, hypertension, HDL cholesterol, total cholesterol, and body mass index.

Table 11. *PTGS2* polymorphism frequency by incident ischemic stroke or CHD case status.

	Caucasian			African-American		
Genotype*	**Non-cases**	**Incident cases**	***P*-value**	**Non-cases**	**Incident cases**	***P*-value**
Stroke						
G-765C						
G/G	457 (70.7%)	111 (74.5%)		154 (50.6%)	44 (38.6%)	
G/C + C/C	195 (29.3%)	38 (25.5%)	*P*=0.353	149 (49.4%)	70 (61.4%)	*P*=0.032
V511A						
T/T	635 (100%)	149 (100%)		290 (91.6%)	104 (92.0%)	
T/C + C/C	0 (0%)	0 (0%)	*P*=N/A	28 (8.4%)	9 (8.0%)	*P*=0.877
CHD						
G-765C						
G/G	425 (71.0%)	546 (70.4%)		147 (49.7%)	113 (50.5%)	
G/C + C/C	182 (29.0%)	230 (29.6%)	*P*=0.808	144 (50.3%)	111 (49.6%)	*P*=0.873
V511A						
T/T	775 (100%)	591 (100%)		280 (91.9%)	202 (90.2%)	
T/C + C/C	0 (0%)	0 (0%)	*P*=N/A	27 (8.1%)	22 (9.8%)	*P*=0.514

*Genotype data presented as absolute (percent) genotype frequency. Frequencies are weighted according to the sampling fraction.

Table 12. Hazard rate ratio between *PTGS2* polymorphisms and risk of incident ischemic stroke or CHD events.

	Caucasian			African-American		
Polymorphism	**HRR**	**95% CI**	***P*-value**	**HRR**	**95% CI**	***P*-value**
Stroke						
G-765C	*G/C + C/C* versus *G/G*			*G/C + C/C* versus *G/G*		
Model 1*	0.78	0.51 – 1.18	*P*=0.236	1.54	0.98 – 2.41	*P*=0.059
Model 2†	0.79	0.50 – 1.25	*P*=0.314	1.76	1.05 – 2.94	*P*=0.031
V511A	*T/C + C/C* versus *T/T*			*T/C + C/C* versus *T/T*		
Model 1*	N/A			0.87	0.39 – 1.95	*P*=0.734
Model 2†	N/A			0.84	0.36 – 2.00	*P*=0.701
CHD						
G-765C	*G/C + C/C* versus *G/G*			*G/C + C/C* versus *G/G*		
Model 1*	1.01	0.79 – 1.29	*P*=0.929	1.00	0.70 – 1.41	*P*=0.991
Model 2†	1.08	0.83 – 1.42	*P*=0.567	1.03	0.69 – 1.52	*P*=0.894
V511A	*T/C + C/C* versus *T/T*			*T/C + C/C* versus *T/T*		
Model 1*	N/A			1.09	0.60 – 1.98	*P*=0.786
Model 2†	N/A			1.03	0.53 – 2.00	*P*=0.932

HRR=hazard rate ratio, CI=confidence interval, N/A=modeling not completed since 0% frequency in case and/or non-case group.

*Adjusted for age, gender, and study center.

†Adjusted for age, gender, study center, current smoker, diabetes, and hypertension.

‡Adjusted for age, gender, study center, current smoker, diabetes, hypertension, high density lipoprotein cholesterol, total cholesterol, and body mass index.

Table 13. *G-765C* polymorphism in *PTGS2*, baseline aspirin utilization, and risk of incident CHD events in Caucasians.

	Non-cases *G/C + C/C*	**CHD cases** *G/C + C/C*	***P*-value**	**HRR*** *G/C + C/C* vs. *G/G*	**95% CI**	***P*-value**
All patients	182 (29.0%)	230 (29.6%)	*P*=0.808	1.08	0.83–1.42	*P*=0.567
No aspirin	122 (28.0%)	171 (31.7%)	*P*=0.231	1.37	0.98–1.92	*P*=0.064
Aspirin	60 (31.5%)	59 (25.0%)	*P*=0.165	0.60	0.36–1.02	*P*=0.058
Interaction[†]				0.57	0.31–1.04	*P*=0.065

HRR=hazard rate ratio, CI=confidence interval.

*Adjusted for age, gender, study center, current smoker, diabetes, hypertension, high density lipoprotein cholesterol, total cholesterol, and body mass index.

[†]Multiplicative *G-765C* by aspirin utilization interaction term.

CHAPTER IV

NOS3 POLYMORPHISMS, CIGARETTE SMOKING, AND CARDIOVASCULAR DISEASE RISK: THE ATHEROSCLEROSIS RISK IN COMMUNITIES (ARIC) STUDY

Lee CR, North KE, Bray MS, Avery CL, Mosher MJ, Couper DJ, Coresh J, Folsom AR, Boerwinkle E, Heiss G, Zeldin DC. Genetic variation in endothelial nitric oxide synthase (*NOS3*), cigarette smoking, and cardiovascular disease risk: the Atherosclerosis Risk in Communities (ARIC) study. Pharmacogenet Genomics 2006; (in press).

Introduction

Ischemic cardiovascular disease is a major public health problem. It is estimated that 1.2 million Americans will experience an acute coronary heart disease (CHD) event and 0.7 million will experience an acute stroke event this year (1). Endothelial dysfunction is integrally involved in the pathogenesis of ischemic cardiovascular disease, and has been associated with an increased risk of myocardial infarction and stroke (10, 11).

Nitric oxide is synthesized by endothelial nitric oxide synthase (eNOS, *NOS3*) in the vasculature, where it possesses potent vasodilatory (12) and anti-inflammatory (13) effects. Impairment in eNOS-mediated nitric oxide biosynthesis contributes to endothelial dysfunction and promotes the development of atherosclerosis (15, 16). Cigarette smoking also contributes to endothelial dysfunction and atherosclerosis (6), eliciting many of its deleterious endothelial effects via attenuation of nitric oxide biosynthesis and activity (17, 18).

Multiple genetic polymorphisms in *NOS3* have been discovered, including the *T-786C* and Glu298Asp (*E298D*) variants which have been associated with reduced nitric oxide

biosynthesis (53, 54). Numerous clinical studies evaluating potential associations between *NOS3* polymorphisms and cardiovascular disease risk have reported inconsistent results (55); however, few have specifically evaluated the contribution of cigarette smoking, even though smoking may modify the influence of these polymorphisms on endothelial function (56, 57, 119, 120). The primary aim of this investigation was to determine if exposure to cigarette smoke significantly modified the association between presence of the *T-786C* or *E298D* polymorphisms in *NOS3* and risk of incident CHD or ischemic stroke events in individuals enrolled in the biethnic Atherosclerosis Risk in Communities (ARIC) study.

Methods

Study Population. Participants were selected from the ARIC study, a longitudinal, population-based cohort study of 15,792 men and women aged 45 to 64 years from four U.S. communities (Forsyth County, NC; Jackson, MS; Minneapolis, MN; and Washington County, MD) enrolled between 1987 and 1989 (102). Since enrollment, participants have been followed prospectively via annual phone interviews, clinic examinations approximately every three years through 1998, and ongoing abstraction of hospital and death certificate records. The study protocol was approved by the Institutional Review Board of each center, and consent was obtained from each participant.

Ascertainment of Incident CHD and Stroke Cases. All incident cases that occurred between baseline and December 31, 1998 were evaluated (median follow-up 9.1 years), excluding participants with history of CHD or stroke at baseline. Incident CHD (n=1085) was defined as 1) definite or probable myocardial infarction (n=520), 2) electrocardiographic

evidence of silent myocardial infarction (n=112), 3) definite CHD death (n=110), or 4) coronary revascularization procedure (n=343). Incident stroke was defined as a definite or probable ischemic stroke (n=300).

The ascertainment of cases and criteria for classification have been previously described (103, 104). All potential events were systematically reviewed and adjudicated by the ARIC Morbidity and Mortality Classification Committee (102-104). Hospitalized myocardial infarction was classified as definite or probable based on chest pain symptoms, cardiac enzyme levels, and electrocardiographic changes. Definite CHD death was classified based on chest pain symptoms, underlying cause of death, hospitalization records, and medical history. Coronary revascularization procedures included coronary artery bypass grafting and percutaneous coronary intervention. Using the National Survey of Stroke criteria (105), a stroke event was classified as definite or probable if there was 1) rapid onset of neurological symptoms that lasted >24 hours or led to death within 24 hours, 2) no evidence of pathology that could have mimicked stroke, and 3) one major (e.g., aphasia or hemiparesis) or two minor (e.g., diplopia or dysarthria) neurological deficits. Qualifying cases were further classified as ischemic (thrombotic brain infarction, cardioembolic stroke) or hemorrhagic (subarachnoid hemorrhage, intracerebral hemorrhage) on the basis of neuroimaging studies and autopsy, when available (104).

Baseline Measurements. Detailed demographic, clinical, and biochemical data were obtained from each participant at baseline. Race was self-reported. Prevalent CHD and stroke were defined as history of a physician-diagnosed event. Hypertension was defined as systolic blood pressure ≥140 mmHg, diastolic blood pressure ≥90 mmHg, or current

antihypertensive medication use. Diabetes was defined as fasting blood glucose ≥126 mg/dL, nonfasting blood glucose ≥200 mg/dL, physician diagnosis, or pharmacologic treatment. Detailed information on cigarette smoking was obtained through an interview-administered questionnaire, and was defined by current smoking status (yes/no) and pack-year smoking history (≥20 or <20 pack-years).

Cohort Random Sample. A random sample of all ARIC participants without history of CHD or stroke at baseline was assembled to serve as the reference group for the case-cohort comparisons [n=1065; 85 (57 Caucasians, 28 African-Americans) and 29 (12 Caucasians, 17 African-Americans)] of which are also incident CHD and stroke cases, respectively). Sampling of the cohort was stratified on age (≥55 or <55 years), gender, and race (Caucasian or African-American). Sampling proportions varied across each stratum.

Genotyping. Genomic DNA from all incident CHD and ischemic stroke cases and the cohort random sample was genotyped for the T>C polymorphism at nucleotide position -786 in the proximal promoter (*T-786C*) and the G>T polymorphism at nucleotide position 5246 in exon 7 (*E298D*) of *NOS3*, using multiplex matrix-assisted laser desorption/ionization time-of-flight (MALDI-TOF) mass spectrometry methods, as described (107) (Appendix II). Briefly, targeted sequences were amplified via polymerase chain reaction using specific forward (*T-786C*: 5'-ACGTTGGATGACTGTAGTTTCCCTAGTCCC-3'; *E298D*: 5'-ACGTTGGATGACCTCAAGGACCAGCTCGG-3') and reverse (*T-786C*: 5'-ACGTTGGATGAGGTCAGCAGAGAGACTAGG-3'; *E298D*: 5'-ACGTTGGATGAAACGGTCGCTTCGACGTGC-3') primers for each polymorphism,

followed by extension reactions utilizing specific oligonucleotide primers that annealed immediately upstream of each polymorphic site and extended the amplification product by a single base pair in the forward direction (*T-786C*: 5'-CATCAAGCTCTTCCCTGGC-3'; *E298D*: 5'-GCTGCAGGCCCCAGATGA-3'). The mass of the extension reaction products was determined and translated into genotype using the MassARRAY RT software (Sequenom Inc., San Diego, CA). Blind replicates were included for quality control. Missing genotypes were present in <5% of individuals.

Data Analysis. Inverse sampling fractions from each stratum were used as weights in variance estimation of adjusted covariate means and proportions by linear and logistic regression, respectively. Cohort random sample allele frequencies were evaluated for deviation from Hardy-Weinberg equilibrium, and pairwise linkage disequilibrium statistics were calculated (Haploview 3.2) (81). Hazard rate ratios (HRR) and 95% confidence intervals (CI) for the development of incident CHD or ischemic stroke in relation to genotype were calculated by weighted proportional hazards regression, using Barlow's method to account for the stratified random sampling and case-cohort design (109). Model 1 included age, gender, and study center as covariates. Model 2 also included significant clinical covariates, which were current smoking status, diabetes, hypertension, high density lipoprotein cholesterol, total cholesterol, and body mass index for the CHD endpoint, and current smoking status, diabetes, and hypertension for the stroke endpoint. Assuming an autosomal dominant mode of inheritance, individuals with one or two variant alleles were combined for comparison to wild-type individuals. All analyses were completed separately in Caucasians and African-Americans. Assuming a case-control design and type I error

α=0.05, there was approximately 99% and 90% power for the CHD endpoint and 90% and 80% power for the stroke endpoint to detect an odds ratio of 2.0 in Caucasians and African-Americans, respectively.

Haplotypes and their frequencies were estimated using the phase reconstruction method (PHASE 2.1), which assigned the most probable haplotype pair to each individual (121), and compared across case status by chi-square. Associations between haplotype (0,1) and risk of CHD or stroke were evaluated using Barlow's method (109), by simultaneously modeling each haplotype relative to the most common haplotype using the model 2 covariate adjustment strategy.

Gene-environment interaction testing was completed on a multiplicative scale between genotype and current smoking status (yes/no) or pack-year smoking history (≥20 or <20 pack-years) at baseline using a Wald chi-square test for significance of the estimated β-coefficient for the interaction term (110). Haplotype-smoking interaction testing was also completed in Caucasians for the reconstructed haplotype containing both the variant *T-786C* and *E298D* alleles; however, this was not completed in African-Americans due to sample size limitations. Because interaction hypothesis testing on a multiplicative scale is underpowered, the critical value for statistical significance was set to α=0.15, two-sided (111). To minimize the impact of the multiple statistical tests conducted in the current analysis, the false discovery rate (FDR) *q*-value was estimated for each interaction test separately for the CHD and stroke endpoints (QVALUE). The FDR *q*-value is defined as the proportion of statistical tests deemed significant that are actually false-positives (112). Stratified weighted proportional hazards regression was also completed according to baseline

current smoking status or pack-year smoking history using the model 2 covariate adjustment strategy (minus current smoking status) to further explore potential interactions.

Results

Study Population. Significant baseline differences in various risk factors were observed between CHD and stroke cases and non-cases included in the cohort random sample (Table 6). Incident CHD and stroke cases were significantly older and more likely to be male, smokers, diabetic, hypertensive and have abnormal fasting lipid panels compared to non-cases. Stroke cases were also more likely to be African-American. In the cohort random sample, 71.5% of current smokers at baseline also had a ≥20 pack-year history.

***NOS3* Genotype.** In the cohort random sample, the *T-786C* (0.371 versus 0.151) and *E298D* (0.330 versus 0.112) minor allele frequencies were significantly different in Caucasians and African-Americans, respectively (P<0.001). Minimal evidence of pairwise linkage disequilibrium was observed between these polymorphisms in both Caucasians (D'=0.47, r^2=0.19) and African-Americans (D'=0.41, r^2=0.12). The allelic distribution of each polymorphism was in Hardy-Weinberg equilibrium (P>0.05).

***E298D* Polymorphism.** The *E298D* variant allele was not significantly associated with CHD or ischemic stroke incidence in either Caucasians or African-Americans (Tables 14 and 15), nor were these relationships modified by gender. However, in Caucasians the relationship between *E298D* genotype and CHD risk was significantly modified by baseline current smoking status (interaction P=0.013, q=0.078) and tended to be modified by pack-

year smoking history (interaction *P*=0.126, *q*=0.247), with the highest risk of CHD observed in smokers carrying the *E298D* variant allele (Table 16). In the stratified analysis, current smokers with the *E298D* variant allele were at significantly greater risk of CHD compared to smokers with two wild-type alleles (HRR 1.84, 95% CI 1.10-3.09, *P*=0.021); however, no association between the *E298D* variant allele and CHD risk was observed in nonsmokers (HRR 0.81, 95% CI 0.59-1.10, *P*=0.168). Current smoking status (interaction *P*=0.762) and pack-year history (interaction *P*=0.641) did not modify the relationship between *E298D* genotype and CHD risk in African-Americans (Table 16). Moreover, neither cigarette smoking exposure estimate modified the relationship between *E298D* genotype and risk of ischemic stroke.

***T-786C* Polymorphism.** In Caucasians, the variant -*786C* allele tended to be more common in CHD cases compared to non-cases (62.7% versus 57.7%, *P*=0.079) (Table 14), and was associated with a trend toward greater CHD risk relative to *T-786* homozygotes (HRR 1.24, 95% CI 0.96-1.62, *P*=0.106) (Table 15); although, this did not attain statistical significance. Pack-year smoking history appeared to modify this association, such that in the stratified analysis ≥20 pack-year smokers carrying the variant -*786C* allele were at significantly greater risk of CHD relative to ≥20 pack-year smokers with two -*786T* alleles (HRR 1.52, 95% CI 1.01-2.27, *P*=0.042). No association was observed between the variant -*786C* allele and CHD risk in <20 pack-year smokers (HRR 1.06, 95% CI 0.75-1.51, *P*=0.731). In African-Americans, no association between the variant -*786C* allele and risk of CHD was observed (*P*=0.421) (Table 15); however, this relationship tended to be modified by current smoking status (interaction *P*=0.142, *q*=0.444) (Table 17).

In African-Americans, the variant -*786C* allele tended to be more common in incident stroke cases compared to non-cases (39.5% versus 30.3%, *P*=0.099) (Table 14), and was associated with a trend toward greater risk of stroke relative to -*786T* homozygotes (HRR 1.63, 95% CI 0.93-2.88, *P*=0.090) (Table 15); although, this did not attain statistical significance. This relationship was not modified by gender. However, cigarette smoking exposure significantly modified this association (interaction *P*=0.037, *q*=0.148), such that the greatest risk of ischemic stroke was observed in ≥20 pack-year smokers carrying the variant -*786C* allele (Table 17). In ≥20 pack-year smokers, stratified analysis demonstrated the -*786C* allele was more common in stroke cases compared to non-cases (41.9% versus 23.4%, *P*=0.083), and was associated with significantly higher risk of stroke relative to ≥20 pack-year smokers with two -*786T* alleles (HRR 4.23, 95% CI 1.34-13.4, *P*=0.014). No relationship between the variant -*786C* allele and risk of stroke was observed in <20 pack-year smokers (HRR 1.08, 95% CI 0.56-2.10, *P*=0.813). A similar association was also observed in current smokers carrying the variant -*786C* allele (HRR 2.65, 95% CI 0.99-7.1, *P*=0.052), but not nonsmokers (HRR 1.16, 95% CI 0.55-2.46, *P*=0.694). In Caucasians, the variant -*786C* allele was not significantly associated with risk of ischemic stroke (*P*=0.665) (Table 15), nor was this relationship modified by current smoking status (interaction *P*=0.892) or pack-year history (interaction *P*=0.488) (Table 17).

NOS3* Haplotypes.** Four potential haplotypes were reconstructed, and in Caucasians only haplotype ***C*G* (uniquely tagged by the variant -*786C* allele) was significantly more frequent in CHD cases compared to non-cases (16.1% versus 13.1%, *P*=0.034) (Table 18) and was associated with a trend toward greater CHD risk relative to the most common haplotype *TG*

(HRR 1.34, 95% CI 0.97-1.85, *P*=0.072); although, this did not attain statistical significance. No significant differences in haplotype copy frequency were observed across CHD case status in African-Americans, or across stroke case status in Caucasians and African-Americans (Table 18).

Haplotype ***CT*** (uniquely tagged by both the variant *T-786C* and *E298D* alleles) was not significantly associated with risk of CHD relative to haplotype *TG* (HRR 1.16, 95% CI 0.88-1.53, *P*=0.296). Although no statistically significant interaction between haplotype ***CT*** and either current smoking status (interaction *P*=0.179) or pack-year history (interaction *P*=0.206) was observed, smokers carrying at least one copy of haplotype ***CT*** appeared to demonstrate higher risk of CHD compared to nonsmokers without this haplotype (Table 19). In the stratified analysis, ≥20 pack-year smokers carrying haplotype ***CT*** were at significantly higher risk of developing CHD relative to ≥20 pack-year smokers with two haplotype *TG* copies (HRR 1.55, 95% CI 1.02-2.36, *P*=0.041). However, no association between haplotype ***CT*** and CHD risk was observed in <20 pack-year smokers (HRR 0.91, 95% CI 0.62-1.33, *P*=0.469). A similar but nonsignificant association was also observed in current smokers carrying haplotype ***CT*** (HRR 1.73, 95% CI 0.99-3.02, *P*=0.054), but not nonsmokers (HRR 1.01, 95% CI 0.72-1.42, *P*=0.937).

Haplotype ***CT*** was not significantly associated with risk of ischemic stroke relative to haplotype *TG* (HRR 1.03, 95% CI 0.67-1.58, *P*=0.642). Moreover, no significant interaction between haplotype ***CT*** and either current cigarette smoking status (interaction *P*=0.309) or pack-year history (interaction *P*=0.610) was observed (Table 19). In the stratified analysis, statistically significant associations were not observed between haplotype ***CT*** and risk of

ischemic stroke in either current smokers (HRR 2.09, 95% CI 0.76-5.77, *P*=0.156) or nonsmokers (HRR 0.85, 95% CI 0.52-1.41, *P*=0.536) relative to haplotype *TG*.

Discussion

The current analysis demonstrated no statistically significant associations between the *T-786C* or *E298D* polymorphisms and risk of either incident CHD or ischemic stroke in Caucasians and African-Americans enrolled in the ARIC study; although, a trend towards higher risk was observed with the variant -*786C* allele for CHD in Caucasians and stroke in African-Americans. Importantly, a potential interaction between genetic variation in *NOS3*, cigarette smoking history, and risk of incident CHD and ischemic stroke events was identified in these individuals. Specifically, the *T-786C* and *E298D* polymorphism variant alleles appeared to be associated with significantly higher risk of developing CHD or ischemic stroke in current cigarette smokers and/or those with a ≥20 pack-year history at baseline, whereas these variant alleles were not significantly associated with disease risk in the absence of the smoking exposure. This interaction was particularly evident with *E298D* genotype and CHD risk in Caucasians, and *T-786C* genotype and ischemic stroke risk in African-Americans.

The role of endothelial dysfunction in the pathogenesis of cardiovascular disease has become increasingly appreciated. Endothelial dysfunction is typically manifested by impairment in endothelial-dependent vasodilation, and is associated with increased risk of myocardial infarction and stroke (10, 11). The vasodilatory, anti-inflammatory, and anti-proliferative properties of nitric oxide are vital mediators of this process, such that impairment in nitric oxide biosynthesis and/or activity elicits a substantial worsening of

endothelial function and promotes the development of atherosclerosis (12, 13, 15, 16). Cigarette smoking also contributes significantly to endothelial dysfunction and atherosclerosis (6), in part through its reduction of eNOS-mediated nitric oxide biosynthesis via enhanced oxidative stress and eNOS uncoupling (17, 18).

Numerous investigations have evaluated associations between *NOS3* polymorphisms and cardiovascular disease. Most have focused on the *T-786C* and *E298D* polymorphisms due to associations between the variant alleles and reduced nitric oxide biosynthesis (53, 54); however, results have been inconsistent (55). Importantly, few investigations have evaluated incident clinical events. Moreover, few have considered the potential influence of cigarette smoking despite their potential synergistic contribution to worsening endothelial function. For instance, the variant *-786C* allele has been significantly associated with risk of coronary spasm (120) and decreased cerebral blood flow (56) in smokers, but not nonsmokers. The *E298D* variant allele has also been associated with significantly lower endothelial-dependent vasodilation in smokers, with no significant effect in nonsmokers (57). Interestingly, the *E298D* variant allele did not influence endothelial-dependent vasodilation in healthy volunteers despite being associated with reduced systemic nitric oxide levels (122). These data suggest that presence of established underlying endothelial dysfunction, as observed in cigarette smokers, may be necessary for these polymorphisms to significantly attenuate endothelial function and predispose patients to increased cardiovascular risk. Findings from the current analysis demonstrating a potential interaction between the *T-786C* and *E298D* polymorphisms, cigarette smoking, and risk of CHD and stroke events are consistent with this hypothesis.

It was observed that associations between the *T-786C* and *E298D* polymorphisms and CHD incidence may be significantly modified by exposure to cigarette smoke, such that smokers carrying these variant alleles were at significantly higher risk of developing CHD compared to nonsmokers without these variants. Smokers carrying the reconstructed haplotype containing both variant alleles also appeared to be at greater risk of CHD. Moreover, pack-year history significantly modified the association between the *-786C* allele and ischemic stroke risk in African-Americans. Collectively, these data suggest the potential existence of a complex interplay between *NOS3* polymorphisms, cigarette smoking exposure, endothelial function, and cardiovascular disease risk.

Although the current study evaluated rigorously ascertained incident events, mechanisms underlying the observed statistical interactions were not elucidated. It also cannot be ruled out that the *T-786C* and *E298D* polymorphisms are simply markers in linkage disequilibrium with the true causative loci. However, it was confirmed that these polymorphisms are not in significant linkage disequilibrium with each other (55). A previous epidemiological study reported a significant interaction between the *NOS3* 27-base pair repeat polymorphism in intron 4, smoking history, and risk of angiographically documented CHD (123). Although this polymorphism was not evaluated in the current analysis, previous studies have demonstrated that it is not in significant linkage disequilibrium with either the *E298D* or *T-786C* polymorphisms (55). The current analysis also identified a potential haplotype-smoking interaction. Since haplotypes are inferred, some uncertainty exists in the haplotype assigned to each individual. However, only two polymorphisms were included in haplotype reconstruction, posterior haplotype probabilities exceeded 0.83 in all individuals (approximately 75% had a probability of 1.0), and similar haplotype distributions were

observed using the expectation-maximization algorithm (81). Unfortunately, validation of reported smoking status via biomarkers of tobacco exposure, such as urinary cotinine, was not completed in the ARIC study; however, misclassification of smoking status was expected to be minor and more likely to involve a smoker who failed to report cigarette consumption in small amounts. Moreover, previous ARIC analyses evaluating smoking and risk of cardiovascular disease outcomes have been consistent with other populations (124). Thus, it is unlikely that misclassification bias, if present, would have a detectable impact on these estimates.

It may be difficult to gauge the statistical significance of these findings considering the number of comparisons completed in the current analysis. Moreover, some of the reported HRR's were imprecise due to small sample sizes and limited power, particularly in the African-American and stroke subsets. However, even though statistical significance was not demonstrated with every comparison, evaluation of two functionally relevant polymorphisms (*T-786C* and *E298D*), two measures of cigarette smoking exposure (current smoking status and pack-year history), and two incident cardiovascular disease endpoints (CHD and ischemic stroke) in Caucasian and African-American individuals enrolled in the rigorously characterized ARIC study cohort provided a conservative mechanism to characterize this potential gene-environment interaction at the population level. Overall, the internal consistency of these results argue in favor of their validity, albeit at the cost of an increased number of statistical comparisons. In order to minimize the impact of the multiple tests completed, the FDR of the interaction test results were also assessed. The estimated q-values for the interactions observed with *E298D* genotype and CHD risk in Caucasians (q=0.078) and *T-786C* genotype and ischemic stroke risk in African-Americans (q=0.148) enhance

confidence in the conclusions drawn from these findings. Moreover, previous studies have demonstrated that the *T-786C* and *E298D* polymorphisms are particularly associated with endothelial dysfunction in cigarette smokers (56, 57, 120), suggesting that existence of a causal interaction between genetic variation in *NOS3* and smoking in the pathogenesis of CHD and stroke is biologically plausible. However, the observation of significant gene-smoking interactions in the absence of significant genotype-disease associations independent of the interaction (i.e., main effects) suggests these findings should be interpreted with caution. Future studies in different populations will undoubtedly be required to validate these findings and improve the current understanding of the complex relationship between *NOS3*, cigarette smoking, and ischemic cardiovascular disease.

Table 14. *T-786C* and *E298D* genotype frequency by incident CHD or stroke case status.

	Caucasian			African-American		
Genotype*	**Non-cases**	**Incident cases**	***P*-value**	**Non-cases**	**Incident cases**	***P*-value**
CHD						
E298D						
G/G	279 (47.2%)	365 (46.7%)		242 (77.3%)	182 (80.2%)	
G/T + T/T	336 (52.8%)	416 (53.3%)	*P*=0.862	70 (22.7%)	45 (19.8%)	*P*=0.437
T-786C						
T/T	248 (42.3%)	276 (37.4%)		212 (68.4%)	155 (74.9%)	
T/C + C/C	362 (57.7%)	463 (62.7%)	*P*=0.079	91 (31.6%)	52 (25.1%)	*P*=0.126
Stroke						
E298D						
G/G	296 (47.0%)	70 (46.7%)		255 (78.5%)	86 (74.1%)	
G/T + T/T	364 (53.0%)	80 (53.3%)	*P*=0.939	68 (21.5%)	30 (25.9%)	*P*=0.362
T-786C						
T/T	268 (42.5%)	56 (39.2%)		223 (69.7%)	66 (60.6%)	
T/C + C/C	386 (57.5%)	87 (60.8%)	*P*=0.466	90 (30.3%)	43 (39.5%)	*P*=0.099

*Genotype data presented as absolute (percent) genotype frequency, and weighted according to sampling fraction.

Table 15. Hazard rate ratio between *T-786C* and *E298D* polymorphisms and risk of incident CHD or stroke.

	Caucasian			African-American		
Polymorphism	**HRR**	**95% CI**	***P*-value**	**HRR**	**95% CI**	***P*-value**
CHD						
E298D	*G/T* + *T/T* versus *G/G*			*G/T* + *T/T* versus *G/G*		
Model 1*	0.94	0.75–1.17	*P*=0.586	0.87	0.57–1.34	*P*=0.526
Model 2†	1.03	0.80–1.33	*P*=0.819	0.66	0.40–1.09	*P*=0.105
T-786C	*T/C* + *C/C* versus *T/T*			*T/C* + *C/C* versus *T/T*		
Model 1*	1.13	0.90–1.42	*P*=0.210	0.80	0.52–1.20	*P*=0.279
Model 2†	1.24	0.96–1.62	*P*=0.106	0.83	0.53–1.31	*P*=0.421
Stroke						
E298D	*G/T* + *T/T* versus *G/G*			*G/T* + *T/T* versus *G/G*		
Model 1*	0.94	0.65–1.36	*P*=0.742	1.50	0.89–2.53	*P*=0.133
Model 2‡	0.97	0.65–1.44	*P*=0.884	1.35	0.76–2.41	*P*=0.311
T-786C	*T/C* + *C/C* versus *T/T*			*T/C* + *C/C* versus *T/T*		
Model 1*	1.06	0.72–1.55	*P*=0.783	1.70	1.05–2.75	*P*=0.032
Model 2‡	1.09	0.73–1.64	*P*=0.665	1.63	0.93–2.88	*P*=0.090

*Adjusted for age, gender, and study center.

†Adjusted for age, gender, study center, current smoker, diabetes, hypertension, HDL cholesterol, total cholesterol, and body mass index.

‡Adjusted for age, gender, study center, current smoker, diabetes, and hypertension.

Table 16. *E298D* genotype by smoking interaction and risk of incident CHD and stroke.*†

	Caucasian			African-American		
Smoking Exposure	***E298D* Genotype**		**Interaction‡**	***E298D* Genotype**		**Interaction‡**
CHD§	*G/G*	*G/T + T/T*		*G/G*	*G/T + T/T*	
Current smoker	n=365/279	n=416/335		n=182/241	n=44/70	
No	1 (referent)	0.83 (0.61–1.13)	2.10 (1.17–3.76)	1 (referent)	0.63 (0.34–1.16)	1.17 (0.43–3.18)
Yes	1.19 (0.77–1.83)	2.07 (1.39–3.07)	*P*=0.013	1.90 (1.17–3.10)	1.40 (0.62–3.18)	*P*=0.762
Pack-years						
<20 years	1 (referent)	0.84 (0.61–1.17)	1.50 (0.89–2.53)	1 (referent)	0.61 (0.35–1.06)	1.30 (0.43–3.90)
≥20 years	1.23 (0.83–1.83)	1.56 (1.08–2.24)	*P*=0.126	1.19 (0.73–1.93)	0.94 (0.35–2.50)	*P*=0.641
Stroke‖	*G/G*	*G/T + T/T*		*G/G*	*G/T + T/T*	
Current smoker	n=70/296	n=80/363		n=85/254	n=30/68	
No	1 (referent)	0.81 (0.51–1.30)	1.70 (0.71–4.06)	1 (referent)	1.26 (0.57–2.77)	1.24 (0.37–4.19)
Yes	1.58 (0.83–3.00)	2.18 (1.19–3.99)	*P*=0.234	2.00 (1.08–3.69)	3.12 (1.22–7.99)	*P*=0.726
Pack-years						
<20 years	1 (referent)	0.80 (0.46–1.38)	1.48 (0.66–3.31)	1 (referent)	1.36 (0.67–2.74)	1.00 (0.25–4.01)
≥20 years	1.49 (0.81–2.75)	1.77 (0.98–3.21)	*P*=0.337	1.39 (0.70–2.75)	1.88 (0.53–6.62)	*P*=0.999

*Number of cases/non-cases in each genotype cell.

†Data presented as HRR (95% CI).

‡Multiplicative *E298D* by smoking interaction term HRR (95% CI), and *P*-value.

§Adjusted for age, gender, study center, diabetes, hypertension, HDL cholesterol, total cholesterol, and body mass index.

‖Adjusted for age, gender, study center, diabetes, hypertension.

Table 17. *T-786C* genotype by smoking interaction and risk of incident CHD and stroke.*†

	Caucasian			African-American		
Smoking Exposure	***T-786C* Genotype**		**Interaction‡**	***T-786C* Genotype**		**Interaction‡**
CHD§	*T/T*	*T/C + C/C*		*T/T*	*T/C + C/C*	
Current smoker	n=276/247	n=463/362		n=154/212	n=52/90	
No	1 (referent)	1.33 (0.97–1.81)	0.83 (0.46–1.49)	1 (referent)	0.60 (0.34–1.07)	2.04 (0.79–5.31)
Yes	1.92 (1.21–3.05)	2.11 (1.41–3.17)	*P*=0.527	1.68 (1.00–2.83)	2.08 (0.95–4.54)	*P*=0.142
Pack-years						
<20 years	1 (referent)	1.08 (0.77–1.50)	1.44 (0.85–2.44)	1 (referent)	0.66 (0.39–1.11)	1.88 (0.68–5.15)
≥20 years	1.22 (0.79–1.88)	1.89 (1.32–2.70)	*P*=0.179	1.07 (0.63–1.82)	1.32 (0.58–3.00)	*P*=0.222
Stroke‖	*T/T*	*T/C + C/C*		*T/T*	*T/C + C/C*	
Current smoker	n=56/267	n=87/386		n=65/223	n=43/89	
No	1 (referent)	1.09 (0.66–1.79)	0.94 (0.39–2.28)	1 (referent)	1.34 (0.66–2.72)	1.49 (0.45–4.96)
Yes	2.17 (1.06–4.43)	2.22 (1.20–4.11)	*P*=0.892	1.86 (0.94–3.68)	3.72 (1.39–9.99)	*P*=0.515
Pack-years						
<20 years	1 (referent)	0.94 (0.54–1.65)	1.33 (0.59–3.02)	1 (referent)	1.06 (0.55–2.06)	3.73 (1.08–12.9)
≥20 years	1.56 (0.80–3.04)	1.97 (1.09–3.57)	*P*=0.488	1.02 (0.49–2.13)	4.03 (1.54–10.6)	*P*=0.037

*Number of cases/non-cases in each genotype cell.

†Data presented as HRR (95% CI).

‡Multiplicative *T-786C* by smoking interaction term HRR (95% CI), and *P*-value.

§Adjusted for age, gender, study center, diabetes, hypertension, HDL cholesterol, total cholesterol, and body mass index.

‖Adjusted for age, gender, study center, diabetes, hypertension.

Table 18. *NOS3* haplotype frequency by incident CHD or stroke case status.

	CHD			Stroke		
Haplotype*	**Non-case†**	**Incident case†**	***P*-value‡**	**Non-case†**	**Incident case†**	***P*-value‡**
Caucasian§	n=606	n=735		n=650	n=142	
TG	54.4%	53.0%	*P*=0.494	54.2%	53.9%	*P*=0.935
CT	23.0%	23.0%	*P*=0.987	23.0%	22.5%	*P*=0.870
C*G*	13.1%	16.1%	*P*=0.034	13.2%	14.8%	*P*=0.496
*T****T***	9.6%	8.0%	*P*=0.160	9.7%	8.8%	*P*=0.648
African-American§	n=303	n=207		n=313	n=109	
TG	78.8%	79.2%	*P*=0.876	79.3%	72.9%	*P*=0.069
CT	6.5%	3.9%	*P*=0.076	6.0%	7.3%	*P*=0.519
C*G*	9.9%	10.1%	*P*=0.891	9.8%	13.8%	*P*=0.145
*T****T***	4.9%	6.8%	*P*=0.230	4.8%	6.0%	*P*=0.536

*Haplotype frequencies weighted according to cohort random sample strata. Tagging polymorphisms are in bold.

†Estimated copy frequency of each haplotype.

‡Chi-square *P*-value for the distribution of each haplotype by CHD or stroke case status.

§Haplotype includes the *T-786C* and *E298D* polymorphisms, respectively.

Table 19. *NOS3* haplotype by smoking interaction and risk of incident CHD and stroke in Caucasians.*†

Smoking Exposure	Haplotype		Interaction‡
CHD§	*Non-CT*	*CT*	
Current smoker	n=430/350	n=305/256	
No	1 (referent)	1.00 (0.74–1.35)	1.50 (0.83–2.70)
Yes	1.46 (1.00–2.13)	2.18 (1.40–3.38)	*P*=0.179
Pack-years			
<20 years	1 (referent)	0.95 (0.68–1.33)	1.39 (0.84–2.30)
≥20 years	1.32 (0.93–1.87)	1.74 (1.21–2.51)	*P*=0.206
Stroke‖	*Non-CT*	*CT*	
Current smoker	n=84/374	n=58/276	
No	1 (referent)	0.87 (0.53–1.45)	1.59 (0.65–3.86)
Yes	1.67 (0.92–3.04)	2.32 (1.18–4.51)	*P*=0.309
Pack-years			
<20 years	1 (referent)	0.92 (0.52–1.63)	1.24 (0.54–2.80)
≥20 years	1.70 (0.98–2.94)	1.93 (0.99–3.74)	*P*=0.610

*Number of cases/non-cases in each haplotype cell.

†Data presented as HRR (95% CI).

‡Multiplicative haplotype by smoking interaction term HRR (95% CI), and *P*-value.

§Adjusted for age, gender, study center, diabetes, hypertension, HDL cholesterol, total cholesterol, and body mass index.

‖Adjusted for age, gender, study center, diabetes, hypertension.

PART II

P450 EPOXYGENASE PATHWAY AND CARDIOVASCULAR DISEASE RISK

CHAPTER V

GENETIC VARIATION IN SOLUBLE EPOXIDE HYDROLASE (*EPHX2*) AND RISK OF CORONARY HEART DISEASE: THE ATHEROSCLEROSIS RISK IN COMMUNITIES (ARIC) STUDY

Lee CR, North KE, Bray MS, Fornage M, Seubert JM, Newman JW, Hammock BD, Couper DJ, Heiss G, Zeldin DC. Genetic variation in soluble epoxide hydrolase (*EPHX2*) and risk of coronary heart disease: the Atherosclerosis Risk in Communities (ARIC) study. Hum Mol Genet. 2006;15:1640-1649.

Introduction

Coronary heart disease (CHD) is a major cause of morbidity and mortality, with 1.2 million Americans estimated to experience an acute coronary event this year (1). Endothelial dysfunction is integrally involved in its pathogenesis (2), and is independently associated with increased risk of acute cardiovascular events (10). Various risk factors including cigarette smoking contribute to this process, which is typically manifested by impairment in nitric oxide synthesis and activity (6). However, dysfunction in other endothelial pathways may also be important.

Arachidonic acid is metabolized to epoxyeicosatrienoic acids (EETs) in endothelial cells by various cytochromes P450 (20). The EETs possess potent vasodilatory (30, 31), anti-inflammatory (32), and fibrinolytic (33) effects, and are considered one of the primary endothelial-derived hyperpolarizing factors (30, 31). The EETs are inactivated by soluble epoxide hydrolase (*EPHX2*) via hydrolysis to dihydroxyeicosatrienoic acids (DHETs) (28, 125). Multiple polymorphisms in *EPHX2* have been recently discovered, including variants with higher (*K55R*) and lower (*R287Q*) epoxide hydrolase activity (68, 69). An

association between *EPHX2* polymorphisms and subclinical atherosclerosis has been previously reported (70); however, associations with risk of clinical events such as myocardial infarction have not been evaluated.

The primary aim was to determine if genetic variation in *EPHX2* was associated with risk of incident CHD events in individuals enrolled in the biethnic Atherosclerosis Risk in Communities (ARIC) study. A secondary aim was to determine if this risk was modified by environmental factors known to impair endothelial function such as cigarette smoking.

Methods

Study Population. Participants were selected from the ARIC study, a longitudinal, population-based cohort study of 15,792 men and women aged 45 to 64 years from four U.S. communities (Forsyth County, NC; Jackson, MS; Minneapolis, MN; and Washington County, MD) enrolled between 1987 and 1989 (102). Since enrollment, participants have been followed prospectively via annual phone interviews, clinic examinations approximately every three years through 1998, and ongoing abstraction of hospital and death certificate records. The study protocol was approved by the Institutional Review Board of each center, and consent was obtained from each participant.

Ascertainment of Incident CHD Cases. All incident cases that occurred between baseline and December 31, 1998 were evaluated (median follow-up 9.1 years), excluding subjects with a history of CHD or stroke at baseline. Incident CHD (n=1085) was defined as 1) definite or probable myocardial infarction (n=520), 2) electrocardiographic evidence of silent

myocardial infarction (n=112), 3) definite CHD death (n=110), or 4) coronary revascularization procedure (n=343).

The ascertainment of cases and criteria for classification have been previously described (103). All potential events were systematically reviewed and adjudicated by the ARIC Morbidity and Mortality Classification Committee (102, 103). Hospitalized myocardial infarction was classified as definite or probable based on chest pain symptoms, cardiac enzyme levels, and electrocardiographic changes. Definite CHD death was classified based on chest pain symptoms, underlying cause of death, hospitalization records, and medical history. Coronary revascularization procedures included coronary artery bypass grafting and percutaneous coronary interventions.

Baseline Measurements. Detailed demographic, clinical, and biochemical data were obtained from each subject at baseline. Race was self-reported. Prevalent CHD and stroke were defined as history of a physician-diagnosed event. Hypertension was defined as systolic blood pressure ≥140 mmHg, diastolic blood pressure ≥90 mmHg, or current antihypertensive medication use. Diabetes was defined as fasting blood glucose ≥126 mg/dL, nonfasting blood glucose ≥200 mg/dL, physician diagnosis, or pharmacologic treatment. Detailed information on cigarette smoking was obtained through an interview-administered questionnaire.

Cohort Random Sample. A random sample of all ARIC participants without history of CHD or stroke at baseline was assembled to serve as the reference group for the case-cohort comparisons (n=1065, 85 of which are also incident CHD cases). Sampling of the cohort

was stratified on age (<55 or ≥55 years), gender, and race (Caucasian or African-American). Sampling proportions varied across each stratum. The term non-case refers to individuals within the cohort random sample who did not develop incident CHD during follow-up (n=980).

Genotyping. Genomic DNA from all incident CHD cases and the cohort random sample was genotyped for ten polymorphisms in coding and noncoding regions of *EPHX2* (Figure 9), using multiplex matrix-assisted laser desorption/ionization time-of-flight (MALDI-TOF) mass spectrometry (Sequenom, Inc., San Diego, CA) (107) (Appendix II) or Taqman® (Applied Biosystems, Foster City, CA) (126) (Appendix IV) methods, as described. Blind replicates were included for quality control. Missing genotypes were present in <5% of individuals. These polymorphisms were identified from a resequencing effort as part of the NIEHS Environmental Genome Single Nucleotide Polymorphism program (https://dir-apps.niehs.nih.gov/egsnp/home.htm) (69), and specifically selected based on their known functional relevance *in vitro* (68, 69) and/or haplotype tagging properties. Briefly, pairwise linkage disequilibrium statistics were calculated and haplotypes were reconstructed separately in European/Caucasians (n=24) and Africans (n=24) using all polymorphisms along *EPHX2* identified by resequencing (Haploview 3.2) (69, 81). Polymorphisms tagging haplotypes with >5% frequency in either population were selected for genotyping (127).

Biomarker Analysis. Plasma from the most recent clinic visit was obtained from 56 participants selected based on their *K55R* genotype [*A/A* (n=19), *A/G* (n=19), *G/G* (n=18)] and matched for age, gender and race. Plasma samples were extracted and

epoxyoctadecenoic acid (EpOME) to dihydroxyoctadecenoic acid (DHOME) concentrations were quantified using a validated HPLC/MS/MS method, as described (128). Previous studies with *Ephx2*$^{-/-}$ mice suggest that plasma EpOME:DHOME ratios are sensitive and specific biomarkers of soluble epoxide hydrolase activity, with lower EpOME:DHOME values indicative of higher apparent soluble epoxide hydrolase activity (46).

Data Analysis. All incident CHD cases and individuals from the cohort random sample were included in the current analysis (n=2065). Inverse sampling fractions from each stratum were used as weights in variance estimation of adjusted covariate means and proportions by linear and logistic regression, respectively, in non-cases included in the cohort random sample. Hazard rate ratios (HRR) and 95% confidence intervals (CI) for the development of incident CHD in relation to *EPHX2* genotype were calculated by weighted proportional hazards regression, using Barlow's method to account for the stratified random sampling and case-cohort design (109). Model 1 was unadjusted and included only genotype. Model 2 included age, gender, and study center as covariates. Model 3 also included current smoking status, diabetes, hypertension, high density lipoprotein cholesterol, total cholesterol, and body mass index. Assuming an autosomal dominant mode of inheritance, individuals with one or two variant alleles were combined for comparison to wild-type individuals. All analyses were completed separately in Caucasians and African-Americans. Assuming a case-control design and type I error α=0.05, there was approximately 99% and 80% power to detect an odds ratio of 2.0 and 70% and 30% power to detect an odds ratio of 1.5 in Caucasians and African-Americans, respectively, for polymorphisms with a 10% variant genotype frequency.

Gene-environment interaction testing was completed on a multiplicative scale between genotype and baseline current smoking status (yes/no) using a Wald chi-square test for significance of the estimated β-coefficient for the interaction term (110). Because interaction hypothesis testing on a multiplicative scale is underpowered, the critical value for statistical significance was set to $\alpha=0.15$, two-sided (111). Stratified weighted proportional hazards regression was also completed according to baseline current smoking status using the model 3 covariate adjustment strategy (minus current smoking status) to further explore potential interactions.

Cohort random sample allele frequencies were evaluated for deviation from Hardy-Weinberg equilibrium, and pairwise linkage disequilibrium statistics were calculated (Haploview 3.2) (81). Haplotypes and their frequencies were estimated using the phase reconstruction method (PHASE 2.1), which assigned the most probable haplotype pair to each individual (121, 129). Only polymorphisms with >5% frequency were considered for haplotype reconstruction, which included polymorphisms 1, 5, 6, 7, and 10 in Caucasians and 1, 2, 4, 5, 6, and 10 in African-Americans (Figure 9). Haplotype frequencies were compared across case status by chi-square, and only haplotypes with >5% frequency were considered. Frequency comparisons were repeated using the expectation-maximization algorithm (Haploview 3.2) (81), which accounted for the uncertainty in haplotype reconstruction by weight-adjusting each inferred haplotype according to its estimated posterior haplotype probability. Associations between haplotype (0,1,2) and risk of incident CHD were also evaluated by modeling each haplotype relative all other haplotypes using Barlow's method (109). The association analysis was repeated after excluding individuals with posterior haplotype probabilities <0.75.

To minimize the impact of the multiple statistical tests conducted in the current analysis, the false discovery rate (FDR) *q*-value was estimated for each comparison, which is defined as the proportion of statistical tests deemed significant that are actually false-positives (QVALUE) (112). In order to calculate conservative *q*-value estimates, statistical tests from the model 1, 2, and 3 association analysis of each nonsynonymous polymorphism and reconstructed haplotype were considered as independent even though each model assessed the same independent variable.

Plasma EpOME:DHOME ratios were compared across *K55R* genotype by analysis of variance, and post-hoc comparisons between genotypes were completed using the Tukey-Kramer test. All data are presented as mean ± standard error of the mean.

Results

Study Population. Significant baseline differences in various risk factors were observed between incident CHD cases and non-cases included in the cohort random sample (Table 6). Cases were significantly older and more likely to be male, cigarette smokers, diabetic, hypertensive and have abnormal fasting lipid panels compared to non-cases.

***EPHX2* Genotype.** The observed race-specific allele frequencies of the 10 polymorphisms evaluated are presented in Figure 9. The distribution of each was in Hardy-Weinberg equilibrium in both Caucasians and African-Americans ($P>0.05$). Minimal evidence of pairwise linkage disequilibrium was observed between polymorphisms within each race; however, polymorphism 10 demonstrated some degree of association with polymorphisms 1

(D'=0.97, r^2=0.28), 5 (D'=0.96, r^2=0.22), and 6 (D'=0.93, r^2=0.28) in Caucasians and 5 (D'=1.0, r^2=0.20) in African-Americans.

***K55R* Biomarker Analysis.** Participants with one (*A/G*) or two (*G/G*) copies of the *K55R* polymorphism variant allele demonstrated significantly lower plasma 12,13-EpOME:DHOME ratios compared to wild-type (*A/A*) individuals (*A/A*: 0.40±0.03 versus *A/G*: 0.31±0.04 versus *G/G*: 0.28±0.03; *P*=0.030), indicative of higher apparent soluble epoxide hydrolase activity *in vivo*. Significant differences in plasma 9,10-EpOME:DHOME ratios were not observed (*A/A*: 0.34±0.03 versus *A/G*: 0.28±0.03 versus *G/G*: 0.26±0.03; *P*=0.155).

In the race-stratified analysis, Caucasians with one or two copies of the *K55R* variant allele demonstrated significantly lower plasma 9,10-EpOME:DHOME (*A/A*: 0.42±0.04 versus *A/G*: 0.28±0.04 versus *G/G*: 0.24±0.04; *P*=0.014) and 12,13-EpOME:DHOME ratios (*A/A*: 0.42±0.04 versus *A/G*: 0.31±0.04 versus *G/G*: 0.25±0.04; *P*=0.011) compared to wild-type individuals (Figure 10A). Significant differences across genotype were not observed in African-Americans for either the 9,10-EpOME:DHOME (*A/A*: 0.28±0.04 versus *A/G*: 0.27±0.05 versus *G/G*: 0.29±0.05; *P*=0.983) or 12,13-EpOME:DHOME ratio (*A/A*: 0.38±0.05 versus *A/G*: 0.31±0.06 versus *G/G*: 0.31±0.06; *P*=0.602) (Figure 10B). Irrespective of genotype, differences in 9,10-EpOME:DHOME (*P*=0.395) and 12,13-EpOME:DHOME ratios (*P*=0.897) were not observed across race.

Genotype Association Analysis. The *K55R* polymorphism variant allele was significantly more common among Caucasian CHD cases compared to cohort random sample non-cases

(20.8% versus 15.3%, respectively, *P*=0.012) (Table 20). This difference in genotype frequency was observed in both heterozygous *A/G* (19.8% versus 14.9%) and homozygous *G/G* (1.0% versus 0.4%) individuals. Significant differences were not observed in African-Americans (*P*=0.344) (Table 20).

Presence of the *K55R* variant allele was associated with significantly higher risk of incident CHD in Caucasians (model 3, HRR 1.45, 95% CI 1.05 to 2.01, *P*=0.026, *q*=0.083) (Table 21). Individuals with the heterozygous *A/G* (model 3, HRR 1.40, 95% CI 1.00 to 1.95, *P*=0.047) and homozygous *G/G* (model 3, HRR 3.47, 95% CI 1.05 to 11.5, *P*=0.041) genotypes were at a significantly greater risk for developing CHD relative to wild-type *A/A* individuals. This association was not modified by gender (*P* for interaction=0.432).

No significant differences in the genotype frequency of other nonsynonymous polymorphisms were observed across case status in either race (Table 20). Moreover, presence of the *R103C*, *R287Q*, *402InsR*, or *E470G* polymorphism variant alleles were not significantly associated with risk of CHD (Table 21). A significant difference in baseline diabetes diagnosis was observed between Caucasians in the cohort random sample with (*G/A* or *A/A*) and without (*G/G*) the *R287Q* polymorphism variant allele (1.6% versus 10.2%, respectively, *P*<0.001). The *R287Q* variant allele was more common in diabetic CHD cases compared to non-cases (20.1% versus 3.6%, respectively, *P*<0.001); however, differences in genotype frequency were not observed in nondiabetics (20.9% versus 20.9%, respectively, *P*=0.987). Inclusion of the *R287Q**diabetes interaction term in model 3 substantially attenuated the observed trend between presence of the *R287Q* variant allele and risk of incident CHD in Caucasians (HRR 1.06, 95% CI 0.76 to 1.48, *P*=0.710). Moreover, stratified analysis demonstrated no association between the *R287Q* variant allele and risk of

CHD in nondiabetic individuals (model 3 minus diabetes, HRR 1.05, 95% CI 0.73 to 1.50, *P*=0.799).

***K55R* Genotype and Smoking.** The interaction between the *K55R* variant allele, cigarette smoking status at baseline and risk of CHD in Caucasians did not attain statistical significance (Table 22). When stratified by current smoking status at baseline, the *K55R* variant allele was significantly more common among Caucasian cases who smoked compared to non-cases (25.6% versus 13.6%, respectively, *P*=0.006). Significant differences were not observed in non-smokers (18.5% versus 15.8%, respectively, *P*=0.291). Caucasian smokers carrying the *K55R* variant allele were at higher risk of CHD compared to smokers without the polymorphism (model 3 minus current smoking, HRR 2.06, 95% CI 0.99 to 4.27, *P*=0.053). No significant association was observed in non-smokers (model 3 minus current smoking, HRR 1.26, 95% CI 0.87 to 1.82, *P*=0.217). Smoking status did not modify risk associated with the *K55R* variant allele in African-Americans (*P* for interaction=0.709).

Haplotype Association Analysis. Haplotype reconstruction including polymorphisms 1, 5, 6, 7, and 10 in Caucasians and 1, 2, 4, 5, 6, and 10 in African-Americans identified six common haplotypes in Caucasians and seven in African-Americans, which accounted for 97.2% and 92.3% of all chromosomes, respectively. A significant difference in the overall haplotype distribution was observed in Caucasians with and without CHD (*P*=0.021) (Table 23); however, no significant difference was observed in African-Americans (*P*=0.315) (Table 24).

In Caucasians, haplotype *AGGDA* (all wild-type alleles) was significantly less frequent (23.6% versus 27.6%, *P*=0.034), and haplotype ***G****GGD****G*** (tagged by the *K55R* and *A53415G* 3'UTR variant alleles) was significantly more frequent (10.7% versus 7.6%, *P*=0.010) in CHD cases compared to non-cases, respectively (Table 23). Similar differences in haplotype *AGGDA* and ***G****GGD****G*** frequency across case status were also observed using the expectation-maximization algorithm (*P*=0.010 and *P*=0.052, respectively). Moreover, presence of haplotype *AGGDA* was associated with significantly lower risk of CHD after covariate adjustment (model 3, HRR 0.78, 95% CI 0.63 to 0.97, *P*=0.028, *q*=0.083), while presence of haplotype ***G****GGD****G*** was associated with significantly higher CHD risk (model 3, HRR 1.45, 95% CI 1.04 to 2.02, *P*=0.030, *q*=0.083) (Table 23). Significant associations were also observed after excluding the 0.8% of individuals with a posterior haplotype probability <0.75 from the analysis (*P*=0.025 and *P*=0.027, respectively).

In African-Americans, haplotype *ACGGGA* (all wild-type alleles) was significantly more frequent (17.3% versus 12.2%, *P*=0.026) in CHD cases compared to non-cases, respectively (Table 24). A similar difference was also observed using the expectation-maximization algorithm (*P*=0.060). Presence of haplotype *ACGGGA* was associated with higher risk of CHD after covariate adjustment (model 3, HRR 1.47, 95% CI 1.01 to 2.13, *P*=0.042, *q*=0.280) (Table 24); however, this association was substantially weakened after exclusion of the 6.7% of individuals with a posterior haplotype frequency <0.75 (model 3, HRR 1.37, 95% CI 0.92 to 2.05, *P*=0.119), and should be interpreted with caution.

Discussion

The current analysis identified a statistically significant association between genetic variation in soluble epoxide hydrolase and risk of incident CHD in Caucasians enrolled in the ARIC study, implicating *EPHX2* as a potential cardiovascular disease-susceptibility gene. Specifically, presence of the *K55R* polymorphism variant allele was associated with significantly higher risk of developing CHD in Caucasians. Consistent with previous *in vitro* findings (69), higher apparent soluble epoxide hydrolase activity was observed *in vivo* in Caucasians carrying the *K55R* variant allele. Variation in *EPHX2* at the haplotype level was also associated with risk of CHD in Caucasians, suggesting multiple variants within or near *EPHX2* may contribute to disease risk.

The role of endothelial dysfunction in the pathogenesis of atherosclerotic cardiovascular disease has become increasingly appreciated. Endothelial dysfunction is typically manifested by impairment in endothelial-dependent vasodilation (2), and is associated with increased risk of acute cardiovascular events (10). The vasodilatory and anti-inflammatory properties of EETs are important mediators of this process (20, 130). Recent data have demonstrated higher CHD risk in individuals carrying the *G-50T* polymorphism variant allele in *CYP2J2*, which exhibits lower promoter activity and EET biosynthesis (64). Soluble epoxide hydrolase rapidly hydrolyzes EETs to DHETs, and is integrally involved in regulation of their cellular levels and vascular effects (28, 125, 131). *EPHX2*$^{-/-}$ mice have significantly lower systolic blood pressures compared to wild-type mice (45). Soluble epoxide hydrolase inhibitors significantly reduce blood pressure in spontaneously and angiotensin II-induced hypertensive rats (28, 47, 132), inhibit vascular smooth muscle cell proliferation (48), possess potent anti-inflammatory effects (49), and represent a therapeutic strategy of

potential clinical utility for the treatment of cardiovascular disease. Moreover, a significant association between genetic variation in *EPHX2* and risk of ischemic stroke events was recently reported (133).

Resequencing efforts have identified nonsynonymous polymorphisms in *EPHX2* with higher (*K55R*, *C154Y*, *E470G*) and lower (*R287Q*, *402InsR*) epoxide hydrolase activity *in vitro* relative to wild-type enzyme (68, 69). Higher apparent epoxide hydrolase activity was observed *in vivo*, as measured by EpOME:DHOME ratios, in Caucasians carrying at least one *K55R* variant allele; however, altered EpOME:DHOME ratios were not observed across *K55R* genotype in African-American individuals. Undetectable plasma EET concentrations precluded calculation of EET:DHET ratios. Based on the role of *EPHX2* in endothelial function, it was hypothesized that higher epoxide hydrolase activity would be associated with higher risk of acute coronary events. A significant association between the *K55R* variant allele and higher risk of incident CHD in Caucasians is consistent with this hypothesis.

Cigarette smoking substantially impairs endothelial-dependent vasodilation in humans (6, 134), in part via inhibition of nitric oxide synthesis and activity (17), and modifies the association between endothelial nitric oxide synthase polymorphisms, endothelial function, and cardiovascular disease risk (57, 123, 135) (Chapter IV). Perhaps presence of established underlying endothelial dysfunction, as observed in cigarette smokers, may be necessary for these genetic variants to significantly influence endothelial function and cardiovascular disease risk. Interestingly, exposure to cigarette smoke also significantly increases vascular *EPHX2* expression in mice (136), suggesting upregulated EET hydrolysis may contribute to the deleterious effects of cigarette smoking in the endothelium. Cigarette smoking history did not appear to influence plasma EpOME:DHOME ratios in the current biomarker study

(data not shown); however, this analysis was not designed or powered to specifically characterize such comparisons. Although preliminary, these findings suggest that the risk of CHD associated with the *K55R* variant allele may be highest in cigarette smokers. Future studies in larger populations will be required to characterize this potential gene-environment interaction and the mechanistic contribution of *EPHX2* to the vascular effects of cigarette smoking.

Using haplotype tagging polymorphisms identified from a previous resequencing effort, the haplotype analysis suggests that variation along the *EPHX2* gene is also an important determinant of CHD risk in Caucasians. Distribution of reconstructed haplotypes differed significantly across individuals with and without incident CHD, and haplotypes ***G****GGD****G*** and *AGGDA* were associated with significantly higher and lower CHD risk, respectively. The ***G****GGD****G*** haplotype was tagged by the *K55R* variant allele, which was associated with significantly higher *in vivo* soluble epoxide hydrolase activity and CHD risk in the genotype analysis. The *R287Q* and *402InsR* variant alleles, which have been associated with lower soluble epoxide hydrolase activity *in vitro* (68, 69), were not located on either the ***G****GGD****G*** or *AGGDA* haplotypes. Since haplotypes are inferred, some uncertainty exists in the haplotype assigned to each individual. This was mitigated by minimizing the number of polymorphisms included in haplotype reconstruction (137). Moreover, similar results were observed using the expectation-maximization algorithm, which accounted for posterior haplotype probabilities in the frequency comparisons across case status (81), and after excluding individuals with posterior haplotype probabilities <0.75.

The lack of an association between CHD and the *K55R* polymorphism in African-Americans could be due to lower statistical power in this subset. However, there was no

apparent influence of *K55R* genotype on *in vivo* soluble epoxide hydrolase activity in African-Americans, whereas significant genotype-dependent differences were observed in Caucasians. Perhaps certain genetic and/or environmental factors not accounted for in the current analysis could have contributed to these racial differences in soluble epoxide hydrolase activity and CHD risk. Future studies evaluating the vascular effects of *EPHX2* in Caucasians and African-Americans appear warranted, particularly since racial differences in endothelial-targeted therapies have been reported in other cardiovascular disease populations (138).

An association between the *R287Q* variant allele and increased coronary artery calcification, a non-invasive measure of atherosclerotic burden, was recently reported in African-Americans (70). The mechanism underlying this association remains unclear since this variant has demonstrated lower soluble epoxide hydrolase activity *in vitro* (68, 69). A significant association between this variant and risk of CHD clinical events was not observed in the current analysis. Although a nonsignificant trend toward higher risk was observed in Caucasians (model 3 only), this relationship was modified by baseline diabetes diagnosis. No association with CHD risk was observed in nondiabetics, while the apparent trend in diabetics was driven by a lower *R287Q* minor allele frequency in diabetic non-cases (0.017) than expected based on previously reported frequencies (approximately 0.10) (69, 70).

Although the current study evaluated rigorously ascertained incident events, mechanisms underlying the observed associations between genetic variation in *EPHX2* and CHD risk were not elucidated. Moreover, the *K55R* polymorphism could simply be a marker in linkage disequilibrium with the true causative locus. However, the current analysis accounted for multiple *EPHX2* polymorphisms and also demonstrated significant associations between

haplotype and CHD risk in Caucasians. Although polymorphisms in this candidate gene with known functional relevance *in vitro* and/or haplotype tagging properties were specifically selected, and a hypothesis-driven approach in the analysis was utilized, it may be difficult to gauge the statistical significance of these findings considering the number of comparisons completed. However, concerns surrounding false negative findings (i.e., missing true associations) are at least as important. In order to minimize the impact of the multiple tests completed in the current analysis the FDR was assessed across all completed tests in the genotype and haplotype association analysis, recognizing that such an approach is likely an over-correction since certain genotype and haplotype associations are not completely independent and the same independent variables were evaluated by each of the three models utilized in the analysis. Since all *q*-values in Caucasians were conservatively estimated to be 0.083 or less, there is a high level of confidence in the reported findings; although, validation in an independent population is necessary.

In conclusion, these findings suggest that genetic variation in *EPHX2*, particularly presence of the *K55R* polymorphism variant allele, may be an important risk factor for the development of CHD clinical events in Caucasians. Association studies in different populations will undoubtedly be required to validate these findings, in addition to molecular and physiological studies evaluating the mechanistic relationship between soluble epoxide hydrolase, endothelial function, and cardiovascular disease risk.

Table 20. Nonsynonymous *EPHX2* polymorphism frequency by CHD case status.

Caucasian				**African-American**			
Genotype*	**Non-cases**	**CHD cases**	***P*-value**	**Genotype***	**Non-cases**	**CHD cases**	***P*-value**
K55R				***K55R***			
A/A	461 (84.7%)	608 (79.2%)		*A/A*	179 (57.6%)	138 (61.9%)	
A/G + G/G	87 (15.3%)	160 (20.8%)	*P*=0.012	*A/G + G/G*	127 (42.4%)	85 (38.1%)	*P*=0.344
A allele	92.1%	89.1%		*A* allele	76.4%	78.9%	
G allele	7.8%	10.9%	*P*=0.009	*G* allele	23.6%	21.1%	*P*=0.351
R103C				***R103C***			
C/C	565 (98.7%)	773 (100%)		*C/C*	247 (80.7%)	180 (81.1%)	
C/T + T/T	8 (1.3%)	0 (0%)	*P*=N/A	*C/T + T/T*	60 (19.3%)	42 (18.9%)	*P*=0.915
C allele	99.4%	100%		*C* allele	90.0%	90.1%	
T allele	0.6%	0%	*P*=N/A	*T* allele	10.0%	9.9%	*P*=0.968
R287Q				***R287Q***			
G/G	496 (80.6%)	616 (79.2%)		*G/G*	258 (82.9%)	190 (86.0%)	
G/A + A/A	118 (19.4%)	162 (20.8%)	*P*=0.525	*G/A + A/A*	49 (17.1%)	31 (14.0%)	*P*=0.361
G allele	89.9%	89.0%		*G* allele	91.3%	92.3%	
A allele	10.1%	11.0%	*P*=0.485	*A* allele	8.7%	7.7%	*P*=0.569

Table 20 (con't).

Caucasian				**African-American**			
Genotype*	**Non-cases**	**CHD cases**	***P*-value**	**Genotype***	**Non-cases**	**CHD cases**	***P*-value**
***402InsR*†**				***402InsR*†**			
D/D	527 (87.6%)	687 (88.1%)		*D/D*	301 (99.2%)	219 (98.2%)	
D/I + I/I	76 (12.4%)	93 (11.9%)	*P*=0.792	*D/I + I/I*	3 (0.8%)	4 (1.8%)	*P*=N/A
D allele	93.5%	93.8%		*D* allele	99.6%	99.1%	
I allele	6.5%	6.2%	*P*=0.694	*I* allele	0.4%	0.9%	*P*=N/A
E470G				***E470G***			
A/A	557 (100%)	774 (100%)		*A/A*	300 (97.8%)	222 (97.8%)	
A/G + G/G	0 (0%)	0 (0%)	*P*=N/A	*A/G + G/G*	5 (2.2%)	5 (2.2%)	*P*=0.974
A allele	100%	100%		*A* allele	98.9%	98.9%	
G allele	0%	0%	*P*=N/A	*G* allele	1.1%	1.1%	*P*=0.975

*Data presented as absolute (percent) genotype frequency and allele frequency. Frequencies are weighted according to the sampling fraction. Data for polymorphism 3 (*C154Y*) and 8 (*V422A*) are not included due to minor allele frequencies ≤0.1% in both races.

†For *402InsR* (polymorphism 7), the deletion allele is designated by *D*, and the *CGT* insertion allele by *I*.

Table 21. Hazard rate ratio between nonsynonymous polymorphisms in *EPHX2* and risk of incident CHD.

	Caucasian			African-American		
Polymorphism	**HRR**	**95% CI**	***P*-value**	**HRR**	**95% CI**	***P*-value**
K55R	*A/G* + *G/G* versus *A/A*			*A/G* + *G/G* versus *A/A*		
Model 1*	1.43	1.07 – 1.90	*P*=0.015	0.87	0.60 – 1.27	*P*=0.474
Model 2†	1.36	1.01 – 1.83	*P*=0.045	0.87	0.61 – 1.25	*P*=0.466
Model 3‡	1.45	1.05 – 2.01	*P*=0.026	0.76	0.50 – 1.16	*P*=0.208
R103C				*C/T* + *T/T* versus *C/C*		
Model 1*	N/A			0.87	0.55 – 1.35	*P*=0.528
Model 2†	N/A			0.95	0.61 – 1.47	*P*=0.801
Model 3‡	N/A			0.94	0.58 – 1.51	*P*=0.787
R287Q	*G/A* + *A/A* versus *G/G*			*G/A* + *A/A* versus *G/G*		
Model 1*	1.03	0.78 – 1.36	*P*=0.827	0.87	0.52 – 1.44	*P*=0.560
Model 2†	1.17	0.88 – 1.54	*P*=0.284	0.90	0.55 – 1.49	*P*=0.685
Model 3‡	1.34	0.96 – 1.87	*P*=0.082	1.13	0.64 – 2.01	*P*=0.676

Table 21 (con't).

	Caucasian			African-American		
Polymorphism	**HRR**	**95% CI**	***P*-value**	**HRR**	**95% CI**	***P*-value**
402InsR[§]	*D/I* + *I/I* versus *D/D*			*D/I* + *I/I* versus *D/D*		
Model 1*	0.96	0.69 – 1.34	*P*=0.819	1.64	0.47 – 5.86	*P*=0.603
Model 2[†]	1.00	0.72 – 1.39	*P*=0.998	1.40	0.39 – 4.97	*P*=0.603
Model 3[‡]	1.00	0.70 – 1.45	*P*=0.990	1.26	0.43 – 3.71	*P*=0.675
E470G				*A/G* + *G/G* versus *A/A*		
Model 1*	N/A			1.33	0.35 – 5.02	*P*=0.679
Model 2[†]	N/A			1.71	0.50 – 5.85	*P*=0.396
Model 3[‡]	N/A			1.87	0.52 – 6.75	*P*=0.338

HRR = hazard rate ratio, CI = confidence interval, N/A = modeling not completed since SNP frequency = 0% in incident coronary heart disease case and/or non-case group. Data for polymorphism 3 (*C154Y*) and 8 (*V422A*) are not included due to minor allele frequencies ≤0.1% in both races.

*Unadjusted.

[†]Adjusted for age, gender, and study center.

[‡]Adjusted for age, gender, study center, current smoker, diabetes, hypertension, high density lipoprotein cholesterol, total cholesterol, and body mass index.

[§]For *402InsR* (polymorphism 7), the deletion allele is designated by *D*, and the *CGT* insertion allele by *I*.

Table 22. *K55R* by smoking interaction and risk of incident CHD in Caucasians.

Smoking Exposure	Susceptibility Genotype (*K55R*)	
	A/A	***A/G + G/G***
Non-current smokers		
Model 2*	1 (referent)	1.16 (0.81 – 1.64)
Model 3†	1 (referent)	1.26 (0.87 – 1.80)
Current Smokers		
Model 2*	1.57 (1.17 – 2.11)	2.84 (1.62 – 4.99)
Model 3†	1.57 (1.14 – 2.16)	2.93 (1.54 – 5.55)

Data presented as Hazard Rate Ratio (95% confidence interval).

*Adjusted for age, gender, and study center (interaction term: HRR 1.57, 95% CI 0.78-3.13, *P*=0.205).

†Adjusted for age, gender, study center, diabetes, hypertension, high density lipoprotein cholesterol, total cholesterol, and body mass index (interaction term: HRR 1.49, 95% CI 0.69-3.18, *P*=0.308).

Table 23. *EPHX2* haplotypes and risk of incident CHD in Caucasians.

	Distribution Analysis			Association Analysis		
Haplotype[*,†,‡]	**Non-cases**	**CHD cases**	***P*-value**[§]	**HRR**[‖]	**95% CI**	***P*-value**
	n=510	n=748				
*A**A**GDA*	41.5%	43.8%		1.02	0.84 – 1.24	*P*=0.842
AGGDA	27.6%	23.6%		0.78	0.63 – 0.97	*P*=0.026
*AGA*D***G***	9.9%	10.7%		1.39	0.97 – 1.99	*P*=0.073
G*GGD****G***	7.6%	10.7%		1.45	1.04 – 2.02	*P*=0.030
*AGG**I**A*	6.5%	6.2%		0.98	0.67 – 1.42	*P*=0.908
*AGGD****G***	6.9%	5.1%	*P*=0.021	0.84	0.58 – 1.22	*P*=0.367

HRR = hazard rate ratio, CI = confidence interval

*Bold nucleotides represent haplotype tagging polymorphisms.

†Estimated copy frequency of each haplotype weighted according to the sampling fraction.

‡Haplotype includes polymorphisms 1, 5, 6, 7, and 10 respectively. For polymorphism 7 (*402InsR*), the deletion allele is designated by *D*, and the *CGT* insertion allele by *I*.

§Chi-square *P*-value for the overall distribution of haplotypes by coronary heart disease case status.

‖Adjusted for age, gender, study center, current smoker, diabetes, hypertension, high density lipoprotein cholesterol, total cholesterol, and body mass index.

Table 24. *EPHX2* haplotypes and risk of incident CHD in African-Americans.

	Distribution Analysis			Association Analysis		
Haplotype[*,†,‡]	**Non-cases**	**CHD cases**	***P*-value**[§]	**HRR**[‖]	**95% CI**	***P*-value**[‖]
	n=305	n=220				
*ACGGG**G***	24.3%	21.8%		0.84	0.57 – 1.24	*P*=0.377
G**CGGG**G	22.6%	20.9%		0.85	0.59 – 1.23	*P*=0.396
*AC**C**GG**G***	15.1%	15.6%		1.09	0.70 – 1.68	*P*=0.703
ACGGGA	12.2%	17.3%		1.47	1.01 – 2.13	*P*=0.042
*ACG**A**GA*	9.8%	10.1%		1.08	0.68 – 1.70	*P*=0.750
*ACGG**AG***	8.8%	6.2%		0.89	0.48 – 1.67	*P*=0.718
*A**T**GGGA*	7.2%	8.2%	*P*=0.315	1.32	0.78 – 2.23	*P*=0.304

*Bold nucleotides represent haplotype tagging polymorphisms.

†Estimated copy frequency of each haplotype weighted according to the sampling fraction.

‡Haplotype includes polymorphisms 1, 2, 4, 5, 6, and 10, respectively.

§Chi-square *P*-value for the overall distribution of haplotypes by coronary heart disease case status.

‖Adjusted for age, gender, study center, current smoker, diabetes, hypertension, high density lipoprotein cholesterol, total cholesterol, and body mass index.

Figure Legends

Figure 9. Nucleotide positions of the 10 polymorphisms evaluated are given relative to the *EPHX2* cDNA start site (Genbank accession number NT_022666). Activity is reported as higher (↑), lower (↓), unchanged (↔), or unknown (?) relative to wild-type enzyme based on previous *in vitro* studies (68, 69). Minor allele frequencies are presented separately by race, and *P*-values for their comparison are reported.

Figure 10. Mean (± standard error of the mean) calculated plasma EpOME:DHOME ratios are presented according to *K55R* genotype in Caucasians (A) and African-Americans (B). 9,10-EpOME:DHOME (black bars, **P*<0.05 versus *A/A*), and 12,13-EpOME:DHOME (white bars, ^*P*<0.05 versus *A/A*) ratios are presented.

Figure 9. Selected *EPHX2* polymorphisms for genotyping.

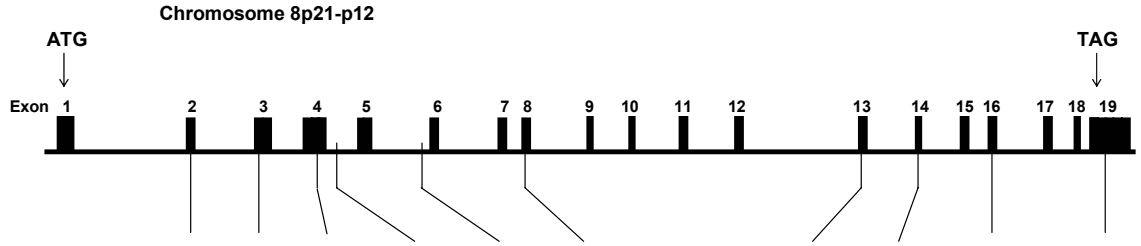

Polymorphism	1	2	3	4	5	6	7	8	9	10
dbSNP ID		rs17057255			rs57816586	rs751141				rs1042032
Nucleotide Position	9846	12582	13928	14029	20675	25206	45678	47539	50360	53415
Major Allele	A	C	G	G	G	G	-	T	A	A
Minor Allele	G	T	A	C	A	A	CGT	C	G	G
Amino Acid Substitution	K55R	R103C	C154Y	-	-	R287Q	402InsR	V422A	E470G	-
Activity	↑	↔	↑	?	?	↓	↓	↔	↑	?
Minor allele frequency										
Caucasian	0.098	0.003	0	0.002	0.427	0.106	0.064	0	0	0.261
AA	0.223	0.100	0.001	0.149	0.090	0.080	0.007	0	0.009	0.670
P-value	<0.001	<0.001	N/A	<0.001	<0.001	0.442	<0.001	N/A	N/A	<0.001

Figure 10. Biomarker of soluble epoxide hydrolase activity by *K55R* genotype and race.

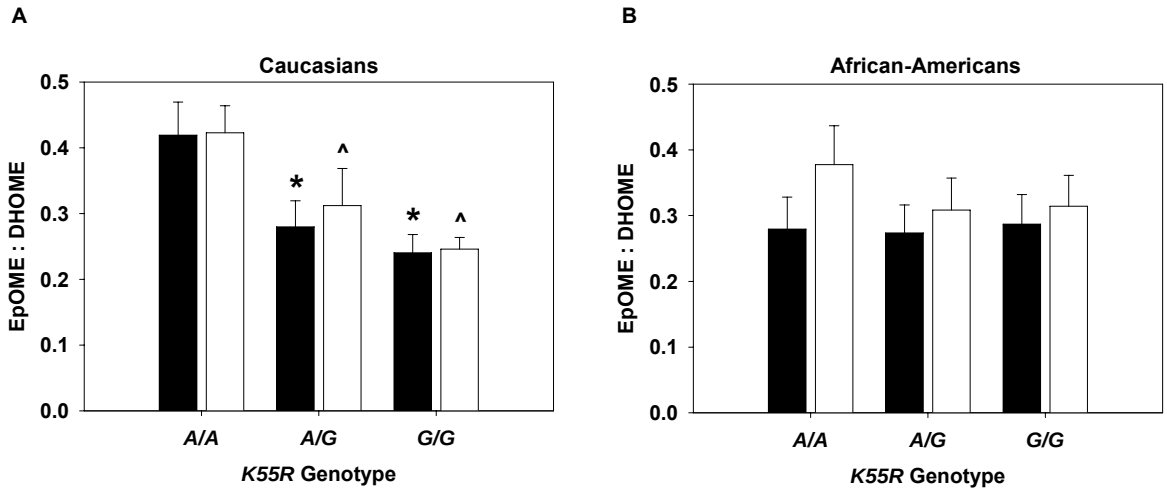

CHAPTER VI

CYP2J2 AND *CYP2C8* POLYMORPHISMS AND CORONARY HEART DISEASE RISK: THE ATHEROSCLEROSIS RISK IN COMMUNITIES (ARIC) STUDY

Introduction

Coronary heart disease (CHD) is a major cause of morbidity and mortality, with 1.2 million Americans estimated to experience a new or recurrent acute coronary syndrome event this year. (1). Endothelial dysfunction is associated with risk of CHD events such as myocardial infarction (10). Various risk factors including cigarette smoking (6) contribute to this process, which has been primarily ascribed to functional impairments in nitric oxide biosynthesis and activity. However, dysfunction in other endothelial pathways also appears to be important.

Arachidonic acid is oxidatively metabolized to epoxyeicosatrienoic acids (EETs) in endothelial cells and cardiomyocytes by the cytochromes P450 epoxygenases CYP2J2 and CYP2C8 (20). The EETs have potent vasodilatory (30, 31), anti-inflammatory (32), fibrinolytic (33) and post-ischemic cardioprotective (34, 35) effects, and are considered one of the primary endothelial-derived hyperpolarizing factors (30, 31). Multiple genetic polymorphisms in *CYP2J2* and *CYP2C8* have been recently discovered (63-66). In *CYP2J2*, the *G-50T* (*CYP2J2*7*) polymorphism in the proximal promoter disrupts a Sp1 transcription factor binding site and leads to reduced *CYP2J2* transcription (64). In *CYP2C8*, the *I269F* (*CYP2C8*2*), *R139K/K399R* (*CYP2C8*3*) and *I264M* (*CYP2C8*4*) nonsynonymous variants possess lower CYP2C8 metabolic activity *in vitro* (65, 66). Case-control studies have

demonstrated an association between the *CYP2J2*7* variant allele and higher risk of angiographically-documented CHD in a German population (64), and between the *CYP2C8*3* variant allele and higher risk of prevalent myocardial infarction in a Swedish cohort (67). However, associations between polymorphisms in these genes and risk of incident CHD clinical events remain to be evaluated.

The primary aim was to determine if genetic variation in *CYP2J2* and *CYP2C8* was associated with risk of incident CHD events in individuals enrolled in the biethnic Atherosclerosis Risk in Communities (ARIC) study. A secondary aim was to determine if this risk was modified by environmental factors known to impair endothelial function such as cigarette smoking.

Methods

Study Population. Participants were selected from the ARIC study, a longitudinal, population-based cohort study of 15,792 men and women aged 45 to 64 years from four U.S. communities (Forsyth County, NC; Jackson, MS; Minneapolis, MN; and Washington County, MD) enrolled between 1987 and 1989 (102). Since enrollment, participants have been followed prospectively via annual phone interviews, clinic examinations approximately every three years through 1998, and ongoing abstraction of hospital and death certificate records. The study protocol was approved by the Institutional Review Board of each center, and consent was obtained from each participant.

Ascertainment of Incident CHD Cases. All incident cases that occurred between baseline and December 31, 1998 were evaluated (median follow-up 9.1 years), excluding participants

with a history of a CHD or stroke event at baseline. Incident CHD (n=1085) was defined as 1) definite or probable myocardial infarction (n=520), 2) electrocardiographic evidence of silent myocardial infarction (n=112), 3) definite CHD death (n=110), or 4) coronary revascularization procedure (n=343).

The ascertainment of cases and criteria for classification have been previously described (103). All potential events were systematically reviewed and adjudicated by the ARIC Morbidity and Mortality Classification Committee (102, 103). Hospitalized myocardial infarction was classified as definite or probable based on chest pain symptoms, cardiac enzyme levels, and electrocardiographic changes. Definite CHD death was classified based on chest pain symptoms, underlying cause of death, hospitalization records, and medical history. Coronary revascularization procedures included coronary artery bypass grafting and percutaneous coronary interventions.

Baseline Measurements. Detailed demographic, clinical, and biochemical data were obtained from each participant at baseline, as described (139) (Chapter V). Briefly, race was self-reported and detailed information on cigarette smoking was obtained through an interview-administered questionnaire.

Cohort Random Sample. A random sample of all ARIC participants without history of CHD or stroke at baseline was assembled to serve as the reference group for the case-cohort comparisons (n=1065, 85 of which are also incident CHD cases). Sampling of the cohort was stratified on age (<55 or ≥55 years), gender, and race (Caucasian or African-American). Sampling proportions varied across each stratum.

Genotyping. Genomic DNA from all incident CHD cases and the cohort random sample was genotyped for ten polymorphisms in coding and noncoding regions of *CYP2J2* (Figure 11) and the nonsynonymous *I269F* (*CYP2C8*2*), *K399R* (*CYP2C8*3*) and *I264M* (*CYP2C8*4*) polymorphisms in *CYP2C8* using either multiplex matrix-assisted laser desorption/ionization time-of-flight (MALDI-TOF) mass spectrometry (Sequenom, Inc., San Diego, CA) (107) (Appendix II) or BeadArray (Illumina, Inc., San Diego, CA) (108) (Appendix III) methods, as described. Blind replicates were included for quality control.

The *CYP2J2* polymorphisms were identified from a resequencing effort as part of the NIEHS Environmental Genome Single Nucleotide Polymorphism program (https://dir-apps.niehs.nih.gov/egsnp/home.htm) (63) and specifically selected based on their known functional relevance *in vitro* and/or haplotype tagging properties. Due to the very low frequency of nonsynonymous variants in *CYP2J2*, evaluation of potential associations between common *CYP2J2* haplotypes and CHD risk were also of particular interest. Briefly, pairwise linkage disequilibrium (LD) statistics were calculated and haplotypes were reconstructed separately in European/Caucasians (n=24) and Africans (n=24) using all polymorphisms in *CYP2J2* identified by resequencing (Haploview 3.2) (63, 81). Polymorphisms tagging haplotypes with >5% frequency in either population were selected for genotyping.

Three nonsynonymous polymorphisms in *CYP2C8* were selected since these represent the most frequent variants in Caucasian or African-American populations with known functional relevance (65, 66). The *CYP2C8*3* variant consists of two nonsynonymous polymorphisms in complete LD (*R139K* and *K399R*) (65); however, only the *K399R* locus was genotyped in

the current analysis. Due to the frequency of these functionally relevant nonsynonymous variants, *CYP2C8* haplotypes were not evaluated.

Data Analysis. All incident CHD cases and individuals from the cohort random sample were included in the current analysis (n=2065). Inverse sampling fractions from each stratum were used as weights in variance estimation of adjusted covariate means and proportions by linear and logistic regression, respectively, in non-cases included in the cohort random sample. Hazard rate ratios (HRR) and 95% confidence intervals (CI) for the development of incident CHD in relation to *CYP2J2* or *CYP2C8* genotype were calculated by weighted proportional hazards regression, using Barlow's method to account for the stratified random sampling and case-cohort design (109). Model 1 included baseline age, gender, and study center as covariates. Model 2 also included current smoking status, diabetes, hypertension, high density lipoprotein cholesterol, total cholesterol, and body mass index at baseline. Assuming an autosomal dominant mode of inheritance, individuals with one or two variant alleles were combined for comparison to wild-type individuals. All analyses were completed separately in Caucasians and African-Americans. Assuming a case-control design, type I error α=0.05 and 10% variant genotype frequency, there was approximately 99% and 80% power to detect an odds ratio of 2.0 in Caucasians and African-Americans, respectively.

Cohort random sample allele frequencies were evaluated for deviation from Hardy-Weinberg equilibrium, and pairwise LD statistics were calculated (Haploview 3.2) (81). *CYP2J2* haplotypes and their frequencies were estimated using the phase reconstruction method (PHASE 2.1), which assigned the most probable haplotype pair to each individual

(121). Only polymorphisms with >5% frequency and pairwise r^2 values <0.80 were considered for haplotype reconstruction, which included polymorphisms 1 and 7 in Caucasians and 1, 7, 9, and 10 in African-Americans (Figure 11). Haplotype frequencies were compared across case status by chi-square. Only haplotypes with >5% frequency were considered. Frequency comparisons were repeated using the expectation-maximization algorithm (Haploview 3.2) (81), which accounted for the uncertainty in haplotype reconstruction by weight-adjusting each inferred haplotype according to its estimated posterior haplotype probability. Associations between haplotype (0,1) and risk of incident CHD were also evaluated by modeling each haplotype relative all other haplotypes using Barlow's method (109). The association analysis was repeated after excluding individuals with posterior haplotype probabilities <0.75.

Gene-environment interaction testing was completed on a multiplicative scale between selected *CYP2J2* and *CYP2C8* variants and baseline current smoking status (yes/no) using a Wald chi-square test for significance of the estimated β-coefficient for the interaction term (110). Because interaction hypothesis testing on a multiplicative scale is underpowered, the critical value for statistical significance was set to α=0.15, two-sided (111). Stratified weighted proportional hazards regression was also completed to further explore potential interactions.

To minimize the impact of the multiple statistical tests conducted in the current analysis, the false discovery rate (FDR) *q*-value was estimated for each comparison, separately for *CYP2J2* and *CYP2C8,* which is defined as the proportion of statistical tests deemed significant that are actually false-positives (QVALUE) (112). In order to calculate conservative *q*-value estimates, statistical tests from the unadjusted, model 1 and model 2

association analysis of each polymorphism and reconstructed haplotype were considered as independent, even though each model assessed the same independent variable and certain genotype and haplotype associations are not completely independent. Additional *q*-value estimates were also calculated for the gene-smoking interaction analysis. Only *q*-values for significant findings are presented.

Results

Study Population. Significant baseline differences in various risk factors were observed between incident CHD cases and non-cases included in the cohort random sample (Table 6). Cases were significantly older and more likely to be male, cigarette smokers, diabetic, hypertensive and have abnormal fasting lipid panels compared to non-cases.

***CYP2J2/CYP2C8* Genotype.** The observed race-specific allele frequencies of the 10 *CYP2J2* polymorphisms are presented in Figure 11. The *R158C* (*CYP2J2*3*), *I192N* (*CYP2J2*4*), and *N404Y* (*CYP2J2*6*) polymorphisms were monomorphic in both Caucasians and African-Americans. Significant LD was observed between certain *CYP2J2* polymorphisms, particularly in Caucasians (Figure 12). The minor allele frequencies of the *I264M* (0.041 versus 0.011), *I269F* (0.002 versus 0.141) and *K399R* (0.108 versus 0.019) polymorphisms in *CYP2C8* were significantly different in Caucasians and African-Americans, respectively, in the cohort random sample ($P<0.001$ for each comparison). No evidence of LD was observed in either subpopulation ($r^2<0.01$). The distribution of all evaluated polymorphisms were in Hardy-Weinberg equilibrium in both Caucasians and African-Americans ($P>0.05$).

***CYP2J2* Polymorphisms and CHD Risk.** In African-Americans, the variant -*50T* allele was significantly less common among CHD cases compared to cohort random sample non-cases (20.9% versus 29.3%, respectively, *P*=0.043) (Table 25). Moreover, presence of at least one variant -*50T* allele was associated with significantly lower risk of incident CHD events relative to -*50G* homozygotes (model 2, HRR 0.58, 95% CI 0.35-0.96, *P*=0.036, *q*=0.051) (Table 26). This association was not modified by gender (*P* for interaction=0.797). In Caucasians, no significant difference in *G-50T* genotype frequency was observed across CHD case status (*P*=0.719) (Table 25), and no significant association between presence of the variant -*50T* allele and CHD risk was observed (model 2, HRR 1.15, 95% CI 0.78-1.70, *P*=0.472) (Table 26).

The rare *R49S* variant allele appeared to be less common in CHD cases compared to non-cases in African-Americans (0.5% versus 2.5%, respectively) and Caucasians (0.1% versus 0.6%, respectively) (Table 25). However, no significant association with risk of CHD was observed in either ethnic group after covariate adjustment (Table 26).

Haplotype reconstruction identified five common haplotypes in African-Americans and three in Caucasians, which accounted for 94.7% and 98.1% of all haplotypes, respectively. In African-Americans, the overall haplotype distribution tended to be different in individuals with and without CHD (*P*=0.086); however, this did not attain statistical significance (Table 27). No difference in haplotype distribution was observed in Caucasians (*P*=0.731) (Table 27).

In African-Americans, haplotype ***TGT****A* [tagged by the polymorphism 1 (*G-50T*), 7 and 9 variant alleles] was less frequent (8.1% versus 12.3%, *P*=0.052) in CHD cases compared to

non-cases, respectively (Table 27). Similar differences in haplotype ***TGT****A* frequency were also observed using the expectation-maximization algorithm (*P*=0.027). Moreover, presence of at least one haplotype ***TGT****A* copy was significantly less common in CHD cases compared to non-cases (14.5% versus 22.9%, respectively, *P*=0.027), and was associated with significantly lower risk of incident CHD (model 2, HRR 0.51, 95% CI 0.29-0.91, *P*=0.023, *q*=0.041) (Table 27). Significant associations were also observed after excluding the 1.5% of individuals with a posterior haplotype probability <0.75 from the analysis (*P*=0.020). In Caucasians, presence of haplotype ***TG*** [tagged by the polymorphism 1 (*G-50T*) and 7 variant alleles] was not significantly associated with risk of incident CHD after covariate adjustment (model 2, HRR 1.33, 95% CI 0.87-2.02, *P*=0.184) (Table 27).

CYP2C8 **Polymorphisms and CHD Risk.** No significant differences in the genotype frequency of the *I264M*, *I269F* or *K399R* polymorphisms in *CYP2C8* were observed across CHD case status in either African-Americans or Caucasians (Table 25). Moreover, presence of the *I264M*, *I269F* or *K399R* variant alleles were not significantly associated with risk of incident CHD after covariate adjustment (Table 26).

Genotype by Smoking Interaction. In Caucasians, cigarette smoking status at baseline appeared to modify the association between CHD risk and both the *I264M* (*P* for interaction=0.104, *q*=0.166) and *K399R* (*P* for interaction=0.060, *q*=0.160) polymorphisms in *CYP2C8* (Table 28). A significant interaction was identified when individuals carrying at least one variant allele in either the *I264M* or *K399R* polymorphisms were compared to those wild-type for both (*P* for interaction=0.008, *q*=0.064) (Table 29). When stratified by

smoking status, smokers carrying at least one variant allele were at significantly higher risk of CHD compared to smokers wild-type at both loci (model 2, HRR 1.89, 95% CI 1.05-3.38, *P*=0.033). Smoking status did not modify risk associated with the *CYP2C8* variant *I269F* allele in African-Americans (*P* for interaction=0.746), or the *CYP2J2* variant *-50T* allele in either African-Americans (*P* for interaction=0.605) or Caucasians (*P* for interaction=0.690).

Discussion

The current analysis demonstrated a statistically significant association between the variant *-50T* allele in *CYP2J2* and lower risk of incident CHD events in African-Americans enrolled in the ARIC study. A common *CYP2J2* haplotype which carried the *-50T* allele was also associated with significantly lower CHD risk in African-Americans. The *I264M*, *I269F* and *K399R* polymorphisms in *CYP2C8* were not associated with risk of CHD in either ethnic group. However, in Caucasians, cigarette smokers carrying either the variant *I264M* or *K399R* allele were at significantly higher risk of incident CHD, whereas no significant association with disease risk was observed in the absence of the smoking exposure.

Endothelial dysfunction is associated with increased risk of acute cardiovascular events (10), and is typically manifested by impairment in endothelial-dependent vasodilation (2). The vasodilatory and anti-inflammatory properties of CYP2J2 and CYP2C8-derived EETs are important mediators of this process (20, 130). Soluble epoxide hydrolase (*EPHX2*) rapidly hydrolyzes EETs and is integrally involved in regulation of their cellular levels and vascular effects (28) The *K55R* variant allele in *EPHX2* was associated with significantly higher soluble epoxide hydrolase activity *in vivo* and higher risk of incident CHD events in Caucasians (139) (Chapter V). Although regulation of EET levels by soluble epoxide

hydrolase *in vivo* is well-documented, variation in CYP2J2 and/or CYP2C8-mediated EET biosynthesis may also be critical. However, the relative contribution of each P450 epoxygenase to the regulation of cellular and systemic EET levels has not been extensively characterized, particularly in humans.

Multiple polymorphisms in *CYP2J2* and *CYP2C8* associated with reduced enzyme expression or metabolic activity have been identified (63-66). In *CYP2J2*, the *R158C*, *I192N*, and *N404Y* polymorphisms possess significantly lower epoxygenase activity *in vitro* (63). However, these variants are extremely infrequent, and were found to be monomorphic in the 2065 individuals genotyped in the current analysis. The *G-50T* polymorphism disrupts a Sp1 transcription factor binding site in the proximal promoter, leads to reduced *CYP2J2* transcription *in vitro* and represents the only common, functionally relevant polymorphism in *CYP2J2* identified to date (64). Importantly, the variant *-50T* allele was associated with significantly lower plasma DHET levels and higher risk of prevalent angiographically-documented CHD in a recently characterized German population (64). However, in the current analysis the variant *-50T* allele was associated with significantly lower risk of incident CHD clinical events in African-Americans at both the polymorphism and haplotype levels, in contrast to these previous findings and current hypotheses related to the beneficial effects of EETs in the vasculature. The rare *R49S* variant allele also appeared to be less frequent in African-American CHD cases; however, the metabolic relevance of this infrequent variant remains to be characterized. In Caucasians, the *-50T* allele was not significantly associated with risk of incident CHD events after covariate adjustment, inconsistent with the previously described German population (64). However, the primary analysis of this investigation by Spiecker et al. defined CHD angiographically, not by clinical

event incidence as defined in the ARIC study. Interestingly, Spiecker et al. also reported a non-significant association between the *-50T* allele and risk of prevalent acute coronary syndrome events (adjusted odds ratio 1.38, 95% CI 0.85-2.25, *P*=0.19) (64), which was similar to the non-significant relationship observed in Caucasians between a common haplotype carrying the *-50T* allele and risk of incident CHD events in the ARIC study (HRR 1.33, 95% CI 0.87-2.02, *P*=0.184). Future studies validating these associations across ethnicities appear warranted.

In *CYP2C8*, the *I264M*, *I269F*, and *R139K/K399R* polymorphisms possess significantly lower metabolic activity *in vitro*; however, only the *R139K/K399R* variant has been associated with significantly reduced CYP2C8-mediated EET biosynthesis (65, 66) and higher risk of prevalent myocardial infarction in a Swedish cohort (67). The *I264M* and *R139K/K399R* polymorphisms are more frequent in Caucasians, while the *I269F* polymorphism is more frequent in African-Americans. Overall, these variants were not significantly associated with risk of incident CHD events in the ARIC population. However, in Caucasians, cigarette smoking history significantly modified the association between the variant *I264M* and *K399R* alleles and CHD incidence, such that smokers carrying either of these variant alleles were at the greatest risk of developing CHD. Smoking did not modify the association between the *G-50T* polymorphism in *CYP2J2* and CHD risk, suggesting such an interaction may be isolated to CYP2C8-mediated epoxygenase activity. Cigarette smoking is a well-characterized environmental risk factor which substantially impairs endothelial function (6). Cigarette smoking modified the association between each the endothelial nitric oxide synthase (eNOS, *NOS3*) *E298D* and *EPHX2 K55R* polymorphisms and risk of incident CHD in Caucasians, with the highest risk observed in smokers carrying

these variant alleles (135, 139) (Chapters IV and V). Perhaps presence of established underlying endothelial dysfunction, as observed in cigarette smokers, may be necessary for genetic variation in *CYP2C8*, *NOS3*, and *EPHX2* to significantly influence endothelial function and cardiovascular disease risk in Caucasians. Future studies will be required to further characterize this potential gene-environment interaction and the mechanistic influence of cigarette smoking on vascular CYP2C8 and CYP2J2-mediated EET biosynthesis.

Importantly, the relationships between genetic variation in both *CYP2J2* and *CYP2C8* and risk of incident CHD events appear to differ substantially across the Caucasian and African-American subsets of the ARIC cohort. In particular, the observed association between the *G-50T* polymorphism in *CYP2J2* and CHD risk in African-Americans existed in the opposite direction of both preclinical findings and previous genetic epidemiological data in Caucasian populations, suggesting reduced P450-mediated EET biosynthesis could have protective effects against the development of CHD clinical events. Despite their well-characterized vasodilatory and anti-inflammatory effects, preclinical evidence has demonstrated that increased EET generation also significantly increases matrix metalloproteinase (MMP) enzyme activity in endothelial cells (140). The MMPs are potent stimulators of vascular remodeling and atherosclerotic plaque destabilization, and are integrally involved in the precipitation of plaque rupture and acute CHD events (141). Perhaps the role of EET-mediated regulation of MMP activity is of particular importance in African-Americans, and genetic determinants of reduced EET generation, such as the *G-50T* polymorphism in *CYP2J2*, significantly reduce the risk of experiencing an acute CHD clinical event via its downregulation of MMP activity. Interestingly, a similar ethnic contrast was observed in the evaluation of *EPHX2* polymorphisms and CHD risk (139) (Chapter V). The variant *K55*R

allele was associated with significantly higher risk of incident CHD in Caucasians (HRR 1.45, 95% CI 1.05-2.01, *P*=0.026); however, a non-significant trend toward lower CHD risk was observed in African-Americans (HRR 0.76, 95% CI 0.50-1.16, *P*=0.208). Although the mechanisms underlying the observed ethnic differences remain unknown, additional genetic and/or environmental factors not accounted for in the current analysis could be contributing to population differences in the likely complex relationship between the P450 epoxygenase pathway, endothelial function and cardiovascular disease risk. In fact, racial differences in endothelial-mediated vasodilatory responses are well-documented, with African-American populations typically demonstrating more pronounced endothelial dysfunction (142). Mechanistic investigations have implicated enhanced NADPH oxidase-mediated reactive oxygen species production and eNOS uncoupling in African-Americans compared to Caucasians (143). However, population-specific differences in P450 epoxygenase-derived EET biosynthesis and its effect on endothelial function, vascular inflammation, and MMP activity in humans remains to be evaluated.

Although the current study evaluated rigorously ascertained incident events, mechanisms underlying the observed population-specific associations between CHD risk and genetic variation in *CYP2J2* and *CYP2C8* were not elucidated. In addition, since haplotypes are inferred some uncertainty exists in the *CYP2J2* haplotype assigned to each individual. However, similar results were observed using the expectation-maximization algorithm and after excluding individuals with posterior haplotype probabilities <0.75. Although polymorphisms with known functional relevance and/or haplotype tagging properties were specifically selected, and a hypothesis-driven approach in the analysis was utilized, it may be difficult to gauge the statistical significance of these findings considering the number of

comparisons completed. Consequently, the FDR was assessed across all completed tests in the genotype and haplotype association analysis. Since all *q*-values related to the association between CHD risk and both the *G-50T* polymorphism and ***TGT****A* haplotype in African-Americans were conservatively estimated to be 0.051 or less, there is a high level of confidence in these findings. Similarly, the FDR analysis enhanced confidence in the *CYP2C8*-smoking interaction findings. However, the observations of significant gene-smoking interactions with the *CYP2C8 I264M* and *K399R* polymorphisms in the absence of significant main effects suggest these findings should be interpreted with caution.

In summary, the current analysis suggests that genetic variation in *CYP2J2* and *CYP2C8* may influence the development of CHD in humans; however, these associations appear to be different across ethnic groups and in the presence of environmental risk factors such as cigarette smoking. Future studies across multiple populations will undoubtedly be required to validate these findings, in addition to molecular and physiological studies evaluating the mechanistic relationship between the P450 epoxygenase pathway, endothelial function and cardiovascular disease risk.

Table 25. *CYP2J2* and *CYP2C8* polymorphism frequency by incident CHD case status.

	Caucasian			African-American		
Genotype*	**Non-cases**	**CHD cases**	***P*-value**	**Non-cases**	**CHD cases**	***P*-value**
CYP2J2						
G-50T (*CYP2J2*7*)						
G/G	501 (88.0%)	648 (88.7%)		189 (70.7%)	167 (79.2%)	
G/T + T/T	65 (12.1%)	83 (11.4%)	*P*=0.719	79 (29.3%)	44 (20.9%)	*P*=0.043
R49S						
C/C	611 (99.5%)	774 (99.9%)		280 (97.5%)	223 (99.6%)	
C/A + A/A	4 (0.6%)	1 (0.1%)	*P*=N/A	8 (2.5%)	1 (0.5%)	*P*=N/A
CYP2C8						
I264M (*CYP2C8*4*)						
C/C	512 (91.9%)	696 (90.0%)		299 (97.7%)	221 (97.7%)	
C/G + G/G	44 (8.1%)	77 (10.0%)	*P*=0.261	6 (2.3%)	5 (2.2%)	*P*=0.950
I269F (*CYP2C8*2*)						
A/A	570 (99.7%)	759 (99.5%)		216 (73.8%)	163 (74.1%)	
A/T + T/T	2 (0.3%)	4 (0.5%)	*P*=N/A	80 (26.2%)	57 (25.9%)	*P*=0.940
K399R (*CYP2C8*3*)						
A/A	461 (81.3%)	618 (80.0%)		299 (96.6%)	213 (95.1%)	
A/G + G/G	116 (18.7%)	155 (20.1%)	*P*=0.552	10 (3.4%)	11 (4.9%)	*P*=0.424

*Genotype data presented as absolute (percent) genotype frequency. Frequencies are weighted according to the sampling fraction. The *R158C* (*CYP2J2*3*), *I192N* (*CYP2J2*4*), and *N404Y* (*CYP2J2*6*) polymorphisms in *CYP2J2* were monomorphic (minor allele frequency 0.0), and the *V113M* (rs11572242) variant allele was identified in only one Caucasian non-case.

Table 26. Hazard rate ratio between *CYP2J2* and *CYP2C8* polymorphisms and risk of incident CHD.

	Caucasian			African-American		
Polymorphism	**HRR**	**95% CI**	***P*-value**	**HRR**	**95% CI**	***P*-value**
CYP2J2						
G-50T (*CYP2J2*7*)	*G/T + T/T* versus *G/G*			*G/T + T/T* versus *G/G*		
Model 1*	1.08	0.75–1.54	*P*=0.692	0.58	0.37–0.89	*P*=0.014
Model 2†	1.15	0.78–1.70	*P*=0.472	0.58	0.35–0.96	*P*=0.036
R49S	*C/A + A/A* versus *C/C*			*C/A + A/A* versus *C/C*		
Model 1*	0.18	0.02–1.67	*P*=0.132	0.17	0.02–1.22	*P*=0.078
Model 2†	0.23	0.02–2.39	*P*=0.220	0.26	0.04–1.84	*P*=0.176
CYP2C8						
I264M (*CYP2C8*4*)	*C/G + G/G* versus *C/C*			*C/G + G/G* versus *C/C*		
Model 1*	1.29	0.86–1.92	*P*=0.222	1.11	0.36–3.42	*P*=0.858
Model 2†	0.98	0.58–1.65	*P*=0.926	1.14	0.36–3.67	*P*=0.823
I269F (*CYP2C8*2*)	*A/T + T/T* versus *A/A*			*A/T + T/T* versus *A/A*		
Model 1*	4.40	0.77–25.1	*P*=0.095	0.90	0.60–1.37	*P*=0.634
Model 2†	5.35	0.93–30.7	*P*=0.060	0.99	0.62–1.56	*P*=0.951
K399R (*CYP2C8*3*)	*A/G + G/G* versus *A/A*			*A/G + G/G* versus *A/A*		
Model 1*	0.97	0.73–1.28	*P*=0.816	1.22	0.55–2.73	*P*=0.627
Model 2†	0.97	0.70–1.34	*P*=0.848	1.20	0.51–2.83	*P*=0.669

HRR=hazard rate ratio, CI=confidence interval.
*Adjusted for age, gender, and study center.
†Adjusted for age, gender, study center, current smoker, diabetes, hypertension, high density lipoprotein cholesterol, total cholesterol, and body mass index.

Table 27. *CYP2J2* haplotypes and risk of incident CHD.

	Distribution Analysis			Association Analysis		
Haplotype*,†	**Non-cases**	**CHD cases**	***P*-value‡**	**HRR§**	**95% CI**	***P*-value**
African-American‖	n=260	n=200				
GTCA	56.3%	56.9%		1.14	0.65–2.00	*P*=0.653
*G**G**CA*	16.1%	13.6%		0.82	0.51–1.31	*P*=0.402
*G**G**C**G***	10.5%	14.9%		1.42	0.83–2.42	*P*=0.201
***TGT**A*	12.3%	8.1%		0.51	0.29–0.91	*P*=0.023
*G**GT**A*	4.8%	6.5%	*P*=0.086	0.93	0.41–2.10	*P*=0.858
Caucasian#	n=493	n=692				
GT	85.7%	86.2%		1.15	0.53 – 2.47	*P*=0.728
*G**G***	8.5%	7.6%		0.96	0.66 – 1.40	*P*=0.831
TG	5.8%	6.2%	*P*=0.731	1.33	0.87 – 2.02	*P*=0.184

*Bold nucleotides represent haplotype tagging polymorphisms.

†Estimated copy frequency weighted according to the sampling fraction.

‡Chi-square *P*-value for the overall distribution of haplotypes by CHD case status.

§Adjusted for age, gender, study center, current smoker, diabetes, hypertension, high density lipoprotein cholesterol, total cholesterol, and body mass index.

‖Haplotype includes polymorphisms 1, 7, 9, and 10 (Figure 11).

#Haplotype includes polymorphisms 1 and 7 (Figure 11).

Table 28. *CYP2C8* polymorphisms, cigarette smoking and risk of incident CHD in Caucasians.

Smoking Exposure	*CYP2C8* Genotype		Interaction	*P*-value
	Wild-type	***Variant***		
I264M	***C/C***	***C/G + G/G***		
Non-current smokers				
Model 1*	1 (referent)	1.13 (0.70 – 1.83)		
Model 2†	1 (referent)	0.72 (0.36 – 1.45)		
Current Smokers				
Model 1*	1.74 (1.32 – 2.31)	3.18 (1.47 – 6.90)	1.61 (0.64 – 4.09)	*P*=0.314
Model 2†	1.62 (1.18 – 2.21)	2.76 (1.28 – 5.95)	2.38 (0.84 – 6.78)	*P*=0.104
K399R	***A/A***	***A/G + G/G***		
Non-current smokers				
Model 1*	1 (referent)	0.87 (0.62 – 1.20)		
Model 2†	1 (referent)	0.79 (0.53 – 1.16)		
Current Smokers				
Model 1*	1.75 (1.30 – 2.36)	2.73 (1.58 – 4.75)	1.80 (0.91 – 3.54)	*P*=0.089
Model 2†	1.64 (1.18 – 2.29)	2.63 (1.46 – 4.74)	2.03 (0.97 – 4.25)	*P*=0.060

Data presented as Hazard Rate Ratio (95% confidence interval).

*Adjusted for age, gender, and study center

†Adjusted for age, gender, study center, diabetes, hypertension, high density lipoprotein cholesterol, total cholesterol, and body mass index.

Table 29. *CYP2C8* polymorphisms, cigarette smoking and risk of incident CHD in Caucasians (2).

Smoking Exposure	*CYP2C8* Genotype (*I264M* or *K399R*)*	
	Wild-type	***Variant***
Non-current smokers		
Model 1†	1 (referent)	0.90 (0.67–1.21)
Model 2‡	1 (referent)	0.73 (0.51–1.05)
Current Smokers		
Model 1†	1.63 (1.19–2.24)	2.88 (1.80–4.62)
Model 2‡	1.48 (1.04–2.11)	2.65 (1.61–4.39)

Data presented as Hazard Rate Ratio (95% confidence interval).

*Individuals carrying at least one variant allele for either the *I264M* (*C/G+G/G*) or *K399R* (*A/G+G/G*) polymorphism were compared to those wild-type for both (*C/C* and *A/A*, respectively).

†Adjusted for age, gender, and study center (interaction term: HRR 1.97, 95% CI 1.08-3.61, *P*=0.028).

‡Adjusted for age, gender, study center, diabetes, hypertension, high density lipoprotein cholesterol, total cholesterol, and body mass index (interaction term: HRR 2.45, 95% CI 1.26-4.75, *P*=0.008).

Figure Legends

Figure 11. Nucleotide positions of the 10 *CYP2J2* polymorphisms evaluated are given relative to the *CYP2J2* transcriptional start site (Genbank accession number AF272142). Activity is reported as lower (↓) or unknown (?) relative to wild-type enzyme based on previous studies (63, 64). Cohort random sample minor allele frequencies are presented separately by race, and *P*-values for their comparison are reported.

Figure 12. Pairwise estimates of linkage disequilibrium (LD) between each *CYP2J2* polymorphism are plotted for (A) Caucasians and (B) African-Americans in the cohort random sample using Haploview 3.2. Each polymorphism is numbered according to its position in the *CYP2J2* gene as presented in Figure 11. Black squares indicate complete LD (r^2=1.0), white squares indicate zero LD (r^2=0.0), and increasing intensity of gray indicates increasing degrees of LD.

Figure 11. Selected *CYP2J2* polymorphisms for genotyping.

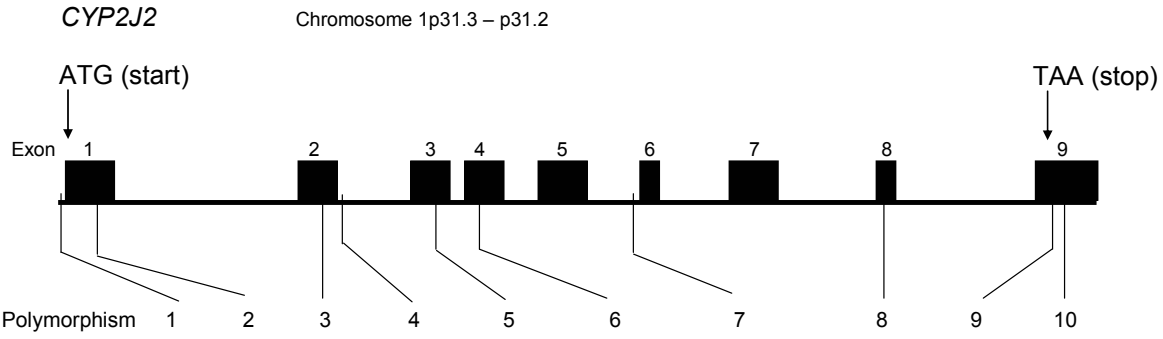

Polymorphism	1	2	3	4	5	6	7	8	9	10
dbSNP ID	rs890293	rs11572190	rs11572242	rs3738474			rs2271800		rs4388726	rs11572327
Nucleotide Position	-50	170	10798	10860	14558	15054	18778	25687	33291	33497
Major Allele	G	C	G	G	C	T	T	A	C	A
Minor Allele	T	A	A	A	T	A	G	T	T	G
Amino Acid Substitution	-	R49S	V113M	-	R158C	I192N	-	N404Y	-	-
Activity	↓	?	?	?	↓	↓	?	↓	?	?
Minor allele frequency										
Caucasian	0.064	0.003	0.001	0.066	0	0	0.159	0	0.069	0.014
AA	0.155	0.014	0	0.014	0	0	0.445	0	0.170	0.106
P-value	<0.001	0.058	N/A	<0.001	N/A	N/A	<0.001	N/A	<0.001	<0.001

Figure 12. *CYP2J2* linkage disequilibrium plots by race.

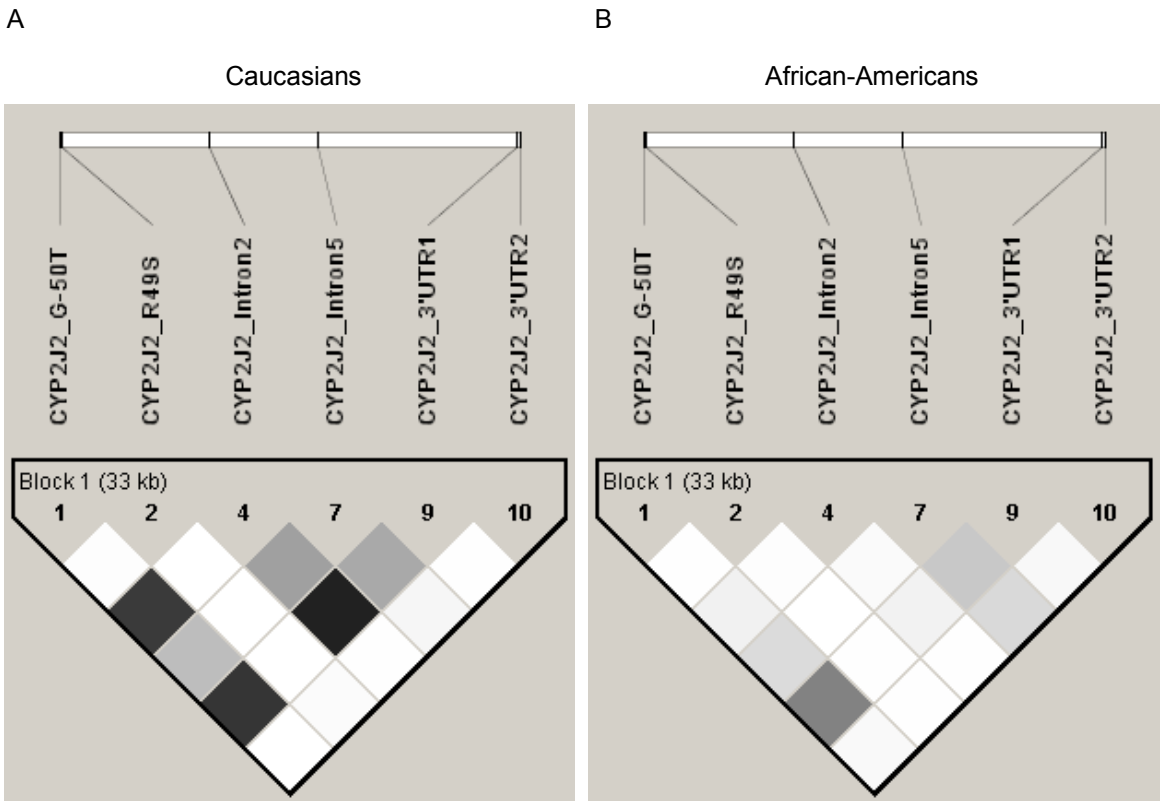

CHAPTER VII

DEVELOPMENT AND BASELINE CHARACTERIZATION OF TIE2-CYP2J2 AND TIE2-CYP2C8 TRANSGENIC MICE

Introduction

Arachidonic acid is oxidatively metabolized to epoxyeicosatrienoic acids (EETs) by cytochrome P450 epoxygenases from the CYP2J and CYP2C subfamilies (20). In humans, CYP2J2 and CYP2C8 are the primary isoforms responsible for the formation of EETs in endothelial cells and cardiomyocytes, where they possess potent biological effects (20, 31, 144). Once formed, EETs are rapidly hydrolyzed to their corresponding dihydroxyeicosatrienoic acid (DHET) metabolites by soluble epoxide hydrolase (sEH, *EPHX2*) (27-29). In general, DHETs are much less active than EETs in the cardiovascular system (20). Previous work has demonstrated that EETs have substantial vasodilatory (30, 31), anti-inflammatory (32), fibrinolytic (33), post-ischemic cardioprotective (34, 35), pro-angiogenic (36), and vascular smooth muscle cell anti-migratory (37) effects. Although both CYP2J and CYP2C isoforms catalyze EET biosynthesis in endothelial cells, the source of EETs may also be a critical factor related to their biological properties.

To date, the majority of the research characterizing the cardiovascular effects of CYP2J and CYP2C-mediated EET biosynthesis and sEH-mediated EET hydrolysis has been conducted *in vitro* and *ex vivo*; however, the biological effects of this pathway have not been extensively characterized in whole animal models *in vivo*. Moreover, evaluation of the potential biological differences between CYP2J2 and CYP2C8-mediated EET biosynthesis

under controlled conditions remains to be characterized. Recent work in genetically altered mouse models has further demonstrated the important role of this pathway in cardiovascular function. Specifically, transgenic mice with cardiomyocyte-specific overexpression of CYP2J2 and enhanced cardiac EET biosynthesis exhibit significant cardioprotection and improvement in post-ischemic recovery of left ventricular function (35). *Ephx2*$^{-/-}$ mice have also demonstrated significantly greater post-ischemic recovery of heart contractile function (46) and lower systemic blood pressure (45) compared to wild-type mice. However, the role of P450-mediated EET biosynthesis in the regulation of endothelial function, vascular inflammation, atherosclerotic lesion development and other vascular processes has not been extensively evaluated *in vivo*.

Importantly, at least 8 CYP2J and 15 CYP2C isoforms in mice have been identified to date, which each possess distinct tissue expression and substrate specificity profiles (145-148). Moreover, specific pharmacological inducers and inhibitors of each isoform have not been developed. Thus, characterization of the vascular effects of the P450 epoxygenase pathway in mice via either 1) pharmacological manipulation of wild-type mice, or 2) development of isoform-specific knock-out mice carries substantial limitations. Development of transgenic mice overexpressing human CYP2J2 or CYP2C8 in the vasculature offers a mechanism to further characterize the *in vivo* role of both CYP2J2 and CYP2C8-derived EETs in vascular function. The primary aim was to develop transgenic mice that exhibit constitutive, vascular endothelial cell-specific expression of either human CYP2J2 or CYP2C8 using the *Tie2* promoter and *Tie2* full enhancer (149), resulting in increased vascular and systemic EET concentrations, for use in future phenotying studies.

Methods

Chemicals. All chemicals were purchased from Sigma (St. Louis, MO), unless otherwise noted.

Generation of Tie2-CYP2J2 and Tie2-CYP2C8 Transgenic Mice. Two separate transgenic mouse lines were developed on a C57BL/6 background to specifically overexpress either human CYP2J2 (Tie2-CYP2J2) or human CYP2C8 (Tie2-CYP2C8) in vascular endothelial cells under control of the *Tie2* promoter and *Tie2* full enhancer (intron 1) (Figure 13A) (149). The human CYP2J2 (Genbank accession number NM_000775) and CYP2C8 (Genbank accession number NM_000770) cDNA sequences were subcloned downstream of the murine *Tie2* promoter (2.1-kb) and upstream of the *Tie2* full enhancer (10-kb) sequences (generously provided by Dr. Tom Sato, University of Texas Southwestern Medical Center, Dallas, TX) to drive endothelial cell-specific expression of CYP2J2 and CYP2C8 in mice.

The full-length human CYP2J2 (1.8-kb) (144) and CYP2C8 (1.8-kb) (150) cDNA sequences were previously subcloned into the pBluescript® SK (+) vector (Stratagene, La Jolla, CA) by reverse transcriptase (RT)-PCR, as described. The CYP2J2 and CYP2C8 cDNA sequences were PCR amplified with specific forward (CYP2J2: 5'-CGCTCTAGAACTAGTGGATC-3'; CYP2C8: 5'-AAGAAGAGAAGGCTTCAATGG-3') and reverse (CYP2J2: 5'-TCTTCTTGCTTTCCTTGCCC-3'; CYP2C8: 5'-AGGTGATAGCAGATCAGCAG-3') primers, and then subcloned into the intermediate pCR®2.1-TOPO vector using the TOPO TA Cloning® system (Invitrogen, Carlsbad, CA) per the manufacturer instructions. *Escherichia coli* TOP10 One Shot® Competent Cells (Invitrogen) were heat transformed with the subcloning reaction, plated out on Luria-Bertani

(LB)-agar plates containing kanamycin (50 μg/mL), and incubated at 37°C overnight. Kanamycin-resistant colonies were selected and grown in 10 mL of LB-media containing kanamycin (50 μg/mL) at 37°C overnight, and plasmid DNA was isolated using the QIAprep Spin Miniprep Kit (QIAGEN, Valencia, CA). The presence and orientation of each cDNA was confirmed by direct sequencing using the BigDye Terminator Reaction Ready Mix (Applied Biosystems, Foster City, CA) and an ABI Prism 377 DNA sequencer (Applied Biosystems).

The CYP2J2 and CYP2C8 cDNA sequences were then PCR amplified with specific forward primers to add a 5'-*Hind*III site (CYP2J2: 5'-GTTACT*AAGCTT*GGAGCC**ATG**CTCGCGGCG-3; CYP2C8: 5'-GTCAGC*AAGCTT*AGAGGCTTCA**ATG**GAACC-3'), and a common reverse primer specific for the pCR®2.1-TOPO vector (5'-GAATTGTAATACGACTCACTATAGGGCCA-3'). The pCR®2.1-TOPO vector contains a *Not*I site immediately downstream of the 3' end of each cDNA sequence. Each cDNA (~1.6-kb) was restriction enzyme digested with *Hind*III and *Not*I, and subcloned into the *Hind*III/*Not*I sites of the pSPTg.T2FpAXK (#52) vector (generously provided by Dr. Tom Sato) downstream of the *Tie2* promoter (2.1-kb) and upstream of the SV40 polyadenylation (polyA) (0.3-kb) and *Tie2* core enhancer (1.7-kb) sequences (149). *Escherichia coli* TOP10 One Shot® Competent Cells (Invitrogen) were heat transformed with the subcloning reaction, plated out on LB-agar plates containing ampicillin (50 μg/mL), and incubated at 37°C overnight. Ampicillin-resistant colonies were selected and grown in 10 mL of LB-media containing ampicillin (50 μg/mL) at 37°C overnight, and plasmid DNA was isolated using the QIAprep Spin Miniprep Kit (QIAGEN). The presence and orientation of each cDNA was confirmed by direct sequencing.

However, since the *Tie2* core enhancer fragment has been found to drive "patchy" endothelial cell transgene expression (data not shown), the *Tie2* promoter-CYP2J2/2C8 cDNA fragment was subcloned upstream of the SV40 polyA (0.3-kb) and *Tie2* full enhancer (10-kb) sequences in order to obtain constitutive and uniform endothelial expression (personal communication with Dr. Tom Sato). First, the polyA and *Tie2* full enhancer were excised from the pT2HLacZp1I.7 (#59) vector (generously provided by Dr. Tom Sato) via a complete *Sal*I digestion and subsequent partial *Xba*I digestion, in order to obtain the linear polyA-*Tie2* full enhancer sequence (10.3-kb) with 5'-*Xba*I and 3'-*Sal*I restriction enzyme sites. This fragment was then subcloned into the *Xba*I/*Sal*I sites of the pBluescript® SK (+) vector (Stratagene), transformed into *Escherichia coli*, and ampicillin-resistant colonies were selected and grown as described above. Plasmid DNA was isolated, and the presence and orientation of the polyA-*Tie2* full enhancer was confirmed by direct sequencing. Second, the *Tie2* promoter-CYP2J2/2C8 cDNA (3.7-kb) fragments were PCR amplified with a common forward primer to add a 5'-*Not*I site to the *Tie2* promoter (5'-GTTACTCA*GCGGCCGC*GTCGACACTAGCTTACTAAGA-3') and a common reverse primer specific for the *Tie2* core enhancer (5'-CTCTATCCCTGCCCTCCTGCCTTGTTTCCC-3'). The amplified products were then restriction enzyme digested with *Not*I, treated with calf intestinal alkaline phosphatase to prevent self-ligation, and subcloned into the *Not*I sites of the pBluescript® SK (+) vector immediately upstream of the polyA-*Tie2* full enhancer. After transformation into *Escherichia coli*, ampicillin-resistant colonies were selected and grown in 250 mL of LB-media containing ampicillin (50 μg/mL) at 37°C overnight, and plasmid DNA was isolated using the QIAGEN plasmid Maxi kit (QIAGEN). The presence and orientation of the *Tie2*

promoter-CYP2J2/2C8 cDNA-polyA-*Tie2* full enhancer (14-kb) constructs were confirmed by direct sequencing and restriction enzyme digestion with *Not*I and *Sal*I.

The 14-kb Tie2-CYP2J2 and Tie2-CYP2C8 transgenic constructs were linearized by *Sal*I restriction enzyme digestion and agarose gel-purified. The constructs were then microinjected in pronuclei of single cell C57BL6/J mouse embryos and implanted into pseudopregnant mice (Dr. Carl Pinkert, University of Rochester Medical Center, Rochester, NY). Hemizygous "founder" pups were identified via PCR genotyping of genomic DNA, as described below.

PCR Genotyping. Genomic DNA isolated from the tails of hemizygous founder mice, and their progeny were genotyped by PCR in order to screen for presence of the transgenic construct in the mouse genome. Two primer pair sets were designed for each construct (Figure 13A). The first amplified a fragment extending from the 3' end of the *Tie2* promoter into the 5' end of each cDNA, using a common forward primer (*Tie2* promoter: 5'-GTCCTCATCGCATACCATAC-3') and a reverse primer specific for each cDNA (CYP2J2: 5'-CGACAGTGCCCAGTAGGAGA-3'; CYP2C8: 5'-AATAGGAAGAGGAGTGGGGC-3'), yielding 526 and 567 base pair products for the Tie2-CYP2J2 and Tie2-CYP2C8 constructs, respectively. The second amplified a fragment extending from the 3' end of each cDNA into the 5' end of the *Tie2* enhancer, using a forward primer specific for each cDNA (CYP2J2: 5'-CATGCCCTACACCAATGCTG-3'; CYP2C8: 5'-AACTTGGTTGGCACTGTAGC-3') and a common reverse primer (*Tie2* enhancer: 5'-GGTGCCGCTGGAATCTGAACT-3'), yielding 967 and 1158 base pair products, respectively. Each amplification reaction was carried out in a 50 μL reaction volume with

200 ng genomic DNA, 0.4 M each primer, 0.2 mM dNTPs, 10X Taq polymerase reaction buffer (5 μL), and 2.5 units of AmpliTaq Gold™ DNA polymerase (Applied Biosystems), and was completed as follows: 15 minutes at 94°C (x 1 cycle); 30 seconds at 94°C, 60 seconds at 66°C (*Tie2* promoter primer pair) or 68°C (*Tie2* enhancer primer pair), and 90 seconds at 72°C (x 30 cycles); and 15 minutes at 72°C (x 1 cycle).

Breeding. Upon identification of hemizygous founder mice, the breeding scheme involved crossing Tie2-CYP2J2 and Tie2-CYP2C8 transgenic (Tg) founder mice with C57BL/6 wild type mice in order to obtain Tie2-CYP2J2 and Tie2-CYP2C8 heterozygous Tg mice and wild-type littermates at an approximate ratio of 1:1. The progeny generated from this breeding scheme were genotyped to identify the founder lines in which the transgene demonstrated germline incorporation into the mouse genome. This breeding scheme was subsequently applied to each germline founder line, and the Tie2-CYP2J2 and Tie2-CYP2C8 Tg and wild-type littermates were evaluated for endothelial expression and function of CYP2J2 and CYP2C8, respectively.

Real Time RT-PCR. Total RNA was isolated from snap frozen lung, aorta, heart, liver and kidney using the QIAgen RNeasy Miniprep Kit and RNase-free DNase (QIAGEN) per the manufacturer instructions. Total RNA was reverse transcribed to cDNA using the ABI High Capacity cDNA Archive Kit (Applied Biosystems) for 10 minutes at 25°C, and then 120 minutes at 37°C. Expression of human CYP2J2 (Hs00356031_m1), human CYP2C8 (Hs00426387_m1), and murine GAPDH (Mm99999915_g1) were quantified by real time quantitative RT-PCR using Taqman® Assays on Demand (Applied Biosystems). Each

amplification reaction was carried out in a 25 μL reaction volume with 100 ng cDNA, 20X Assay on Demand Gene Expression kit (1.25 μL), and 2X Taqman Universal PCR Master Mix (12.5 μL), and was completed as follows: 2 minutes at 50°C (x 1 cycle); 10 minutes at 95°C (x 1 cycle); 15 seconds at 95°C, and 60 seconds at 60°C (x 40 cycles). All reactions were performed in triplicate using the ABI Prism 7900HT Sequence Detection System (Applied Biosystems).

The human CYP2J2 and CYP2C8 assays demonstrated minimal cross-reactivity with murine CYP2Js and CYP2Cs, respectively, in various tissues from wild-type animals (data not shown). Thus, these assays provided a sensitive means to detect presence of the human CYP2J2 and CYP2C8 transgenes at the transcript level in Tie2-CYP2J2 and Tie2-CYP2C8 Tg mice, respectively, relative to wild-type littermates. Murine GAPDH expression was used as an endogenous reference to account for potential differences in the amount of total RNA and/or differences in amplification efficiency across each reaction. Expression data were calculated using the $2^{-\Delta\Delta Ct}$ method (151), and presented as the relative fold-difference of CYP2J2 and CYP2C8 expression in Tie2-CYP2J2 and Tie2-CYP2C8 Tg mice, respectively, normalized to GAPDH and compared to wild-type littermates (defined as 1.0 for each comparison).

Immunoblotting. Microsomal fractions from whole lung, heart, liver and kidney, and 12 pooled aortas for each genotype were also prepared. Briefly, snap frozen tissue was homogenized on ice in a 0.25 M sucrose, 10 mM Tris-Cl buffer (pH=7.5) containing protease inhibitors. Tissue homogenates were centrifuged at 5000 rpm at 4°C for 20 minutes, 12000 rpm at 4°C for 20 minutes, and 12000 rpm at 4°C for 20 minutes consecutively to remove

cellular debris. Supernatants were then ultracentrifuged at 40,000 rpm (Beckman 70Ti) at 4°C for 90 minutes. The microsomal pellets were resuspended in 50-100 μL of a 50 mM Tris, 1 mM DTT, 1 mM EDTA buffer (pH=7.5) containing 20% glycerol. Protein concentrations of the microsomal fractions were quantified using the Bio-Rad protein assay (Bio-Rad, Hercules, CA), and then stored in aliquots at -80°C.

Microsomes (70 μg) were thawed on ice, added to 4X sample buffer containing β-mercaptoethanol, and boiled for 5 minutes. Proteins were separated by 10% Novex Tris-glycine polyacrylamide gels (Invitrogen) and transferred to nitrocellulose membranes (Invitrogen) in transfer buffer containing 20% methanol. The membranes were blocked in 5% nonfat milk in Tris-buffered saline (TBS) for 2 hours. For Tie2-CYP2J2 mice, membranes were then incubated in a 1:1000 dilution of anti-CYP2J2pep1 antibody in 5% nonfat milk at 4°C overnight. Anti-CYP2J2pep1 is a purified rabbit polyclonal antibody raised against a CYP2J2-specific peptide (amino acids 103-117) immunospecific for human CYP2J2 (63). For Tie2-CYP2C8 mice, membranes were incubated in a 1:1000 dilution of anti-CYP2C8 antibody (kindly provided by Dr. Joyce Goldstein, NIEHS, Research Triangle Park, NC) in 3% nonfat milk at 4°C overnight. Anti-CYP2C8 is a purified rabbit polyclonal antibody raised against recombinant human CYP2C8; although, some cross-reactivity with mouse CYP2Cs exists. Subsequently, the membranes were washed in 0.05% TBS-Tween 20 four times, and then incubated with a 1:2000 (CYP2J2) or 1:1000 (CYP2C8) dilution of horseradish peroxidase conjugated bovine anti-rabbit secondary antibody (Santa Cruz Biotechnology, Santa Cruz, CA) in 5% nonfat milk at room temperature for 1 hour. After additional washing in 0.05% TBS-Tween 20 and TBS, CYP2J2 and CYP2C8

immunoreactive bands were detected by chemiluminescence using the SuperSignal West Pico chemiluminescent substrate (Pierce, Rockford, IL).

Immunohistochemistry. Lung and aorta tissue were also fixed in 10% neutral buffered formalin, and embedded in paraffin. Serial sections (6 μm) were stained immunohistochemically for evaluation endothelial cell-specific transgene expression. Briefly, sections were deparaffinized in xylene, hydrated through a graded series of ethanols to 1X Automation Buffer (Biomeda, Foster City, CA), and then blocked for endogenous peroxidase activity with 3% (v/v) hydrogen peroxide. Enzyme-based antigen retrieval was completed using 0.05% pronase (Dako Corporation, Carpinterina, CA) for 5 minutes at room temperature prior to 15 minutes of blocking with 10% normal donkey serum in 1.25% normal mouse serum (Jackson Immunoresearch Labs, West Grove, PA). Following blocking for endogenous biotin using the Avidin-Biotin blocking kit (Vector Laboratories, Burlingame, CA), sections were incubated with primary antibody. For Tie2-CYP2J2 mice, sections were incubated with anti-CYP2J2pep1 or normal rabbit serum (1:50 dilution) for 30 minutes at room temperature. For Tie2-CYP2C8 mice, sections were incubated with anti-CYP2C8 (kindly provided by Dr. Joyce Goldstein) or normal rabbit serum (1:100 dilution) for 30 minutes at room temperature. Sections were rinsed in 1X Automation Buffer, and then incubated with a donkey anti-rabbit secondary antibody (Vector Laboratories) (1:500 dilution) for 30 minutes at room temperature. Sections were subsequently rinsed in 1X Automation Buffer, followed by a 30 minute incubation with a pre-diluted streptavidin complex (BioGenex, San Ramon, CA). Visualization of the antibody complex was completed using liquid 3,3'-diaminobenzidine solution (Dako Corporation) for 6 minutes in

the dark. Slides were counterstained with Harris hematoxylin (Harelco, Gibbston, NJ), rinsed in 1X Automation Buffer, dehydrated through a graded series of ethanol to xylene washes, and coverslipped with Permount (Surgipath, Richmond, IL). Stained sections were observed under a light microscope.

Quantification of Systemic EETs. Plasma samples were analyzed for epoxy and dihydroxy fatty acid metabolites of arachidonic acid and linoleic acid using established HPLC/MS/MS methods (128). In particular, plasma concentrations of each EET regioisomer (5,6-EET, 8,9-EET, 11,12-EET, 14-15-EET) were quantified.

Plasma samples were extracted by solid phase extraction using 60 mg Oasis-HLB SPE cartridges (Waters, Milford, MA) (46). Briefly, the cartridges were preconditioned with 2 mL of a 0.1% acetic acid-10% methanol solution, and then 10 μL of a 0.17 mg/mL solution of EDTA and butylated hydroxytoluene (BHT) in 50% methanol. Plasma samples (250 μL) were added to the column, diluted 1:1 (v/v) with 0.1% acetic acid-10% methanol, and then spiked with 30 ng of the following analytical surrogates for the epoxide [10,11-epoxyheptadecanoic acid (10,11-EpHep)] and diol [10,11-dihydroxynonadecanoic acid (10,11-DHN)] metabolites of the P450 epoxygenase pathway. After sample loading, the cartridges were washed with 2 mL of 0.1% acetic acid-10% methanol. Analytes were then eluted in 2 mL of ethyl acetate, and dried under nitrogen. Oxylipids were separated by reverse phase HPLC on a 2x150 mm, 5 μm Luna C18(2) column, (Phenomenex, Torrance, CA) and quantified using a MDS Sciex API 3000 triple quadrupole mass spectrometer (Applied Biosystems) with negative mode electrospray ionization and multiple reaction monitoring, as previously described (128). The relative response ratios of each analyte were

used to calculate concentrations, while correcting for surrogate losses via quantification relative to the internal standard.

Data analysis. All data are expressed as mean ± standard error of the mean (SEM). Data were analyzed by analysis of variance (ANOVA) or Student's t test, where applicable. A *P*-value <0.05 was considered statistically significant.

Results

Generation of Tie2-CYP2J2 and Tie2-CYP2C8 Transgenic Mice. The Tie2-CYP2J2 and Tie2-CYP2C8 transgenic constructs were successfully synthesized (Figures 13A and 13B). Microinjection of the linearized 14-kb constructs produced three Tie2-CYP2J2 and six Tie2-CYP2C8 hemizygous founder mice. Two Tie2-CYP2J2 and four Tie2-CYP2C8 founder mice successfully produced progeny for screening for germline transmission of the transgene. Genotyping of the progeny from the Tie2-CYP2J2 founder mice demonstrated that both founder lines (designated as Lines 1-2) exhibited germline incorporation of the transgene into the mouse genome (Figure 14). Genotyping of the progeny from the Tie2-CYP2C8 founder mice demonstrated that three founder lines (designated as Lines 1-3) exhibited germline incorporation into the mouse genome (Figure 14). Subsequent breeding of Tg mice from each germline founder line with wild-type C57BL/6 mice demonstrated Mendelian inheritance of the transgene, producing Tg (heterozygous) and wild-type pups at an approximate ratio of 1:1. Moreover, male and female Tg and wild-type mice were fertile with no impaired reproductive capacity, and expression of the transgene was not lethal and did not result in developmental defects.

Real Time RT-PCR. Quantitative real-time RT-PCR demonstrated that Tie2-CYP2J2 and Tie2-CYP2C8 Tg mice exhibit significantly higher expression of the human CYP2J2 and CYP2C8 transgenes, respectively, at the RNA level in lung and aorta relative to wild-type littermates (Figure 15A and 15B). The Tie2-CYP2J2 and Tie2-CYP2C8 Tg mice also had higher RNA expression of their respective transgene in heart, kidney and liver compared to wild-type littermates (n=2-3 per genotype, data not shown).

The apparent lower degree of transgene expression in lung (Figure 15A, ~100-150-fold) compared to aorta (Figure 15B, ~10,000-15,000-fold) in Tg mice relative to wild-type littermates was driven by the substantially greater degree of cross-reactivity of the human CYP2J2 and CYP2C8 real time RT-PCR assays with murine CYP2Js and CYP2Cs, respectively, in wild-type lung compared to wild-type aorta. These apparent differences were not due to lower RNA expression of the human CYP2J2 or CYP2C8 transgenes in Tg lung compared to Tg aorta.

Immunoblotting. Immunoblotting demonstrated that Tie2-CYP2J2 and Tie2-CYP2C8 Tg mice exhibit significantly higher expression of the human CYP2J2 and CYP2C8 transgenes, respectively, at the protein level in lung microsomes relative to wild-type littermates (Figure 16A and 16B). In Tie2-CYP2J2 mice, immunoreactivity with the anti-CYP2J2pep1 antibody was observed in Tg mice of germline founder lines 1 and 2, whereas no immunoreactivity was observed in wild-type littermates (Figure 16A). In Tie2-CYP2C8 mice, a substantially greater degree of immunoreactivity with the anti-CYP2C8 antibody was observed in Tg mice of germline founder lines 1, 2 and 3 compared to wild-type littermates (Figure 16B).

Interestingly, no differences in immunoreactivity to either antibody were observed in Tg mice compared to wild-type littermates in aorta, heart, liver or kidney microsomes (data not shown).

Immunohistochemistry. Immunohistochemical staining demonstrated that Tie2-CYP2J2 and Tie2-CYP2C8 Tg mice exhibit endothelial cell-specific expression of the human CYP2J2 and CYP2C8 transgenes, respectively (Figures 17-20). In Tie2-CYP2J2 mice, CYP2J2 expression was observed in pulmonary endothelial cells in Tg mice, whereas no detectable expression was observed in wild-type littermates or with normal rabbit serum (Figure 17A-17D). This expression profile was observed across multiple vessels located throughout the lung, and was consistent with the immunoblotting results observed in lung microsomes. Endothelial cell expression of CYP2J2 was also observed in the aorta of Tg mice, with minimal to no detectable expression observed in wild-type littermates (Figure 18A-18D).

In Tie2-CYP2C8 mice, CYP2C8 expression was observed in pulmonary endothelial cells in Tg mice, whereas minimal to no detectable expression was observed in wild-type littermates (Figure 19A-19B). No expression was observed with normal rabbit serum (Figure 19C-19D). This expression profile was observed across multiple vessels located throughout the lung, and was consistent with the immunoblotting results observed in lung microsomes. Endothelial cell expression of CYP2C8 was also observed in the aorta of Tg mice, with minimal to no detectable expression observed in wild-type littermates (Figure 20A-20D).

Quantification of Systemic EETs. Tie2-CYP2J2 and Tie2-CYP2C8 Tg mice have significantly higher plasma concentrations of EETs compared to wild-type littermates (Figures 21A and 21B), demonstrating enhanced CYP2J2 and CYP2C8-mediated EET biosynthesis, respectively, in mice expressing the transgene. Tie2-CYP2J2 Tg mice had a mean 1.5-fold higher concentration of total EETs in plasma compared to WT littermates (P=0.019) (Figure 21A). Tie2-CYP2C8 Tg mice had a mean 1.6-fold higher concentration of total EETs in plasma compared to WT littermates (P=0.039) (Figure 21B).

Discussion

Preclinical studies have demonstrated that CYP2J2 and CYP2C8-derived EETs play an important role in the regulation of cardiovascular function. However, the vascular effects of this pathway have not been extensively characterized in whole animal models *in vivo*, including the potential biological differences related to CYP2J2 versus CYP2C8-mediated EET generation. In order to further characterize the *in vivo* role of both CYP2J2 and CYP2C8-mediated EET biosynthesis in the regulation of endothelial function, vascular inflammation and atherosclerotic lesion development, *in vivo* models enabling alteration of the P450 epoxygenase pathway must be developed. Due to the complexity of the murine CYP2J and CYP2C subfamilies and their relative tissue distribution in mice (145), both pharmacological manipulation of wild-type mice and the development of isoform-specific knock-out mice carry substantial limitations. Consequently, transgenic mice which overexpress either human CYP2J2 or CYP2C8 in vascular endothelial cells were developed.

Transgenic constructs were synthesized via subcloning human CYP2J2 or CYP2C8 cDNA downstream of the *Tie2* promoter and upstream of the *Tie2* full enhancer (intron 1) sequences

(149). Utilizing this approach, Tie2-CYP2J2 and Tie2-CYP2C8 Tg mice which exhibit constitutive, vascular endothelial cell-specific expression of CYP2J2 and CYP2C8, respectively, were successfully generated. Transgene expression was observed at the RNA level by real time quantitative RT-PCR in various tissues, including lung and aorta. Moreover, transgene expression at the protein level was observed by immunoblotting in lung microsomal fractions. Endothelial-specific expression was confirmed by immunohistochemical staining of lung and aorta sections. Overall, Tie2-CYP2J2 and Tie2-CYP2C8 Tg mice demonstrated significantly enhanced expression of CYP2J2 and CYP2C8, respectively, compared to wild-type littermates. Importantly, Tie2-CYP2J2 and Tie2-CYP2C8 Tg mice also had significantly higher plasma EET concentrations compared to their wild-type littermates, demonstrating enhanced CYP2J2 and CYP2C8-mediated EET biosynthesis in mice expressing the transgene.

In order to confirm transgene expression at the RNA level, real time quantitative RT-PCR and assays which quantified expression of human CYP2J2 and CYP2C8 in mice were utilized. Due to the high degree of homology between human and murine CYP2J and CYP2C isoforms, assays with primers that exhibited minimal homology to murine CYP2Js and CYP2Cs, respectively, via sequence alignment were specifically selected. However, some cross-reactivity between these "human" assays and murine CYP2J and CYP2C isoforms was present, particularly in lung. Consequently, the relative differences in transgene expression observed between Tg mice and wild-type littermates should not be compared across tissues. This is apparent by comparing the substantial differences in relative expression (Tg versus wild-type) observed across lung and aorta (Figure 15), which was driven by differences in CYP2J2 and CYP2C8 cross-reactivity in the lung and aorta of wild-

type mice. Importantly, the data presented in Figure 15 demonstrate that Tie2-CYP2J2 and Tie2-CYP2C8 Tg mice have significantly higher RNA expression of CYP2J2 and CYP2C8, respectively, compared to wild-type littermates within both lung and aorta.

CYP2J2 protein expression was clearly observed in lung microsomes by immunoblotting in Tie2-CYP2J2 Tg mice, whereas no detectable expression was observed in wild-type littermates. The anti-CYP2J2pep1 antibody utilized in these analyses is specific for human CYP2J2, and does not cross-react with murine CYP2Js (63). Immunohistochemistry demonstrated that CYP2J2 expression in Tg mice was specifically present in endothelial cells in both lung and aorta sections. In Tie2-CYP2C8 Tg mice, CYP2C8 protein expression was also observed in lung microsomes by immunoblotting and specifically in endothelial cells in both lung and aorta by immunohistochemistry. Although some CYP2C8 expression was observed in wild-type littermates, this was due to cross-reactivity of the anti-CYP2C8 antibody with certain murine CYP2C isoforms such as CYP2C29 and CYP2C40 (data not shown). Importantly, the level of expression in Tg mice was substantially greater than that observed in wild-type mice. However, overexpression of the CYP2J2 and CYP2C8 transgenes was not detectable by immunoblotting in aorta, heart, liver or kidney microsomes. This was likely due to the greater degree of vascularization in lung tissue, which has been reported to have a greater proportion of endothelial cells per given amount of tissue compared to other organs in mice (152). The substantial degree of vascularization in lung was evident in the immunohistochemistry analysis, in which multiple vessels throughout the lung exhibited clear endothelial cell expression of each transgene. Moreover, development of other endothelial transgenic mice using the *Tie2* promoter and *Tie2* full enhancer has

demonstrated that transgene expression is most readily detectable in lung, particularly when expression was evaluated by immunoblotting (152).

Since microinjected transgenic constructs are randomly inserted into the mouse genome when generating transgenic mice, the goal was to obtain at least two germline founder lines which express the transgene for each the Tie2-CYP2J2 and Tie2-CYP2C8 mice. Evaluation of more than one founder line in future phenotyping studies will enhance confidence that any observed phenotype is due to the expression and function of the transgene, and not due to disruption of the genome region in which the transgene was randomly inserted. The results of the reported baseline studies have confirmed that two Tie2-CYP2J2 and three Tie2-CYP2C8 distinct founder lines exhibit expression of the transgene in vascular endothelial cells.

Development of these novel Tie2-CYP2J2 and Tie2-CYP2C8 transgenic mice (in addition to existing *Ephx2*$^{-/-}$ mice) will enable investigators to characterize the effects of altered CYP2J2 and CYP2C8-mediated EET biosynthesis (or decreased EET hydrolysis) on endothelial function, vascular inflammation and atherosclerotic lesion development *in vivo*. Collectively, phenotypic studies in these genetically altered mouse models will improve the mechanistic understanding of the role of CYP2J2, CYP2C8 and sEH in these processes *in vivo*, which have proven vital to the development and progression of cardiovascular disease. Moreover, future phenotypic studies in these mouse models will help to provide a mechanistic rationale for the observed associations at the population level between genetic variation in *CYP2J2*, *CYP2C8* and *EPHX2* and cardiovascular disease susceptibility in humans.

Figure Legends

Figure 13. (A) Diagram of the linear 14-kb Tie2-CYP2J2 and Tie2-CYP2C8 transgenic constructs. (B) Restriction enzyme digested Tie2-CYP2J2 and Tie2-CYP2C8 transgenic constructs run on an ethidium bromide-stained, 0.8% agarose gel and visualized under ultraviolet light. *Not*I digestion produced the linearized *Tie2* promoter-CYP2J2/2C8 cDNA (~3.7-kb) and pBS vector-polyA-*Tie2* full enhancer (~13.3-kb) fragments. *Sal*I digestion produced the linearized *Tie2* promoter-CYP2J2/2C8 cDNA-*Tie2* full enhancer (~14-kb) and pBS vector (~3-kb) fragments. *Not*I and *Sal*I digestion produced the linearized *Tie2* promoter-CYP2J2/2C8 cDNA (~3.7-kb), polyA-*Tie2* full enhancer (~10.3-kb), and pBS vector (~3-kb) fragments.

Figure 14. PCR genotyping of transgenic (Tg) and wild-type (WT) littermate mice from the (A) two Tie2-CYP2J2 and (B) three Tie2-CYP2C8 germline founder lines, and 0.1 pg (0.5 gene copies per cell) of each transgenic construct as a positive control. Both PCR reactions were run on an ethidium bromide-stained, 1% agarose gel and visualized under ultraviolet light. The Tg mice demonstrate bands at approximately 600 and 1000 base pairs for PCR reaction #1 and #2, respectively, while WT mice demonstrate no detectable bands.

Figure 15. Mean±SEM expression of human CYP2J2 and CYP2C8 RNA in Tie2-CYP2J2 and Tie2-CYP2C8 transgenic (Tg) mice and wild-type (WT) littermates in (A) lung and (B) aorta (n=4-7 per genotype group). CYP2J2 and CYP2C8 RNA expression was quantified by real-time quantitative RT-PCR, and normalized to murine GAPDH expression. Data are

presented as relative expression compared to WT littermates (reference 1.0) using the $2^{-\Delta\Delta Ct}$ method (151). *P<0.05 versus wild-type.

Figure 16. Representative immunoblot of lung microsomal fractions (70 μg per lane) in (A) Tie2-CYP2J2 and (B) Tie2-CYP2C8 transgenic (Tg) mice and wild-type (WT) littermates, using the anti-CYP2J2pep1 and anti-CYP2C8 antibodies, respectively. Lane 1 includes recombinant CYP2J2 or CYP2C8 (0.5 pg), respectively, as a positive control. Subsequent lanes include Tg and WT littermate pairs from each germline founder line.

Figure 17. Immunohistochemical staining of a representative lung section in (A, B) Tie2-CYP2J2 transgenic (Tg) mice and (C, D) wild-type (WT) littermates. Staining was completed using the anti-CYP2J2pep1 antibody (A, C) or normal rabbit serum negative control (B, D). Arrows indicate the presence and absence of endothelial cell staining in Tg and WT mice.

Figure 18. Immunohistochemical staining of a representative aorta section in (A, B) Tie2-CYP2J2 transgenic (Tg) mice and (C, D) wild-type (WT) littermates. Staining was completed using the anti-CYP2J2pep1 antibody (A, C) or normal rabbit serum negative control (B, D). Arrows indicate the presence and absence of endothelial cell staining in Tg and WT mice.

Figure 19. Immunohistochemical staining of a representative lung section in (A, B) Tie2-CYP2C8 transgenic (Tg) mice and (C, D) wild-type (WT) littermates. Staining was

completed using the anti-CYP2C8 antibody (A, C) or normal rabbit serum negative control (B, D). Arrows indicate the presence and absence of endothelial cell staining in Tg and WT mice.

Figure 20. Immunohistochemical staining of a representative aorta section in (A, B) Tie2-CYP2C8 transgenic (Tg) mice and (C, D) wild-type (WT) littermates. Staining was completed using the anti-CYP2C8 antibody (A, C) or normal rabbit serum negative control (B, D). Arrows indicate the presence and absence of endothelial cell staining in Tg and WT mice.

Figure 21. Mean±SEM plasma EET concentrations in (A) Tie2-CYP2J2 and (B) Tie2-CYP2C8 transgenic (Tg) mice and wild-type (WT) littermates (n=5-6 per genotype group), quantified by HPLC/MS/MS. Concentrations of the four individual EET regioisomers (5,6-EET, 8,9-EET, 11,12-EET, 14,15-EET) and their sum total (Sum EETs) are presented in ng/mL. *$P<0.05$ and ^$P<0.10$ versus WT.

Figure 13. Tie2-CYP2J2 and Tie2-CYP2C8 transgenic constructs.

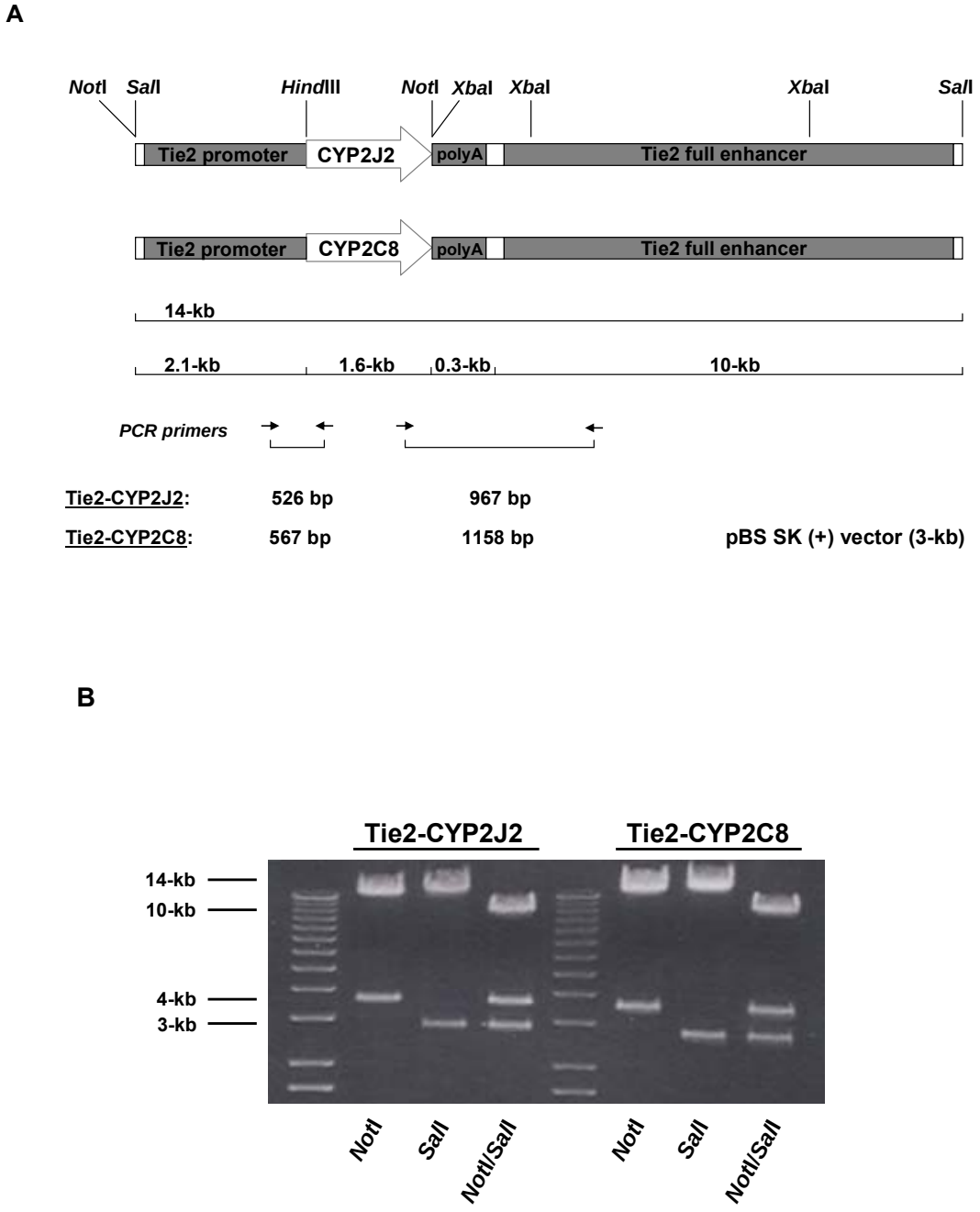

Figure 14. Genotyping Tie2-CYP2J2 and Tie2-CYP2C8 mice.

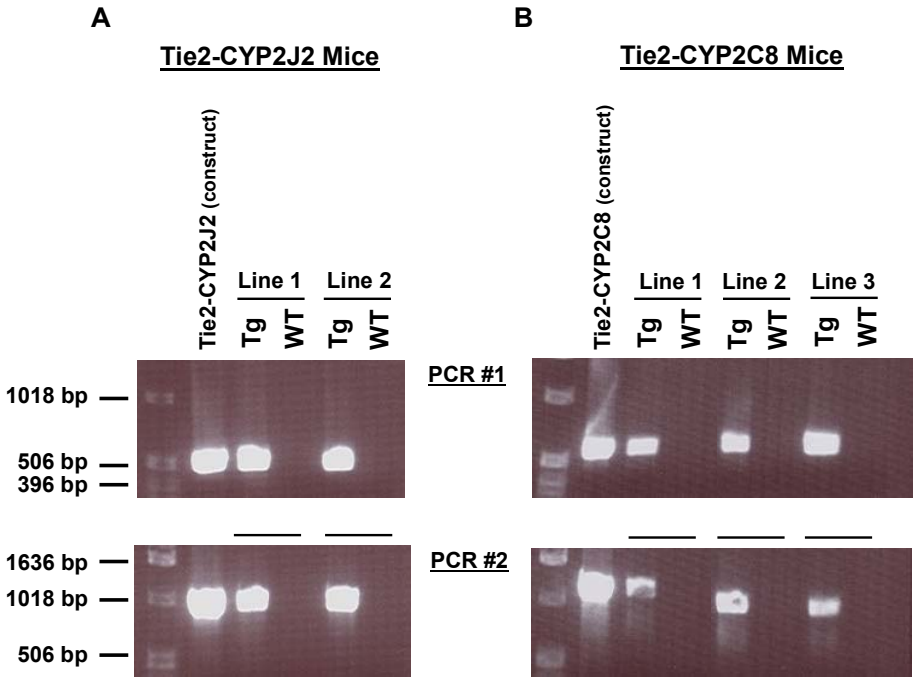

Figure 15. CYP2J2 and CYP2C8 RNA expression by real time quantitative RT-PCR.

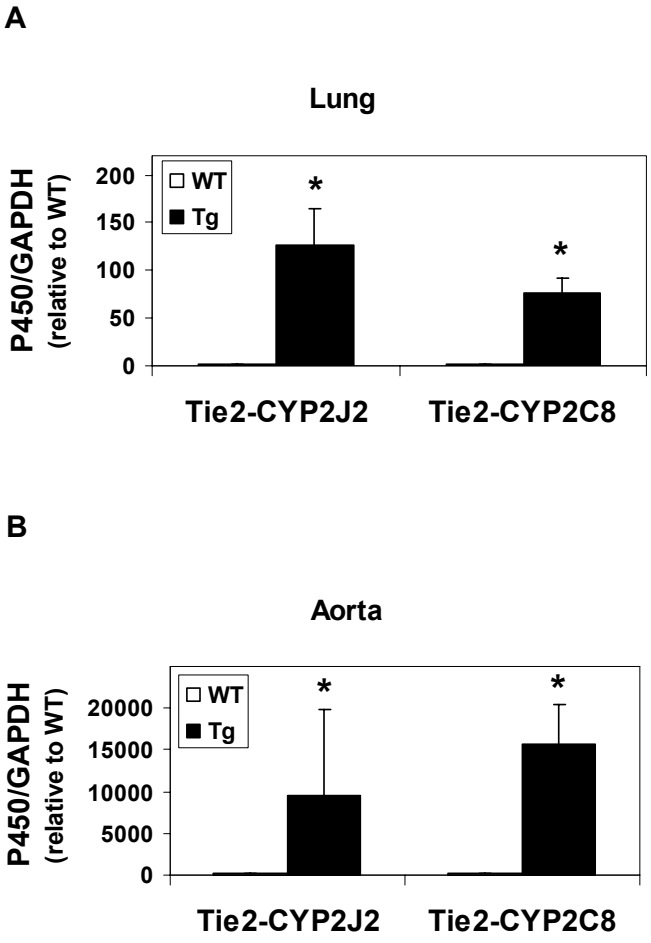

Figure 16. CYP2J2 and CYP2C8 protein expression in lung microsomes by immunoblotting.

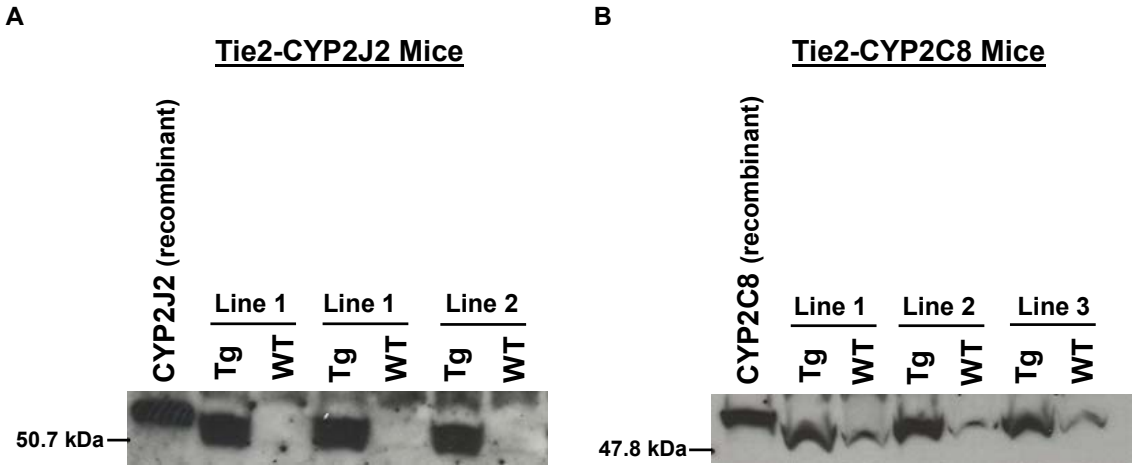

Figure 17. Endothelial cell expression of CYP2J2 in lung by immunohistochemical staining in Tie2-CYP2J2 mice.

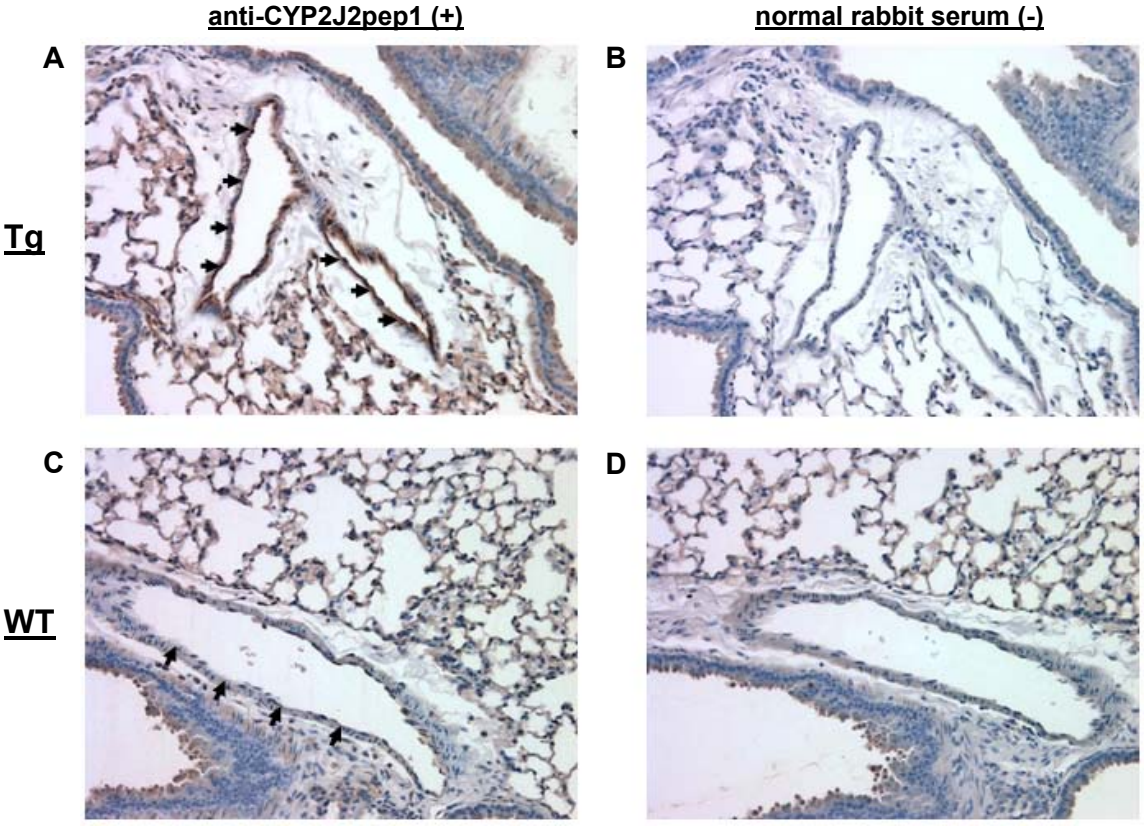

Figure 18. Endothelial cell expression of CYP2J2 in aorta by immunohistochemical staining in Tie2-CYP2J2 mice.

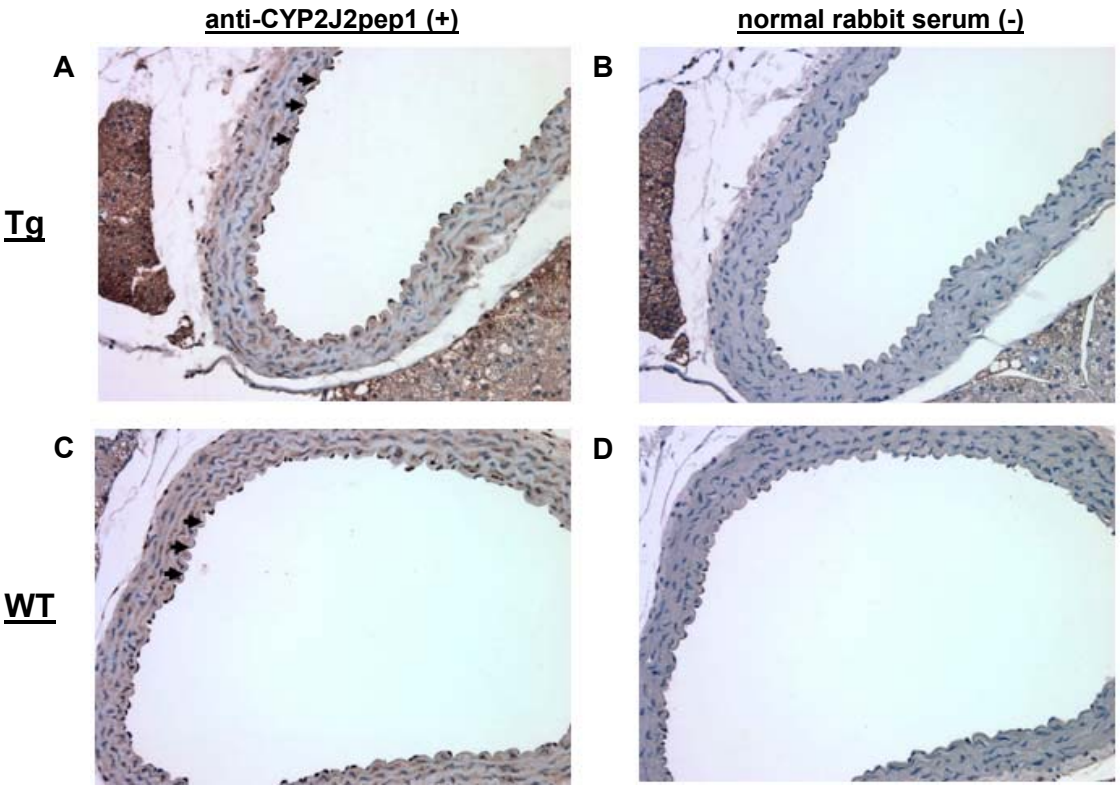

Figure 19. Endothelial cell expression of CYP2C8 in lung by immunohistochemical staining in Tie2-CYP2C8 mice.

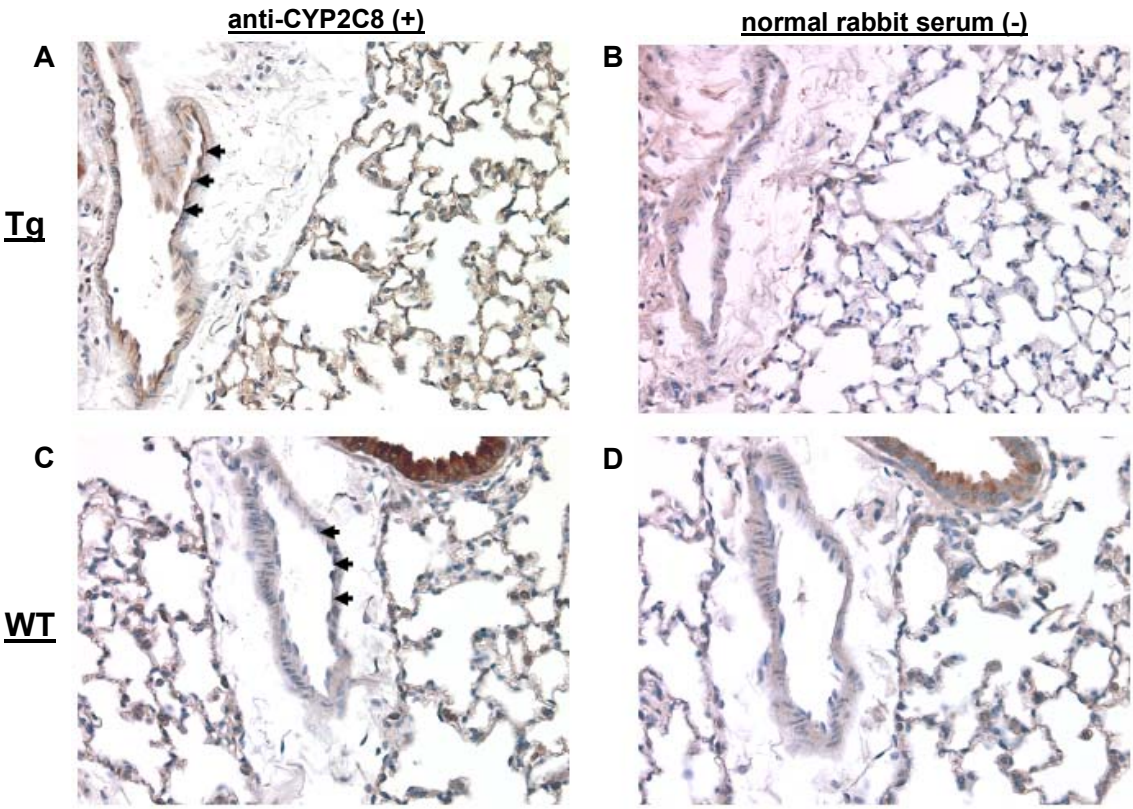

Figure 20. Endothelial cell expression of CYP2C8 in aorta by immunohistochemical staining in Tie2-CYP2C8 mice.

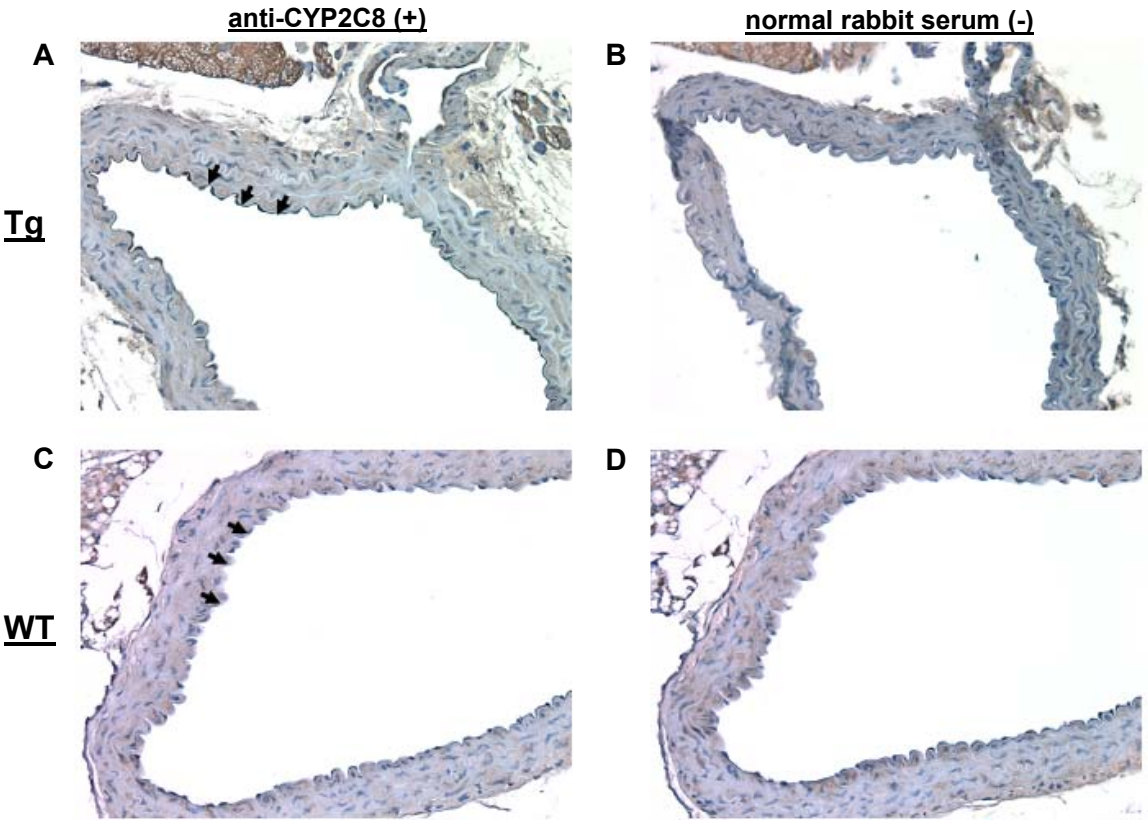

Figure 21. Plasma EETs in Tie2-CYP2J2 and Tie2-CYP2C8 mice.

A

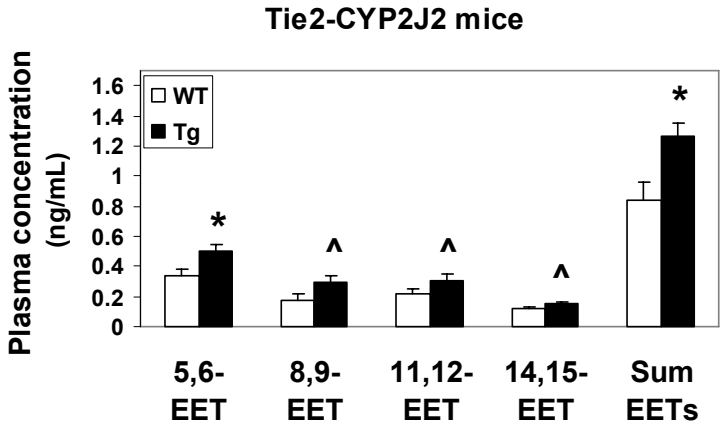

B

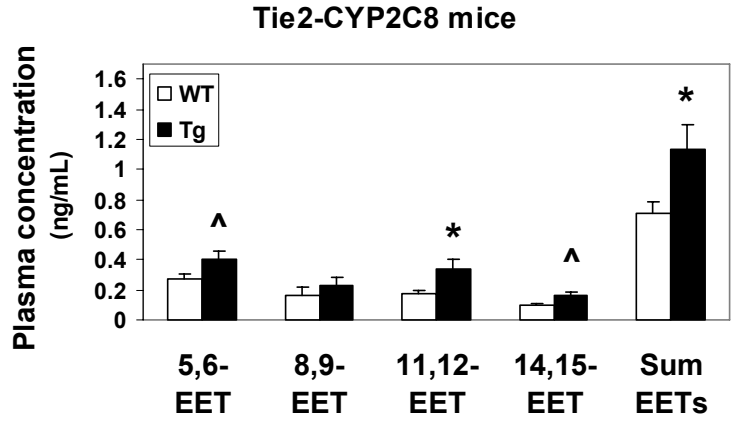

CHAPTER VIII

DISCUSSION AND PERSPECTIVE

Endothelial dysfunction plays an integral role in the pathogenesis and progression of ischemic cardiovascular disease in humans (2). Risk factors including cigarette smoking significantly contribute to endothelial dysfunction (6), which is independently associated with an increased risk of myocardial infarction and ischemic stroke events in patients (10, 11). The development of endothelial dysfunction has been primarily ascribed to functional impairments in nitric oxide biosynthesis and activity; however, arachidonic acid metabolism by the cyclooxygenase (COX) and P450 epoxygenase pathways also appear to be important regulators of endothelial function (Figures 1 and 2). Consequently, genetic variation in these pathways may be important modifiers of cardiovascular disease risk in humans. Numerous polymorphisms in the genes encoding endothelial nitric oxide synthase (*NOS3*), COX-1 (*PTGS1*), COX-2 (*PTGS2*), CYP2J2 (*CYP2J2*), CYP2C8 (*CYP2C8*) and soluble epoxide hydrolase (*EPHX2*) have been recently discovered. However, their contribution to cardiovascular disease susceptibility remains poorly understood. The collective objective of the studies outlined in this doctoral dissertation was to determine if genetic variation in these established (*NOS3*, *PTGS1* and *PTGS2*) and recently characterized (*CYP2J2*, *CYP2C8* and *EPHX2*) pathways are significantly associated with cardiovascular disease risk.

The identification and functional characterization of genetic polymorphisms in *PTGS2* and *NOS3* have been reported (53, 54, 58, 59); however, characterization of *PTGS1*

polymorphisms and their influence on COX-1-mediated arachidonic acid metabolism has not been extensively investigated. Consequently, the first aim was to determine if nonsynonymous polymorphisms in *PTGS1* significantly alter COX-1 metabolic activity *in vitro*, in order to guide the design and interpretation of epidemiological studies evaluating associations between *PTGS1* variants and cardiovascular disease risk. The relatively infrequent R53H, R78W, K185T, G230S and L237M variants demonstrated significantly lower metabolic activity (35-60%) relative to wild-type COX-1, suggesting individuals carrying these variant alleles may have significantly altered prostaglandin biosynthesis *in vivo* (Chapter II). No significant differences in enzymatic activity were detected with the R8W and P17L variants, which are prevalent at higher frequencies in European/Caucasian and African populations.

Subsequently, the second aim was to determine if genetic variation in *PTGS1*, *PTGS2* and/or *NOS3* is significantly associated with the development of incident coronary heart disease (CHD) or ischemic stroke clinical events in individuals enrolled in the Atherosclerosis Risk in Communities (ARIC) study. Genetic variation in *PTGS1* and *PTGS2* was associated with risk of incident ischemic cardiovascular disease events (Chapter III). Interestingly, these associations appeared most prominent for risk of ischemic stroke events, consistent with various preclinical studies implicating both COX-1 and COX-2-mediated arachidonic acid metabolism in ischemic brain injury (113-118). Specifically, the variant -*1006A* allele in *PTGS1* was associated with higher risk of ischemic stroke events in Caucasians. Although the functional relevance of this polymorphism has not been characterized, evaluation of linkage disequilibrium in *PTGS1* demonstrated that seven polymorphisms in the 5'UTR (*T-1749C*, *G-1598A*, *A-1202G*, *A-1201G*, *G-1006A*, *A-918G*

and *A-707G*) were present on the same haplotype in individuals of either European/Caucasian or African descent (Chapter II). Consequently, the *G-1006A* polymorphism may not be the functionally relevant locus driving the observed association with ischemic stroke risk in the ARIC study. Future studies evaluating the functional relevance of these variants appear necessary. Moreover, the rare *G230S* variant allele in *PTGS1* was associated with significantly higher risk of both ischemic stroke and CHD events in African-Americans. This variant was associated with reduced COX-1 metabolic activity *in vitro* (Chapter II). Moreover, protein modeling suggested that this variant may disrupt the active conformation of COX-1, leading to the observed reductions in metabolic activity. Future studies validating this association and confirming the functional relevance of the *G230S* variant allele *in vivo* are necessary.

Previous studies have demonstrated that the *G-765C* polymorphism in the proximal promoter of *PTGS2* disrupts a Sp1 binding site and is associated with significantly lower *PTGS2* transcription (59). Due to its anti-inflammatory effects, the variant *-765C* allele was associated with significantly lower risk of prevalent myocardial infarction or ischemic stroke events in a high-risk Italian population (60). In contrast, the variant *-765C* allele was associated with higher risk of incident ischemic stroke events in African-Americans, but not Caucasians, in the ARIC study (Chapter III). Moreover, although the *G-765C* polymorphism in *PTGS2* was not significantly associated with CHD incidence, aspirin utilization appeared to modify this relationship in Caucasians. The variant *-765C* allele appeared to be associated with higher risk of CHD in aspirin non-users and lower risk in those receiving aspirin therapy, suggesting presence of a potential gene-drug interaction. This observation is consistent with the hypothesis that concomitant aspirin utilization may mitigate the

cardiovascular hazard associated with selective COX-2 inhibition via restoration of prostacyclin-thromboxane A_2 balance (24), and could explain the contrasting results observed by Cipollone et al. (60). However, due to the power limitations and lack of data elucidating the underlying mechanism, this interaction must be interpreted with caution and confirmed in an independent population.

Numerous studies evaluating potential associations between *NOS3* polymorphisms and cardiovascular disease risk have reported inconsistent results (55). However, few have considered the potential influence of cigarette smoking despite their potential synergistic contribution to worsening endothelial function *in vivo* (56, 57). No statistically significant associations between the *T-786C* or *E298D* polymorphisms and risk of either incident CHD or ischemic stroke events in Caucasians and African-Americans enrolled in the ARIC study were observed (Chapter IV). Importantly, a potential interaction between genetic variation in *NOS3*, cigarette smoking history, and risk of incident CHD and ischemic stroke events was identified in these individuals. Specifically, the *T-786C* or *E298D* polymorphism variant alleles appeared to be associated with significantly higher risk of developing CHD or ischemic stroke in cigarette smokers, whereas no associations were observed in the absence of the smoking exposure. This interaction was particularly evident with the *E298D* polymorphism and CHD risk in Caucasians, and the *T-786C* polymorphism and ischemic stroke risk in African-Americans. These data 1) suggest that presence of established underlying endothelial dysfunction, as observed in cigarette smokers, may be necessary for these variant alleles to significantly attenuate endothelial function and predispose patients to increased risk of cardiovascular events, and 2) demonstrate the potential existence of a complex interplay between *NOS3* polymorphisms, cigarette smoking and cardiovascular

disease risk (i.e., a gene-environment interaction). Similar interactions with cigarette smoking were not observed with polymorphisms in *PTGS1* and *PTGS2*. Collectively, the observed associations between genetic variation in *PTGS1*, *PTGS2* and *NOS3* and risk of incident cardiovascular disease events in the ARIC study further implicate these established pathways in the development of ischemic cardiovascular disease in humans.

Since the identification and functional characterization of genetic polymorphisms in *EPHX2*, *CYP2J2* and *CYP2C8* have been previously reported (63-66, 68, 69), the third aim was to determine if genetic variation in *EPHX2*, *CYP2J2* and/or *CYP2C8* is significantly associated with the development of incident CHD clinical events in individuals enrolled in the ARIC study. Although potential associations between genetic variants in these pathways and ischemic stroke risk are also of interest (133), the results of those analyses were not included in this doctoral dissertation. First, a significant association between genetic variation in *EPHX2* and risk of incident CHD events in Caucasians was observed, implicating *EPHX2* as a potential cardiovascular disease-susceptibility gene (Chapter V). Specifically, presence of the *K55R* polymorphism variant allele was associated with significantly higher risk of CHD incidence in Caucasians. Consistent with previous *in vitro* findings (69), higher soluble epoxide hydrolase activity in Caucasians carrying the *K55R* variant allele was also observed *in vivo*. Based on the role of *EPHX2* in endothelial function, it was hypothesized that higher epoxide hydrolase activity would be associated with higher risk of acute coronary events. A significant association between the *K55R* variant allele and higher risk of incident CHD in Caucasians are consistent with this hypothesis. Variation in *EPHX2* at the haplotype level was also associated with risk of CHD in Caucasians, suggesting multiple variants within or near *EPHX2* may contribute to CHD risk. Genetic

variation in *EPHX2* was not associated with risk of incident CHD in African-Americans. Interestingly, no apparent influence of *K55R* genotype on soluble epoxide hydrolase activity was observed in African-Americans *in vivo*.

Second, a significant association between the variant *-50T* allele in *CYP2J2* and lower risk of incident CHD events was observed in African-Americans, whereas no significant association was observed in Caucasians (Chapter VI). The *G-50T* polymorphism disrupts a Sp1 transcription factor binding site in the proximal promoter and leads to reduced *CYP2J2* transcription *in vitro* (64). Importantly, the variant *-50T* allele was associated with higher risk of prevalent angiographically-documented CHD in a recently characterized German population (64). However, the findings in African-Americans exist in contrast to these previous findings and current hypotheses related to the beneficial effects of EETs in the vasculature. Interestingly, a similar ethnic contrast was observed in the evaluation of both *NOS3* and *EPHX2* polymorphisms and CHD risk (135, 139) (Chapters IV and V). Specifically, the *E298D* variant allele in *NOS3* and the *K55R* variant allele in *EPHX2*, which were hypothesized to be associated with higher CHD risk, were each associated with a non-significant trend toward lower CHD risk in African-Americans. Additional genetic and/or environmental factors not accounted for in this analysis could be contributing to population differences in the likely complex relationship between these pathways, endothelial function and cardiovascular disease risk, particularly since ethnic differences in endothelial function are well-documented (142). Future studies further characterizing the mechanisms underlying these contrasting observations at the population level appear necessary.

Third, the *I264M*, *I269F* and *K399R* polymorphisms in *CYP2C8*, which have been associated with reduced CYP2C8 metabolic activity *in vitro* (65, 66), were not associated

with risk of CHD in either ethnic group (Chapter VI). However, in Caucasians, cigarette smokers carrying either the variant *I264M* or *K399R* allele were at significantly higher risk of incident CHD, whereas no significant association with disease risk was observed in the absence of the smoking exposure. Similar interactions were observed with each the *E298D* polymorphism in *NOS3* and *K55R* polymorphism in *EPHX2* and risk of incident CHD in Caucasians, with the highest risk observed in smokers carrying these variant alleles (135, 139) (Chapters IV and V). However, a similar interaction was not observed with the *G-50T* polymorphism in *CYP2J2* (Chapter VI), demonstrating potential biological differences related to CYP2J2 versus CYP2C8-mediated epoxyeicosatrienoic acid (EET) biosynthesis in humans. Perhaps presence of established underlying endothelial dysfunction, as observed in cigarette smokers, may be necessary for genetic variation in *CYP2C8*, *NOS3* and *EPHX2* to significantly influence endothelial function and cardiovascular disease risk in Caucasians. Interestingly, similar interactions with CHD risk were not observed in African-Americans in the ARIC study, further demonstrating potential differences in the contribution of these endothelial pathways to cardiovascular disease risk across populations. Future mechanistic studies will be required to further characterize this potential gene-environment interaction. Collectively, the observed associations between genetic variation in *EPHX2*, *CYP2J2* and *CYP2C8* and risk of incident CHD events in the ARIC study demonstrate the potential importance of the P450 epoxygenase pathway in the pathogenesis of ischemic cardiovascular disease in humans.

Importantly, the mechanisms underlying the role of P450-mediated EET biosynthesis in the regulation of endothelial function, vascular inflammation and atherosclerotic lesion development *in vivo* remain poorly understood. Moreover, evaluation of the potential

biological differences between CYP2J2 and CYP2C8-mediated EET biosynthesis under controlled conditions has not been extensively characterized. Due to the complexity of the murine CYP2J and CYP2C subfamilies and their relative tissue distribution in mice (145), both pharmacological manipulation of wild-type mice and the development of isoform-specific knock-out mice carry substantial limitations. Thus, the fourth aim was to develop transgenic mice that exhibit vascular endothelial cell-specific overexpression of either human CYP2J2 or CYP2C8 for use in future phenotyping studies. Using the murine *Tie2* promoter and *Tie2* full enhancer fragments (149), Tie2-CYP2J2 and Tie2-CYP2C8 transgenic mice which exhibit constitutive, vascular endothelial cell-specific expression of CYP2J2 and CYP2C8, respectively, were successfully generated (Chapter VII). Transgene expression was observed at the RNA level by real time quantitative RT-PCR and the protein level by both immunoblotting and immunohistochemistry. Importantly, Tie2-CYP2J2 and Tie2-CYP2C8 transgenic mice also had significantly higher plasma EET concentrations compared to their wild-type littermates, demonstrating enhanced CYP2J2 and CYP2C8-mediated EET biosynthesis in mice expressing the transgene.

Development of these Tie2-CYP2J2 and Tie2-CYP2C8 transgenic mice (in addition to existing *Ephx2*$^{-/-}$ mice) will enable further characterization of the effects of altered CYP2J2 and CYP2C8-mediated EET biosynthesis (or decreased EET hydrolysis) on endothelial function, vascular inflammation and atherosclerotic lesion development *in vivo* in order to improve the mechanistic understanding of the role of CYP2J2, CYP2C8 and soluble epoxide hydrolase in these processes, which have proven vital to the development and progression of cardiovascular disease in humans. Moreover, future phenotypic studies in these mouse models will help to provide a mechanistic rationale for the observed associations at the

population level between genetic variation in *CYP2J2*, *CYP2C8* and *EPHX2* and cardiovascular disease susceptibility in the ARIC study. Collectively, the results of these current and future translational investigations will enable investigators to more extensively determine if modulation of the P450 epoxygenase pathway using genetic and/or pharmacological approaches represents a useful therapeutic strategy for the prevention and/or treatment of cardiovascular disease in patients.

APPENDIX I

The reality of pharmacogenomics: optimizing therapeutic decision making (editorial)

Lee CR and Zeldin DC. The reality of pharmacogenomics: optimizing therapeutic decision making. Environ Health Perpesct. 2003;111:A566-67.

It is now well established that significant interindividual variability exists in the disposition and pharmacological effects of certain medications. Influences such as environmental exposures, nutritional status, comorbidities, severity of disease, and concomitant medications have all been associated with heterogeneity in drug responses. In addition, the profound contribution of genetics has been appreciated for some time and is receiving greater emphasis in recent years.

Approximately 1.8 million single nucleotide polymorphisms (SNPs) in the human genome have been identified by the SNP Consortium (http://snp.cshl.org), a collaboration of several companies and institutions. Numerous SNPs in genes encoding various drug metabolizing enzymes, drug transporters, and drug targets (e.g., receptors, enzymes involved in metabolism of endogenous substrates, etc.) have been shown to be associated with interindividual differences in the pharmacokinetics and pharmacodynamics of certain medications (153). Many *in vitro* and *in vivo* "pharmacogenetic" studies performed to date have evaluated the association between SNPs in a single gene and a specific drug's pharmacological properties. Preclinical and clinical investigations have evaluated genetic determinants of drug metabolism, and demonstrated that polymorphisms in genes encoding drug metabolizing enzymes can markedly influence a drug's pharmacokinetics, change its efficacy and/or toxicity profile, and necessitate dosing changes in certain individuals. More recent studies have begun to evaluate the association between drug target polymorphisms and pharmacodynamic effects.

Due to the complex interplay between the pharmacological effects of drugs and disease pathophysiology, inherited differences in drug responses are most likely polygenic, rather than monogenic, in nature (153). Hence, "pharmacogenomics" has emerged as a new field of study which attempts to identify and elucidate the contribution of multiple, interrelated genes to the efficacy and toxicity of certain medications. Ultimately, the goal of pharmacogenomics is to account for and minimize interindividual variability in drug response, thus allowing clinicians to enhance the efficacy and minimize the toxicities associated with drug therapy. By considering the role of multiple genes, pharmacogenomics seeks to divide a given patient population into smaller, less variable, more predictable subgroups, which enables clinicians to individualize drug therapy (i.e., to administer the right drug, at the right dose, to the right patient) (154).

For example, it has been increasingly recognized that SNPs can impact the activity of drug transporters and drug metabolizing enzymes, and substantially influence an individual's systemic exposure to certain agents. Genetic variation in a given drug's target can also contribute to its pharmacological effect. Moreover, variation in a disease-modifying gene can impact the rate and/or extent of disease progression, ultimately influencing the therapeutic effect of a drug. Therefore, simultaneously characterizing genetic determinants of drug exposure, drug effect, and disease progression will likely improve the ability to predict a drug's overall effect in an individual patient. In other words, genomic data will divide a given patient population into subpopulations of "responders" and "nonresponders," allowing prescribers to better predict the potential therapeutic effect of a drug. Pharmacogenomic testing may also lead to more predictable toxicity profiling for individual patients, thus prospectively identifying and eventually minimizing idiosyncratic or

unexpected drug reactions. Such testing might also offer new insight into the mechanisms of such toxicities. Overall, this approach has the potential to account for variability in drug response, maximize beneficial and minimize untoward drug effects, optimize therapeutic decision making, and ultimately improve clinical outcomes.

In order to facilitate utilization of pharmacogenomic-guided therapy, genomic diagnostics are also being developed at a rapid rate. Microarray and "chip" technologies have enabled the simultaneous evaluation of multiple SNPs in multiple genes. We envision that a variety of diagnostic pharmacogenomic "packages" will be developed for certain patient populations at risk for or recently diagnosed with specific diseases (e.g. breast cancer, cardiovascular disease, asthma). These packages will provide critical genomic information that will help predict disease susceptibility, the likelihood of disease progression, drug efficacy, and drug toxicity. Together with other clinical information (e.g. breast cancer stage, lipid profile, lung function studies), the genomic data will substantially improve a clinician's ability to identify subpopulations of patients most likely to respond to specific preventive or therapeutic strategies, as well as identify specific drugs and dosing regimens that can be used in individual patients to optimize outcomes. In addition, pharmacogenomic concepts will be applied to the development of novel therapeutic agents by the pharmaceutical industry, which has already reported substantial increases in the use of pharmacogenomic testing in clinical trials (154). This approach will eventually yield medicines which directly modify genetically validated targets.

The future of pharmacogenomics is quickly becoming a reality. Indeed, preclinical and clinical investigations are already evaluating the contribution of multiple genes to the observed variability in drug response. However, unraveling the full potential of

pharmacogenomics will require the translation of discoveries from basic to clinical science, and eventually the application of these findings to patient care (i.e. from bench to bedside). Current approaches to pharmacogenomic research involve 1) SNP discovery, 2) *in vitro* studies which characterize the functional and mechanistic significance of known SNPs, and 3) *in vivo* studies in healthy volunteers or patients which investigate the clinical relevance of known SNPs. Clinical evaluations have included prospective clinical pharmacology studies with pharmacokinetic and pharmacodynamic endpoints, and retrospective outcome analyses of genetic subgroups from randomized, controlled clinical trials. Future prospective clinical trials that evaluate the safety and efficacy of pharmacogenomic-guided drug therapy will be necessary to determine if these strategies can actually improve patient outcomes. Furthermore, detailed economic analyses, which evaluate the cost-effectiveness of such approaches, will be crucial before widespread implementation into clinical practice can occur.

Understanding the relevance of genomic information will be crucial to close the gap between basic science and patient care. Moreover, open dialogue regarding the numerous ethical issues surrounding genomic testing, such as the protection of privacy as it relates to insurance and employment, will need to occur as this field moves towards clinical application. Ultimately, the factors essential to the appropriate utilization of pharmacogenomic data include collaboration between basic researchers and clinicians, development of a multidisciplinary approach to patient care, and education of clinician-scientists in pharmacogenomic medicine. Perhaps the biggest challenge to effective utilization of pharmacogenomic strategies in clinical practice will involve educating the public on its availability, uses, and limitations.

The recent sequencing of the human genome has facilitated identification of polymorphic variants in genes involved in the disposition and pharmacological action of numerous drugs. The rapidly growing field of pharmacogenomics offers enormous potential to improve the way clinicians utilize medications. Pharmacogenomics will ultimately serve to minimize variability in the way patients respond to medications, enabling clinicians to individualize therapy and improve overall clinical outcome.

APPENDIX II

Methods used for genotyping *PTGS1*, *PTGS2*, *NOS3*, *EPHX2*, *CYP2J2* and *CYP2C8* polymorphisms by MALDI-TOF

Polymorphism	Amplification Primers	Extension Primer	Alleles
PTGS1			
G-1006A	F: 5'-ACGTTGGATGCCAGGAGCCAGCACAAGAAC-3'	F: 5'-AGCACAAGAACCTCTGA-3'	G
	R: 5'-ACGTTGGATGATCTCCCTCAGTTTCCCCAG-3'		A
R8W (rs1236913)	F: 5'-ACGTTGGATGCTGGGTCCGCGAGCAGGA-3'	R: 5'-GAGCAGGAACAGCAAGAACC-3'	C
	R: 5'-ACGTTGGATGTCATCTCTCTCCTCTGCAGG-3'		T
P17L (rs3842787)	F: 5'-ACGTTGGATGTCATCTCTCTCCTCTGCAGG-3'	F: 5'-GTTCCTGCTCCTGCTCC-3'	C
	R: 5'-ACGTTGGATGCTGGGTCCGCGAGCAGGA-3'		T
R53H (rs3842789)	F: 5'-ACGTTGGATGAGGGCATCTGTGTCCGCTTC-3'	F: 5'-CCGCTTCGGCCTTGACC-3'	G
	R: 5'-ACGTTGGATGAGCTCACGGATGGTGCAGTT-3'		A
G230S	F: 5'-ACGTTGGATGGTATGTCATCGACAGTGGGC-3'	F: 5'-CTCTGTCCACAGGTAGACCTC-3'	G
	R: 5'-ACGTTGGATGCGCTCCAGATTGTCTCCATA-3'		A
L237M (rs5789)	F: 5'-ACGTTGGATGTCTGTCCACAGGTAGACCTC-3'	F: 5'-CCACATTTATGGAGACAAT-3'	C
	R: 5'-ACGTTGGATGTTCCCATCCTTAAAGAGCCG-3'		A
PTGS2			
V511A (rs5273)	F: 5'-ACGTTGGATGCTTCTGGTAGAAAAGCCTCG-3'	F: 5'-GTGAAACCATGGTAGAAG-3'	T
	R: 5'-ACGTTGGATGCCATAAGTCCTTTCAAGGAG-3'		C

Polymorphism	Amplification Primers	Extension Primer	Alleles
NOS3			
T-786C (rs2070744)	F: 5'-ACGTTGGATGACTGTAGTTTCCCTAGTCCC-3'	F: 5'-CATCAAGCTCTTCCCTGGC-3'	T
	R: 5'-ACGTTGGATGAGGTCAGCAGAGAGACTAGG-3'		C
E298D (rs1799983)	F: 5'-ACGTTGGATGACCTCAAGGACCAGCTCGG-3'	F: 5'-GCTGCAGGCCCCAGATGA-3'	G
	R: 5'-ACGTTGGATGAAACGGTCGCTTCGACGTGC-3'		T
EPHX2			
K55R	F: 5'-ACGTTGGATGATGATGCTTTCCAGAAAGGG-3'	F: 5'-CACTACCCGGCTTATGA-3'	A
	R: 5'- ACGTTGGATGTCACCTGGGAAAGTGTGATC-3'		G
R103C (rs17057255)	F: 5'-ACGTTGGATGAGGCGATTTCAGCCAGAAAG-3'	F: 5'-CAGCCAGAAAGATCAAC-3'	C
	R: 5'-ACGTTGGATGGCCAGTATCAGATCCTTACC-3'		T
C154Y	F: 5'-ACGTTGGATGAGCTGATGTGTGAGCTGAAG-3'	F: 5'-TGACTTCCTGATAGAGTCGT-3'	G
	R: 5'-ACGTTGGATGGTTCAGGTTTGACCATTCCC-3'		A
G14029C	F: 5'-ACGTTGGATGCCCTGGTTGCAATATCTCTG-3'	R: 5'-CAATATCTCTGAACATCCTTCT-3'	G
	R: 5'-ACGTTGGATGACAAGTTTCTGCTGGACACC-3'		C
G20675A (rs57816586)	F: 5'-ACGTTGGATGGGGTATTGAGAAGCTGTAAG-3'	R: 5'-CTGTAAGCAGGAAAGGTA-3'	G
	R: 5'-ACGTTGGATGTATTCAGGAGAGCCTCTCAC-3'		A
402InsR	F: 5'-ACGTTGGATGTGTTTTAGGGAGTGGCTGAG-3'	F: 5'-GGAACAGAACCTGAGTCG-3'	CGT
	R: 5'-ACGTTGGATGTTGCTCTGAAGAGGCTTTTG-3'		-
V422A	F: 5'-ACGTTGGATGTGGTTCCAGATATGGCTCTC-3'	R: 5'-CTCTTACCCGCTTCACAG-3'	T
	R: 5'-ACGTTGGATGTCCTTCAGAGTGTTTTATCC-3'		C
E470G	F: 5'-ACGTTGGATGAGCTTTTGCAAGCCCACTTC-3'	R: 5'-CCCACTTCCAGTTCCTT-3'	A
	R: 5'-ACGTTGGATGACTTTCTGATCTCTCCCCAG-3'		G

Polymorphism	Amplification Primers	Extension Primer	Alleles
CYP2J2			
G10860A (rs3738474)	F: 5'-ACGTTGGATGGGTAAGTTTCTTGGCCAACG-3'	F: 5'-CTTGGCCAACGAAAGGT-3'	G
	R: 5'-ACGTTGGATGGTCACCAAGGTGCCTTTAAC-3'		A
R158C (**3*)	F: 5'-ACGTTGGATGCTCTGACAGCACTAAGGAAC-3'	F: 5'-AGGAAAGAAGAGCTTAGAGGAA-3'	C
	R: 5'-ACGTTGGATGTTGCTTCAGTGAGGTGTTGG-3'		T
T18778G (rs2271800)	F: 5'-ACGTTGGATGGGGACCTTTTCTTCCAAATG-3'	F: 5'-CCTCCTAGGATGAAGCCCCT-3'	T
	R: 5'-ACGTTGGATGTCAGAGGATTCCTGATTGCC-3'		G
N404Y (**6*)	F: 5'-ACGTTGGATGGTCCGGATTGAATGTGTCAG-3'	R: 5'-CCTGTGCAGCGCCGTCAAAT-3'	A
	R: 5'-ACGTTGGATGGCTTTCTCTAGGGTACCATG-3'		T
CYP2C8			
I264M (**4*, rs1058930)	F: 5'-ACGTTGGATGAGAACACCAAGCATCACTGG-3'	F: 5'-TAACAATCCTCGGGACTTTAT-3'	C
	R: 5'-ACGTTGGATGGCTAATATCTTACCTGCTCC-3'		G
I269F (**2*, rs11572103)	F: 5'-ACGTTGGATGGCTAATATCTTACCTGCTCC-3'	F: 5'-CTTACCTGCTCCATTTTGA-3'	A
	R: 5'-ACGTTGGATGAGAACACCAAGCATCACTGG-3'		T
K399R (**3*, rs10509681)	F: 5'-ACGTTGGATGACTGACTTCCGTGCTACATG-3'	F: 5'-TTCCGTGCTACATGATGACA-3'	A
	R: 5'-ACGTTGGATGTATCTAGAAAGTGGCCAGGG-3'		G

*Targeted sequences were amplified via polymerase chain reaction using the designated forward (F) and reverse (R) primers, followed by extension reactions utilizing specific oligonucleotide primers that annealed immediately upstream of each polymorphic site and extended the amplification product by a single base pair in either the forward (F) or reverse (R) direction, as indicated. The mass of the extension reaction products was determined and translated into genotype using the MassARRAY RT software (Sequenom Inc., San Diego, CA) (107).

APPENDIX III

Methods used for genotyping *PTGS2* and *CYP2J2* polymorphisms by BeadArray

Polymorphism
PTGS2
G-765C (rs20417)
CYP2J2:
G-50T (*CYP2J2*7*, rs890293)
R49S (rs11572190)
V113M (rs11572242)
I192N (*CYP2J2*4*)
C33291T (rs4388726)
A33497G (rs11572327)

*Genotyping was performed using the BeadStation system (Illumina, Inc., San Diego, CA) and a custom oligonucleotide pool comprised of 384 single nucleotide polymorphism variants in multiple genes (108). Briefly, double-stranded genomic DNA was labeled with biotin to facilitate the capture of single stranded DNA onto streptavidin-coated sepharose beads for purification of PCR template. The PCR template was created using a highly specific polymerase and ligase that extend and ligate allele-specific primers that bind to complementary sequences surrounding the variant sites and include universal primer sequences and an "address" sequence that is ultimately hybridized to the genotyping array. The PCR template was amplified via the use of universal primers labeled with either Cy3 or Cy5 fluorescent tags, and the amplified products were hybridized to a fiber optic bundle array and imaged with the BeadArray Reader (Illumina). Allele detection and genotype calling were performed using the GenCall and GTS Reports software (Illumina). Primer sequences are available upon request.

APPENDIX IV

Methods used for genotyping *EPHX2* polymorphisms by Taqman®

Polymorphism	Amplification Primers	Probe Primers	Alleles
EPHX2			
R287Q (rs751141)	F: 5'-ATCCCTGCTCTGGCCCA-3'	5'-ATGTCCATAGCTAGGACC**C**GGTAACCT-3'	G
	R: 5'-GGAGGAGCAGATGACTCTCCATA-3'	5'-ATGTCCATAGCTAGGACC**T**GGTAACCT-3'	A
A53415G (rs1042032)	F: 5'-GTGCCCACGCTCAGCAG-3'	5'-TGTGCC**A**TCCTTCCA-3'	A
	R: 5'-TAAGAATGGTGCCCCAGCAG-3'	5'-TGCC**G**TCCTTCCA-3'	G

*Targeted sequences were amplified via polymerase chain reaction using the designated forward (F) and reverse (R) primers, and hybridized with two allele-specific probes that differed at the polymorphic site (bold) and were labeled with the distinct fluorescent reporter dyes VIC and TAM. The fluorescent intensity of each reported dye was quantified and translated into genotype (Applied Biosystems, Foster City, CA) (126).

REFERENCES

1. American Heart Association. 2003. *Heart Disease and Stroke Statistics - 2004 Update*. Dallas, TX.

2. Widlansky, M.E., Gokce, N., Keaney, J.F., Jr., and Vita, J.A. 2003. The clinical implications of endothelial dysfunction. *J Am Coll Cardiol* 42:1149-1160.

3. Hansson, G.K. 2005. Inflammation, atherosclerosis, and coronary artery disease. *N Engl J Med* 352:1685-1695.

4. Charo, I.F., and Taubman, M.B. 2004. Chemokines in the pathogenesis of vascular disease. *Circ Res* 95:858-866.

5. de Winther, M.P., Kanters, E., Kraal, G., and Hofker, M.H. 2005. Nuclear factor kappaB signaling in atherogenesis. *Arterioscler Thromb Vasc Biol* 25:904-914.

6. Ambrose, J.A., and Barua, R.S. 2004. The pathophysiology of cigarette smoking and cardiovascular disease: an update. *J Am Coll Cardiol* 43:1731-1737.

7. Chowienczyk, P.J., Watts, G.F., Cockcroft, J.R., and Ritter, J.M. 1992. Impaired endothelium-dependent vasodilation of forearm resistance vessels in hypercholesterolaemia. *Lancet* 340:1430-1432.

8. Wheatcroft, S.B., Williams, I.L., Shah, A.M., and Kearney, M.T. 2003. Pathophysiological implications of insulin resistance on vascular endothelial function. *Diabet Med* 20:255-268.

9. Schachinger, V., Britten, M.B., and Zeiher, A.M. 2000. Prognostic impact of coronary vasodilator dysfunction on adverse long-term outcome of coronary heart disease. *Circulation* 101:1899-1906.

10. Halcox, J.P., Schenke, W.H., Zalos, G., Mincemoyer, R., Prasad, A., Waclawiw, M.A., Nour, K.R., and Quyyumi, A.A. 2002. Prognostic value of coronary vascular endothelial dysfunction. *Circulation* 106:653-658.

11. Targonski, P.V., Bonetti, P.O., Pumper, G.M., Higano, S.T., Holmes, D.R., Jr., and Lerman, A. 2003. Coronary endothelial dysfunction is associated with an increased risk of cerebrovascular events. *Circulation* 107:2805-2809.

12. Ohashi, Y., Kawashima, S., Hirata, K., Yamashita, T., Ishida, T., Inoue, N., Sakoda, T., Kurihara, H., Yazaki, Y., and Yokoyama, M. 1998. Hypotension and reduced nitric oxide-elicited vasorelaxation in transgenic mice overexpressing endothelial nitric oxide synthase. *J Clin Invest* 102:2061-2071.

13. De Caterina, R., Libby, P., Peng, H.B., Thannickal, V.J., Rajavashisth, T.B., Gimbrone, M.A., Jr., Shin, W.S., and Liao, J.K. 1995. Nitric oxide decreases cytokine-induced endothelial activation. Nitric oxide selectively reduces endothelial

expression of adhesion molecules and proinflammatory cytokines. *J Clin Invest* 96:60-68.

14. Kawashima, S., Yamashita, T., Ozaki, M., Ohashi, Y., Azumi, H., Inoue, N., Hirata, K., Hayashi, Y., Itoh, H., and Yokoyama, M. 2001. Endothelial NO synthase overexpression inhibits lesion formation in mouse model of vascular remodeling. *Arterioscler Thromb Vasc Biol* 21:201-207.

15. Knowles, J.W., Reddick, R.L., Jennette, J.C., Shesely, E.G., Smithies, O., and Maeda, N. 2000. Enhanced atherosclerosis and kidney dysfunction in eNOS(-/-)/ApoE(-/-) mice are ameliorated by enalapril treatment. *J Clin Invest* 105:451-458.

16. Kawashima, S., and Yokoyama, M. 2004. Dysfunction of endothelial nitric oxide synthase and atherosclerosis. *Arterioscler Thromb Vasc Biol* 24:998-1005.

17. Barua, R.S., Ambrose, J.A., Eales-Reynolds, L.J., DeVoe, M.C., Zervas, J.G., and Saha, D.C. 2001. Dysfunctional endothelial nitric oxide biosynthesis in healthy smokers with impaired endothelium-dependent vasodilatation. *Circulation* 104:1905-1910.

18. Barua, R.S., Ambrose, J.A., Srivastava, S., DeVoe, M.C., and Eales-Reynolds, L.J. 2003. Reactive oxygen species are involved in smoking-induced dysfunction of nitric oxide biosynthesis and upregulation of endothelial nitric oxide synthase: an in vitro demonstration in human coronary artery endothelial cells. *Circulation* 107:2342-2347.

19. Smith, W.L., Garavito, R.M., and DeWitt, D.L. 1996. Prostaglandin endoperoxide H synthases (cyclooxygenases)-1 and -2. *J Biol Chem* 271:33157-33160.

20. Zeldin, D.C. 2001. Epoxygenase pathways of arachidonic acid metabolism. *J Biol Chem* 276:36059-36062.

21. Brash, A.R. 1999. Lipoxygenases: occurrence, functions, catalysis, and acquisition of substrate. *J Biol Chem* 274:23679-23682.

22. Davidge, S.T. 2001. Prostaglandin H synthase and vascular function. *Circ Res* 89:650-660.

23. Antman, E.M., DeMets, D., and Loscalzo, J. 2005. Cyclooxygenase inhibition and cardiovascular risk. *Circulation* 112:759-770.

24. Grosser, T., Fries, S., and Fitzgerald, G.A. 2006. Biological basis for the cardiovascular consequences of COX-2 inhibition: therapeutic challenges and opportunities. *J Clin Invest* 116:4-15.

25. Patrono, C., Garcia Rodriguez, L.A., Landolfi, R., and Baigent, C. 2005. Low-dose aspirin for the prevention of atherothrombosis. *N Engl J Med* 353:2373-2383.

26. Capdevila, J.H., Falck, J.R., and Harris, R.C. 2000. Cytochrome P450 and arachidonic acid bioactivation. Molecular and functional properties of the arachidonate monooxygenase. *J Lipid Res* 41:163-181.

27. Zeldin, D.C., Kobayashi, J., Falck, J.R., Winder, B.S., Hammock, B.D., Snapper, J.R., and Capdevila, J.H. 1993. Regio- and enantiofacial selectivity of epoxyeicosatrienoic acid hydration by cytosolic epoxide hydrolase. *J Biol Chem* 268:6402-6407.

28. Yu, Z., Xu, F., Huse, L.M., Morisseau, C., Draper, A.J., Newman, J.W., Parker, C., Graham, L., Engler, M.M., Hammock, B.D., et al. 2000. Soluble epoxide hydrolase regulates hydrolysis of vasoactive epoxyeicosatrienoic acids. *Circ Res* 87:992-998.

29. Fang, X., Kaduce, T.L., Weintraub, N.L., Harmon, S., Teesch, L.M., Morisseau, C., Thompson, D.A., Hammock, B.D., and Spector, A.A. 2001. Pathways of epoxyeicosatrienoic acid metabolism in endothelial cells. Implications for the vascular effects of soluble epoxide hydrolase inhibition. *J Biol Chem* 276:14867-14874.

30. Campbell, W.B., Gebremedhin, D., Pratt, P.F., and Harder, D.R. 1996. Identification of epoxyeicosatrienoic acids as endothelium-derived hyperpolarizing factors. *Circ Res* 78:415-423.

31. Fisslthaler, B., Popp, R., Kiss, L., Potente, M., Harder, D.R., Fleming, I., and Busse, R. 1999. Cytochrome P450 2C is an EDHF synthase in coronary arteries. *Nature* 401:493-497.

32. Node, K., Huo, Y., Ruan, X., Yang, B., Spiecker, M., Ley, K., Zeldin, D.C., and Liao, J.K. 1999. Anti-inflammatory properties of cytochrome P450 epoxygenase-derived eicosanoids. *Science* 285:1276-1279.

33. Node, K., Ruan, X.L., Dai, J., Yang, S.X., Graham, L., Zeldin, D.C., and Liao, J.K. 2001. Activation of Galpha s mediates induction of tissue-type plasminogen activator gene transcription by epoxyeicosatrienoic acids. *J Biol Chem* 276:15983-15989.

34. Wu, S., Chen, W., Murphy, E., Gabel, S., Tomer, K.B., Foley, J., Steenbergen, C., Falck, J.R., Moomaw, C.R., and Zeldin, D.C. 1997. Molecular cloning, expression, and functional significance of a cytochrome P450 highly expressed in rat heart myocytes. *J Biol Chem* 272:12551-12559.

35. Seubert, J., Yang, B., Bradbury, J.A., Graves, J., Degraff, L.M., Gabel, S., Gooch, R., Foley, J., Newman, J., Mao, L., et al. 2004. Enhanced postischemic functional recovery in CYP2J2 transgenic hearts involves mitochondrial ATP-sensitive K+ channels and p42/p44 MAPK pathway. *Circ Res* 95:506-514.

36. Pozzi, A., Macias-Perez, I., Abair, T., Wei, S., Su, Y., Zent, R., Falck, J.R., and Capdevila, J.H. 2005. Characterization of 5,6- and 8,9-epoxyeicosatrienoic acids (5,6- and 8,9-EET) as potent in vivo angiogenic lipids. *J Biol Chem* 280:27138-27146.

37. Sun, J., Sui, X., Bradbury, J.A., Zeldin, D.C., Conte, M.S., and Liao, J.K. 2002. Inhibition of vascular smooth muscle cell migration by cytochrome p450 epoxygenase-derived eicosanoids. *Circ Res* 90:1020-1027.

38. Wink, D.A., Osawa, Y., Darbyshire, J.F., Jones, C.R., Eshenaur, S.C., and Nims, R.W. 1993. Inhibition of cytochromes P450 by nitric oxide and a nitric oxide-releasing agent. *Arch Biochem Biophys* 300:115-123.

39. Bauersachs, J., Popp, R., Hecker, M., Sauer, E., Fleming, I., and Busse, R. 1996. Nitric oxide attenuates the release of endothelium-derived hyperpolarizing factor. *Circulation* 94:3341-3347.

40. Cowart, L.A., Wei, S., Hsu, M.H., Johnson, E.F., Krishna, M.U., Falck, J.R., and Capdevila, J.H. 2002. The CYP4A isoforms hydroxylate epoxyeicosatrienoic acids to form high affinity peroxisome proliferator-activated receptor ligands. *J Biol Chem* 277:35105-35112.

41. Liu, Y., Zhang, Y., Schmelzer, K., Lee, T.S., Fang, X., Zhu, Y., Spector, A.A., Gill, S., Morisseau, C., Hammock, B.D., et al. 2005. The antiinflammatory effect of laminar flow: the role of PPARgamma, epoxyeicosatrienoic acids, and soluble epoxide hydrolase. *Proc Natl Acad Sci U S A* 102:16747-16752.

42. Kozak, W., Aronoff, D.M., Boutaud, O., and Kozak, A. 2003. 11,12-epoxyeicosatrienoic acid attenuates synthesis of prostaglandin E2 in rat monocytes stimulated with lipopolysaccharide. *Exp Biol Med (Maywood)* 228:786-794.

43. Wang, H., Lin, L., Jiang, J., Wang, Y., Lu, Z.Y., Bradbury, J.A., Lih, F.B., Wang, D.W., and Zeldin, D.C. 2003. Up-regulation of endothelial nitric-oxide synthase by endothelium-derived hyperpolarizing factor involves mitogen-activated protein kinase and protein kinase C signaling pathways. *J Pharmacol Exp Ther* 307:753-764.

44. Michaelis, U.R., Falck, J.R., Schmidt, R., Busse, R., and Fleming, I. 2005. Cytochrome P4502C9-derived epoxyeicosatrienoic acids induce the expression of cyclooxygenase-2 in endothelial cells. *Arterioscler Thromb Vasc Biol* 25:321-326.

45. Sinal, C.J., Miyata, M., Tohkin, M., Nagata, K., Bend, J.R., and Gonzalez, F.J. 2000. Targeted disruption of soluble epoxide hydrolase reveals a role in blood pressure regulation. *J Biol Chem* 275:40504-40510.

46. Seubert, J.M., Sinal, C.J., Goralski, K.B., Graves, J.P., DeGraff, L.M., Lee, C.R., Carey, M.A., Lauria, A., J.W., N., Hammock, B.D., et al. 2006. Role of soluble epoxide hydrolase in postischemic recovery of heart contractile function. *Circ Res* (submitted for publication).

47. Imig, J.D., Zhao, X., Capdevila, J.H., Morisseau, C., and Hammock, B.D. 2002. Soluble epoxide hydrolase inhibition lowers arterial blood pressure in angiotensin II hypertension. *Hypertension* 39:690-694.

48. Davis, B.B., Thompson, D.A., Howard, L.L., Morisseau, C., Hammock, B.D., and Weiss, R.H. 2002. Inhibitors of soluble epoxide hydrolase attenuate vascular smooth muscle cell proliferation. *Proc Natl Acad Sci U S A* 99:2222-2227.

49. Schmelzer, K.R., Kubala, L., Newman, J.W., Kim, I.H., Eiserich, J.P., and Hammock, B.D. 2005. Soluble epoxide hydrolase is a therapeutic target for acute inflammation. *Proc Natl Acad Sci U S A* 102:9772-9777.

50. Yang, B., Graham, L., Dikalov, S., Mason, R.P., Falck, J.R., Liao, J.K., and Zeldin, D.C. 2001. Overexpression of cytochrome P450 CYP2J2 protects against hypoxia-reoxygenation injury in cultured bovine aortic endothelial cells. *Mol Pharmacol* 60:310-320.

51. Fleming, I., Michaelis, U.R., Bredenkotter, D., Fisslthaler, B., Dehghani, F., Brandes, R.P., and Busse, R. 2001. Endothelium-derived hyperpolarizing factor synthase (Cytochrome P450 2C9) is a functionally significant source of reactive oxygen species in coronary arteries. *Circ Res* 88:44-51.

52. Lee, C.R., and Zeldin, D.C. 2003. The reality of pharmacogenomics: optimizing therapeutic decision making. *Environ Health Perspect* 111:A566-567.

53. Miyamoto, Y., Saito, Y., Nakayama, M., Shimasaki, Y., Yoshimura, T., Yoshimura, M., Harada, M., Kajiyama, N., Kishimoto, I., Kuwahara, K., et al. 2000. Replication protein A1 reduces transcription of the endothelial nitric oxide synthase gene containing a -786T-->C mutation associated with coronary spastic angina. *Hum Mol Genet* 9:2629-2637.

54. Tesauro, M., Thompson, W.C., Rogliani, P., Qi, L., Chaudhary, P.P., and Moss, J. 2000. Intracellular processing of endothelial nitric oxide synthase isoforms associated with differences in severity of cardiopulmonary diseases: cleavage of proteins with aspartate vs. glutamate at position 298. *Proc Natl Acad Sci U S A* 97:2832-2835.

55. Casas, J.P., Bautista, L.E., Humphries, S.E., and Hingorani, A.D. 2004. Endothelial nitric oxide synthase genotype and ischemic heart disease: meta-analysis of 26 studies involving 23028 subjects. *Circulation* 109:1359-1365.

56. Nasreen, S., Nabika, T., Shibata, H., Moriyama, H., Yamashita, K., Masuda, J., and Kobayashi, S. 2002. T-786C polymorphism in endothelial NO synthase gene affects cerebral circulation in smokers: possible gene-environmental interaction. *Arterioscler Thromb Vasc Biol* 22:605-610.

57. Leeson, C.P., Hingorani, A.D., Mullen, M.J., Jeerooburkhan, N., Kattenhorn, M., Cole, T.J., Muller, D.P., Lucas, A., Humphries, S.E., and Deanfield, J.E. 2002. Glu298Asp endothelial nitric oxide synthase gene polymorphism interacts with environmental and dietary factors to influence endothelial function. *Circ Res* 90:1153-1158.

58. Fritsche, E., Baek, S.J., King, L.M., Zeldin, D.C., Eling, T.E., and Bell, D.A. 2001. Functional characterization of cyclooxygenase-2 polymorphisms. *J Pharmacol Exp Ther* 299:468-476.

59. Papafili, A., Hill, M.R., Brull, D.J., McAnulty, R.J., Marshall, R.P., Humphries, S.E., and Laurent, G.J. 2002. Common promoter variant in cyclooxygenase-2 represses gene expression: evidence of role in acute-phase inflammatory response. *Arterioscler Thromb Vasc Biol* 22:1631-1636.

60. Cipollone, F., Toniato, E., Martinotti, S., Fazia, M., Iezzi, A., Cuccurullo, C., Pini, B., Ursi, S., Vitullo, G., Averna, M., et al. 2004. A polymorphism in the cyclooxygenase 2 gene as an inherited protective factor against myocardial infarction and stroke. *JAMA* 291:2221-2228.

61. Ulrich, C.M., Bigler, J., Sibert, J., Greene, E.A., Sparks, R., Carlson, C.S., and Potter, J.D. 2002. Cyclooxygenase 1 (COX1) polymorphisms in African-American and Caucasian populations. *Hum Mutat* 20:409-410.

62. Halushka, M.K., Walker, L.P., and Halushka, P.V. 2003. Genetic variation in cyclooxygenase 1: effects on response to aspirin. *Clin Pharmacol Ther* 73:122-130.

63. King, L.M., Ma, J., Srettabunjong, S., Graves, J., Bradbury, J.A., Li, L., Spiecker, M., Liao, J.K., Mohrenweiser, H., and Zeldin, D.C. 2002. Cloning of CYP2J2 gene and identification of functional polymorphisms. *Mol Pharmacol* 61:840-852.

64. Spiecker, M., Darius, H., Hankeln, T., Soufi, M., Sattler, A.M., Schaefer, J.R., Node, K., Borgel, J., Mugge, A., Lindpaintner, K., et al. 2004. Risk of coronary artery disease associated with polymorphism of the cytochrome P450 epoxygenase CYP2J2. *Circulation* 110:2132-2136.

65. Dai, D., Zeldin, D.C., Blaisdell, J.A., Chanas, B., Coulter, S.J., Ghanayem, B.I., and Goldstein, J.A. 2001. Polymorphisms in human CYP2C8 decrease metabolism of the anticancer drug paclitaxel and arachidonic acid. *Pharmacogenetics* 11:597-607.

66. Bahadur, N., Leathart, J.B., Mutch, E., Steimel-Crespi, D., Dunn, S.A., Gilissen, R., Houdt, J.V., Hendrickx, J., Mannens, G., Bohets, H., et al. 2002. CYP2C8 polymorphisms in Caucasians and their relationship with paclitaxel 6alpha-hydroxylase activity in human liver microsomes. *Biochem Pharmacol* 64:1579-1589.

67. Yasar, U., Bennet, A.M., Eliasson, E., Lundgren, S., Wiman, B., De Faire, U., and Rane, A. 2003. Allelic variants of cytochromes P450 2C modify the risk for acute myocardial infarction. *Pharmacogenetics* 13:715-720.

68. Sandberg, M., Hassett, C., Adman, E.T., Meijer, J., and Omiecinski, C.J. 2000. Identification and functional characterization of human soluble epoxide hydrolase genetic polymorphisms. *J Biol Chem* 275:28873-28881.

69. Przybyla-Zawislak, B.D., Srivastava, P.K., Vazquez-Matias, J., Mohrenweiser, H.W., Maxwell, J.E., Hammock, B.D., Bradbury, J.A., Enayetallah, A.E., Zeldin, D.C., and Grant, D.F. 2003. Polymorphisms in human soluble epoxide hydrolase. *Mol Pharmacol* 64:482-490.

70. Fornage, M., Boerwinkle, E., Doris, P.A., Jacobs, D., Liu, K., and Wong, N.D. 2004. Polymorphism of the soluble epoxide hydrolase is associated with coronary artery calcification in African-American subjects: The Coronary Artery Risk Development in Young Adults (CARDIA) study. *Circulation* 109:335-339.

71. Yokoyama, C., and Tanabe, T. 1989. Cloning of human gene encoding prostaglandin endoperoxide synthase and primary structure of the enzyme. *Biochem Biophys Res Commun* 165:888-894.

72. Wang, L.H., Hajibeigi, A., Xu, X.M., Loose-Mitchell, D., and Wu, K.K. 1993. Characterization of the promoter of human prostaglandin H synthase-1 gene. *Biochem Biophys Res Commun* 190:406-411.

73. Warner, T.D., and Mitchell, J.A. 2004. Cyclooxygenases: new forms, new inhibitors, and lessons from the clinic. *FASEB J* 18:790-804.

74. Scott, B.T., Hasstedt, S.J., Bovill, E.G., Callas, P.W., Valliere, J.E., Wang, L., Wu, K.K., and Long, G.L. 2002. Characterization of the human prostaglandin H synthase 1 gene (PTGS1): exclusion by genetic linkage analysis as a second modifier gene in familial thrombosis. *Blood Coagul Fibrinolysis* 13:519-531.

75. Hillarp, A., Palmqvist, B., Lethagen, S., Villoutreix, B.O., and Mattiasson, I. 2003. Mutations within the cyclooxygenase-1 gene in aspirin non-responders with recurrence of stroke. *Thromb Res* 112:275-283.

76. Maree, A.O., Curtin, R.J., Chubb, A., Dolan, C., Cox, D., O'Brien, J., Crean, P., Shields, D.C., and Fitzgerald, D.J. 2005. Cyclooxygenase-1 haplotype modulates platelet response to aspirin. *J Thromb Haemost* 3:2340-2345.

77. Fries, S., Grosser, T., Price, T.S., Lawson, J.A., Kapoor, S., DeMarco, S., Pletcher, M.T., Wiltshire, T., and FitzGerald, G.A. 2006. Marked interindividual variability in the response to selective inhibitors of cyclooxygenase-2. *Gastroenterology* 130:55-64.

78. Ulrich, C.M., Bigler, J., Sparks, R., Whitton, J., Sibert, J.G., Goode, E.L., Yasui, Y., and Potter, J.D. 2004. Polymorphisms in PTGS1 (=COX-1) and risk of colorectal polyps. *Cancer Epidemiol Biomarkers Prev* 13:889-893.

79. Collins, F.S., Brooks, L.D., and Chakravarti, A. 1998. A DNA polymorphism discovery resource for research on human genetic variation. *Genome Res* 8:1229-1231.

80. Bleasby, K., Hall, L.A., Perry, J.L., Mohrenweiser, H.W., and Pritchard, J.B. 2005. Functional consequences of single nucleotide polymorphisms in the human organic anion transporter hOAT1 (SLC22A6). *J Pharmacol Exp Ther* 314:923-931.

81. Barrett, J.C., Fry, B., Maller, J., and Daly, M.J. 2005. Haploview: analysis and visualization of LD and haplotype maps. *Bioinformatics* 21:263-265.

82. Knuppel, R., Dietze, P., Lehnberg, W., Frech, K., and Wingender, E. 1994. TRANSFAC retrieval program: a network model database of eukaryotic transcription regulating sequences and proteins. *J Comput Biol* 1:191-198.

83. Chenna, R., Sugawara, H., Koike, T., Lopez, R., Gibson, T.J., Higgins, D.G., and Thompson, J.D. 2003. Multiple sequence alignment with the Clustal series of programs. *Nucleic Acids Res* 31:3497-3500.

84. Picot, D., Loll, P.J., and Garavito, R.M. 1994. The X-ray crystal structure of the membrane protein prostaglandin H2 synthase-1. *Nature* 367:243-249.

85. Kurumbail, R.G., Stevens, A.M., Gierse, J.K., McDonald, J.J., Stegeman, R.A., Pak, J.Y., Gildehaus, D., Miyashiro, J.M., Penning, T.D., Seibert, K., et al. 1996. Structural basis for selective inhibition of cyclooxygenase-2 by anti-inflammatory agents. *Nature* 384:644-648.

86. Kiefer, J.R., Pawlitz, J.L., Moreland, K.T., Stegeman, R.A., Hood, W.F., Gierse, J.K., Stevens, A.M., Goodwin, D.C., Rowlinson, S.W., Marnett, L.J., et al. 2000. Structural insights into the stereochemistry of the cyclooxygenase reaction. *Nature* 405:97-101.

87. Davis, I.W., Murray, L.W., Richardson, J.S., and Richardson, D.C. 2004. MOLPROBITY: structure validation and all-atom contact analysis for nucleic acids and their complexes. *Nucleic Acids Res* 32:W615-619.

88. Baek, S.J., Wilson, L.C., Lee, C.H., and Eling, T.E. 2002. Dual function of nonsteroidal anti-inflammatory drugs (NSAIDs): inhibition of cyclooxygenase and induction of NSAID-activated gene. *J Pharmacol Exp Ther* 301:1126-1131.

89. Barnett, J., Chow, J., Ives, D., Chiou, M., Mackenzie, R., Osen, E., Nguyen, B., Tsing, S., Bach, C., Freire, J., et al. 1994. Purification, characterization and selective inhibition of human prostaglandin G/H synthase 1 and 2 expressed in the baculovirus system. *Biochim Biophys Acta* 1209:130-139.

90. Gierse, J.K., Hauser, S.D., Creely, D.P., Koboldt, C., Rangwala, S.H., Isakson, P.C., and Seibert, K. 1995. Expression and selective inhibition of the constitutive and inducible forms of human cyclo-oxygenase. *Biochem J* 305 (Pt 2):479-484.

91. Kulmacz, R.J., and Lands, W.E.M. 1987. Cyclo-oxygenase: measurement, purification and properties. In *Prostaglandins and Related Substances: A Practical Approach*. C.C. Denedetto, R.G. McDonald-Gibson, S. Nigam, and T.F. Slater, editors. Washington, DC: IRL Press. 209-227.

92. Lee, Y.S., Kim, H., Wu, T.X., Wang, X.M., and Dionne, R.A. 2006. Genetically mediated interindividual variation in analgesic responses to cyclooxygenase inhibitory drugs. *Clin Pharmacol Ther* 79:407-418.

93. Shimokawa, T., Kulmacz, R.J., DeWitt, D.L., and Smith, W.L. 1990. Tyrosine 385 of prostaglandin endoperoxide synthase is required for cyclooxygenase catalysis. *J Biol Chem* 265:20073-20076.

94. Bhattacharyya, D.K., Lecomte, M., Rieke, C.J., Garavito, M., and Smith, W.L. 1996. Involvement of arginine 120, glutamate 524, and tyrosine 355 in the binding of arachidonate and 2-phenylpropionic acid inhibitors to the cyclooxygenase active site of ovine prostaglandin endoperoxide H synthase-1. *J Biol Chem* 271:2179-2184.

95. Garavito, R.M., and DeWitt, D.L. 1999. The cyclooxygenase isoforms: structural insights into the conversion of arachidonic acid to prostaglandins. *Biochim Biophys Acta* 1441:278-287.

96. Thuresson, E.D., Lakkides, K.M., Rieke, C.J., Sun, Y., Wingerd, B.A., Micielli, R., Mulichak, A.M., Malkowski, M.G., Garavito, R.M., and Smith, W.L. 2001. Prostaglandin endoperoxide H synthase-1: the functions of cyclooxygenase active site residues in the binding, positioning, and oxygenation of arachidonic acid. *J Biol Chem* 276:10347-10357.

97. Thuresson, E.D., Lakkides, K.M., and Smith, W.L. 2000. Different catalytically competent arrangements of arachidonic acid within the cyclooxygenase active site of prostaglandin endoperoxide H synthase-1 lead to the formation of different oxygenated products. *J Biol Chem* 275:8501-8507.

98. Shi, J., Misso, N.L., Duffy, D.L., Bradley, B., Beard, R., Thompson, P.J., and Kedda, M.A. 2005. Cyclooxygenase-1 gene polymorphisms in patients with different asthma phenotypes and atopy. *Eur Respir J* 26:249-256.

99. Camitta, M.G., Gabel, S.A., Chulada, P., Bradbury, J.A., Langenbach, R., Zeldin, D.C., and Murphy, E. 2001. Cyclooxygenase-1 and -2 knockout mice demonstrate increased cardiac ischemia/reperfusion injury but are protected by acute preconditioning. *Circulation* 104:2453-2458.

100. Kobayashi, T., Tahara, Y., Matsumoto, M., Iguchi, M., Sano, H., Murayama, T., Arai, H., Oida, H., Yurugi-Kobayashi, T., Yamashita, J.K., et al. 2004. Roles of thromboxane A(2) and prostacyclin in the development of atherosclerosis in apoE-deficient mice. *J Clin Invest* 114:784-794.

101. Lee, C.R., Bottone, F.G., Krahn, J.M., Li, L., Mohrenweiser, H.W., Cook, M.E., Petrovich, R.M., Bell, D.A., Eling, T.E., and Zeldin, D.C. 2006. Identification and functional characterization of polymorphisms in human cyclooxygenase-1 (PTGS1). *Pharmacogenet Genomics* (in press).

102. The ARIC investigators. 1989. The Atherosclerosis Risk in Communities (ARIC) Study: design and objectives. *Am J Epidemiol* 129:687-702.

103. White, A.D., Folsom, A.R., Chambless, L.E., Sharret, A.R., Yang, K., Conwill, D., Higgins, M., Williams, O.D., and Tyroler, H.A. 1996. Community surveillance of coronary heart disease in the Atherosclerosis Risk in Communities (ARIC) Study: methods and initial two years' experience. *J Clin Epidemiol* 49:223-233.

104. Rosamond, W.D., Folsom, A.R., Chambless, L.E., Wang, C.H., McGovern, P.G., Howard, G., Copper, L.S., and Shahar, E. 1999. Stroke incidence and survival among middle-aged adults: 9-year follow-up of the Atherosclerosis Risk in Communities (ARIC) cohort. *Stroke* 30:736-743.

105. 1981. The National Survey of Stroke. National Institute of Neurological and Communicative Disorders and Stroke. *Stroke* 12:I1-91.

106. Shahar, E., Folsom, A.R., Romm, F.J., Bisgard, K.M., Metcalf, P.A., Crum, L., McGovern, P.G., Hutchinson, R.G., and Heiss, G. 1996. Patterns of aspirin use in middle-aged adults: the Atherosclerosis Risk in Communities (ARIC) Study. *Am Heart J* 131:915-922.

107. Bray, M.S., Boerwinkle, E., and Doris, P.A. 2001. High-throughput multiplex SNP genotyping with MALDI-TOF mass spectrometry: practice, problems and promise. *Hum Mutat* 17:296-304.

108. Shen, R., Fan, J.B., Campbell, D., Chang, W., Chen, J., Doucet, D., Yeakley, J., Bibikova, M., Wickham Garcia, E., McBride, C., et al. 2005. High-throughput SNP genotyping on universal bead arrays. *Mutat Res* 573:70-82.

109. Barlow, W.E., Ichikawa, L., Rosner, D., and Izumi, S. 1999. Analysis of case-cohort designs. *J Clin Epidemiol* 52:1165-1172.

110. Li, R., Folsom, A.R., Sharrett, A.R., Couper, D., Bray, M., and Tyroler, H.A. 2001. Interaction of the glutathione S-transferase genes and cigarette smoking on risk of lower extremity arterial disease: the Atherosclerosis Risk in Communities (ARIC) study. *Atherosclerosis* 154:729-738.

111. Hosmer, D., and Lemeshow, S. 1989. *Applied Logistic Regression*. New York: John Wiley & Sons.

112. Storey, J.D., and Tibshirani, R. 2003. Statistical significance for genomewide studies. *Proc Natl Acad Sci U S A* 100:9440-9445.

113. Niwa, K., Haensel, C., Ross, M.E., and Iadecola, C. 2001. Cyclooxygenase-1 participates in selected vasodilator responses of the cerebral circulation. *Circ Res* 88:600-608.

114. Iadecola, C., Sugimoto, K., Niwa, K., Kazama, K., and Ross, M.E. 2001. Increased susceptibility to ischemic brain injury in cyclooxygenase-1-deficient mice. *J Cereb Blood Flow Metab* 21:1436-1441.

115. Lin, H., Lin, T.N., Cheung, W.M., Nian, G.M., Tseng, P.H., Chen, S.F., Chen, J.J., Shyue, S.K., Liou, J.Y., Wu, C.W., et al. 2002. Cyclooxygenase-1 and bicistronic cyclooxygenase-1/prostacyclin synthase gene transfer protect against ischemic cerebral infarction. *Circulation* 105:1962-1969.

116. Brian, J.E., Jr., Faraci, F.M., and Moore, S.A. 2001. COX-2-dependent delayed dilatation of cerebral arterioles in response to bradykinin. *Am J Physiol Heart Circ Physiol* 280:H2023-2029.

117. Iadecola, C., Niwa, K., Nogawa, S., Zhao, X., Nagayama, M., Araki, E., Morham, S., and Ross, M.E. 2001. Reduced susceptibility to ischemic brain injury and N-methyl-D-aspartate-mediated neurotoxicity in cyclooxygenase-2-deficient mice. *Proc Natl Acad Sci U S A* 98:1294-1299.

118. Dore, S., Otsuka, T., Mito, T., Sugo, N., Hand, T., Wu, L., Hurn, P.D., Traystman, R.J., and Andreasson, K. 2003. Neuronal overexpression of cyclooxygenase-2 increases cerebral infarction. *Ann Neurol* 54:155-162.

119. Wang, J., Dudley, D., and Wang, X.L. 2002. Haplotype-specific effects on endothelial NO synthase promoter efficiency: modifiable by cigarette smoking. *Arterioscler Thromb Vasc Biol* 22:e1-4.

120. Nakayama, M., Yoshimura, M., Sakamoto, T., Shimasaki, Y., Nakamura, S., Ito, T., Abe, K., Yamamuro, M., Miyamoto, Y., Saito, Y., et al. 2003. Synergistic interaction of T-786-->C polymorphism in the endothelial nitric oxide synthase gene and smoking for an enhanced risk for coronary spasm. *Pharmacogenetics* 13:683-688.

121. Stephens, M., and Donnelly, P. 2003. A comparison of bayesian methods for haplotype reconstruction from population genotype data. *Am J Hum Genet* 73:1162-1169.

122. Sofowora, G., Dishy, V., Xie, H.G., Imamura, H., Nishimi, Y., Morales, C.R., Morrow, J.D., Kim, R.B., Stein, C.M., and Wood, A.J. 2001. In-vivo effects of Glu298Asp endothelial nitric oxide synthase polymorphism. *Pharmacogenetics* 11:809-814.

123. Wang, X.L., Sim, A.S., Badenhop, R.F., McCredie, R.M., and Wilcken, D.E. 1996. A smoking-dependent risk of coronary artery disease associated with a polymorphism of the endothelial nitric oxide synthase gene. *Nat Med* 2:41-45.

124. Howard, G., Wagenknecht, L.E., Burke, G.L., Diez-Roux, A., Evans, G.W., McGovern, P., Nieto, F.J., and Tell, G.S. 1998. Cigarette smoking and progression of atherosclerosis: The Atherosclerosis Risk in Communities (ARIC) Study. *JAMA* 279:119-124.

125. Fang, X., Weintraub, N.L., McCaw, R.B., Hu, S., Harmon, S.D., Rice, J.B., Hammock, B.D., and Spector, A.A. 2004. Effect of soluble epoxide hydrolase inhibition on epoxyeicosatrienoic acid metabolism in human blood vessels. *Am J Physiol Heart Circ Physiol* 287:H2412-2420.

126. Livak, K.J., Flood, S.J., Marmaro, J., Giusti, W., and Deetz, K. 1995. Oligonucleotides with fluorescent dyes at opposite ends provide a quenched probe system useful for detecting PCR product and nucleic acid hybridization. *PCR Methods Appl* 4:357-362.

127. Carlson, C.S., Eberle, M.A., Rieder, M.J., Yi, Q., Kruglyak, L., and Nickerson, D.A. 2004. Selecting a maximally informative set of single-nucleotide polymorphisms for association analyses using linkage disequilibrium. *Am J Hum Genet* 74:106-120.

128. Newman, J.W., Watanabe, T., and Hammock, B.D. 2002. The simultaneous quantification of cytochrome P450 dependent linoleate and arachidonate metabolites in urine by HPLC-MS/MS. *J Lipid Res* 43:1563-1578.

129. Stephens, M., Smith, N.J., and Donnelly, P. 2001. A new statistical method for haplotype reconstruction from population data. *Am J Hum Genet* 68:978-989.

130. Spiecker, M., and Liao, J.K. 2005. Vascular protective effects of cytochrome p450 epoxygenase-derived eicosanoids. *Arch Biochem Biophys* 433:413-420.

131. Enayetallah, A.E., French, R.A., Thibodeau, M.S., and Grant, D.F. 2004. Distribution of soluble epoxide hydrolase and of cytochrome P450 2C8, 2C9, and 2J2 in human tissues. *J Histochem Cytochem* 52:447-454.

132. Imig, J.D., Zhao, X., Zaharis, C.Z., Olearczyk, J.J., Pollock, D.M., Newman, J.W., Kim, I.H., Watanabe, T., and Hammock, B.D. 2005. An orally active epoxide hydrolase inhibitor lowers blood pressure and provides renal protection in salt-sensitive hypertension. *Hypertension* 46:975-981.

133. Fornage, M., Lee, C.R., Doris, P.A., Bray, M.S., Heiss, G., Zeldin, D.C., and Boerwinkle, E. 2005. The soluble epoxide hydrolase gene harbors sequence variation associated with susceptibility to and protection from incident ischemic stroke. *Hum Mol Genet* 14:2829-2837.

134. Celermajer, D.S., Sorensen, K.E., Georgakopoulos, D., Bull, C., Thomas, O., Robinson, J., and Deanfield, J.E. 1993. Cigarette smoking is associated with dose-related and potentially reversible impairment of endothelium-dependent dilation in healthy young adults. *Circulation* 88:2149-2155.

135. Lee, C.R., North, K.E., Bray, M.S., Avery, C.L., Mosher, M.J., Couper, D.J., Coresh, J., Folsom, A.R., Boerwinkle, E., Heiss, G., et al. 2006. Genetic variation in endothelial nitric oxide synthase (NOS3), cigarette smoking, and cardiovascular disease risk: the Atherosclerosis Risk in Communities (ARIC) study. *Pharmacogenet Genomics* (in press).

136. Maresh, J.G., Xu, H., Jiang, N., Gairola, C.G., and Shohet, R.V. 2005. Tobacco smoke dysregulates endothelial vasoregulatory transcripts in vivo. *Physiol Genomics* 21:308-313.

137. Avery, C.L., Martin, L.J., Williams, J.T., and North, K.E. 2005. Accuracy of haplotype estimation in a region of low linkage disequilibrium. *BMC Genet* 6 Suppl 1:S80.

138. Taylor, A.L., Ziesche, S., Yancy, C., Carson, P., D'Agostino, R., Jr., Ferdinand, K., Taylor, M., Adams, K., Sabolinski, M., Worcel, M., et al. 2004. Combination of isosorbide dinitrate and hydralazine in blacks with heart failure. *N Engl J Med* 351:2049-2057.

139. Lee, C.R., North, K.E., Bray, M.S., Fornage, M., Seubert, J.M., Newman, J.W., Hammock, B.D., Couper, D.J., Heiss, G., and Zeldin, D.C. 2006. Genetic variation in soluble epoxide hydrolase (EPHX2) and risk of coronary heart disease: The Atherosclerosis Risk in Communities (ARIC) study. *Hum Mol Genet* 15:1640-1649.

140. Michaelis, U.R., Fisslthaler, B., Barbosa-Sicard, E., Falck, J.R., Fleming, I., and Busse, R. 2005. Cytochrome P450 epoxygenases 2C8 and 2C9 are implicated in hypoxia-induced endothelial cell migration and angiogenesis. *J Cell Sci* 118:5489-5498.

141. Galis, Z.S., and Khatri, J.J. 2002. Matrix metalloproteinases in vascular remodeling and atherogenesis: the good, the bad, and the ugly. *Circ Res* 90:251-262.

142. Lang, C.C., Stein, C.M., Brown, R.M., Deegan, R., Nelson, R., He, H.B., Wood, M., and Wood, A.J. 1995. Attenuation of isoproterenol-mediated vasodilatation in blacks. *N Engl J Med* 333:155-160.

143. Kalinowski, L., Dobrucki, I.T., and Malinski, T. 2004. Race-specific differences in endothelial function: predisposition of African Americans to vascular diseases. *Circulation* 109:2511-2517.

144. Wu, S., Moomaw, C.R., Tomer, K.B., Falck, J.R., and Zeldin, D.C. 1996. Molecular cloning and expression of CYP2J2, a human cytochrome P450 arachidonic acid epoxygenase highly expressed in heart. *J Biol Chem* 271:3460-3468.

145. Nelson, D.R., Zeldin, D.C., Hoffman, S.M., Maltais, L.J., Wain, H.M., and Nebert, D.W. 2004. Comparison of cytochrome P450 (CYP) genes from the mouse and human genomes, including nomenclature recommendations for genes, pseudogenes and alternative-splice variants. *Pharmacogenetics* 14:1-18.

146. Luo, G., Zeldin, D.C., Blaisdell, J.A., Hodgson, E., and Goldstein, J.A. 1998. Cloning and expression of murine CYP2Cs and their ability to metabolize arachidonic acid. *Arch Biochem Biophys* 357:45-57.

147. Tsao, C.C., Coulter, S.J., Chien, A., Luo, G., Clayton, N.P., Maronpot, R., Goldstein, J.A., and Zeldin, D.C. 2001. Identification and localization of five CYP2Cs in murine extrahepatic tissues and their metabolism of arachidonic acid to regio- and stereoselective products. *J Pharmacol Exp Ther* 299:39-47.

148. Wang, H., Zhao, Y., Bradbury, J.A., Graves, J.P., Foley, J., Blaisdell, J.A., Goldstein, J.A., and Zeldin, D.C. 2004. Cloning, expression, and characterization of three new mouse cytochrome p450 enzymes and partial characterization of their fatty acid oxidation activities. *Mol Pharmacol* 65:1148-1158.

149. Schlaeger, T.M., Bartunkova, S., Lawitts, J.A., Teichmann, G., Risau, W., Deutsch, U., and Sato, T.N. 1997. Uniform vascular-endothelial-cell-specific gene expression in both embryonic and adult transgenic mice. *Proc Natl Acad Sci U S A* 94:3058-3063.

150. Zeldin, D.C., DuBois, R.N., Falck, J.R., and Capdevila, J.H. 1995. Molecular cloning, expression and characterization of an endogenous human cytochrome P450 arachidonic acid epoxygenase isoform. *Arch Biochem Biophys* 322:76-86.

151. Livak, K.J., and Schmittgen, T.D. 2001. Analysis of relative gene expression data using real-time quantitative PCR and the 2(-Delta Delta C(T)) Method. *Methods* 25:402-408.

152. Alp, N.J., Mussa, S., Khoo, J., Cai, S., Guzik, T., Jefferson, A., Goh, N., Rockett, K.A., and Channon, K.M. 2003. Tetrahydrobiopterin-dependent preservation of nitric oxide-mediated endothelial function in diabetes by targeted transgenic GTP-cyclohydrolase I overexpression. *J Clin Invest* 112:725-735.

153. Evans, W.E., and McLeod, H.L. 2003. Pharmacogenomics--drug disposition, drug targets, and side effects. *N Engl J Med* 348:538-549.

154. Roses, A.D. 2000. Pharmacogenetics and the practice of medicine. *Nature* 405:857-865.